Study of the pathogenesis of highly pathogenic influenza A virus (H7N1) infection in chickens with special focus in the central nervous system

Aida J. Chaves Hernández.

PhD Thesis, 2011

Study of the pathogenesis of highly pathogenic influenza A virus (H7N1) infection in chickens, with special focus in the central nervous system.

Aida J. Chaves Hernández.

PhD Thesis, 2011

Study of the pathogenesis of highly pathogenic influenza A virus (H7N1) infection in chickens, with special focus in the central nervous system.

Author: Aida J. Chaves Hernández.

Director: Natàlia Majó i Masferrer.

Departament de Sanitat i d'Anatomia Animals de la

Facultat de Veterinària de la

Universitat Autònoma de Barcelona.

2011

PhD studies of Miss. Aida J. Chaves Hernández were supported by the Programme Alβan, the European Union Programme of High Level Scholarships for Latin America, scholarship No. E07D400404CR and by the Universidad Nacional de Costa Rica.

This work was partially supported by the European Project Specific Target Research Project, Euroflu, funded by the sixth Framework Programme (FP6) of the EU (grant 5B-CT-2007-044098).

NATÀLIA MAJÓ i MASFERRER, profesora titular del *Departament de Sanitat i d'Anatomia Animals* de la *Facultat de Veterinària* de la *Universitat Autònoma de Barcelona* e investigadora del *Centre de Recerca en Sanitat Animal (CReSA).*

Certifica:

Que la memoria titulada, "Study of the pathogenesis of highly pathogenic influenza A virus (H7N1) infection in chickens, with special focus in the central nervous system" presentada por Aida Jeannette Chaves Hernández para la obtención del grado de Doctor en Veterinaria, se ha realizado bajo su surpervisión en la *Universitat Autònoma de Barcelona* y el *Centre de Recerca en Sanitat Animal*.

Para que conste a los efectos oportunos, firma el presente certificado en Bellaterra (Barcelona), a 28 de septiembre de 2011.

Natàlia Majó i Masferrer

Para y por la mujer que más admiro,
mi hermosa Mamá.

El diseño de la portada y la dedicatoria hacen referencia a las esferas precolombinas y la idea del Génesis del escultor costarricense Jorge Jiménez Deheredia.

Agradecimientos

Tantas gracias no caben en una hoja… ni cinco… ni diez, son necesarias muchas, como muchos son los momentos vividos, los amigos con los que he compartido y mucho lo que he aprendido….

Gracias al ser supremo que sustenta la vida, porque mientras yo buscaba razones para creer, Él está siempre ahí, a cada paso… cuidando de mí.

Quiero además dar las gracias…

A mi mami, mi papá y mi familia, porque nos une algo más fuerte que la sangre, que es lo que permite que aunque estén tan lejos, los sienta tan cerca.

A mi mentor y mi mayor ejemplo profesional, el que me dio el empujón para emprender esta tarea… Dr. Morales, cuanto me falta por saber, pero primero la salud!

A mi directora de tesis, Natàlia, porque ha luchado junto conmigo en el desarrollo de este proyecto con gran disposición, siempre dándome su apoyo y confianza.

A Fernando, mi compañero y ángel de la guarda "oficial", con quien desde hace más de tres años, he formado una bonita, mágica y extraña simbiosis… como ramas de dos árboles que crecen cerca, se entrecruzan, se sostienen y se necesitan…TQM. También agradezco a mi "suegra postiza-mamá" Amalia, por adoptarme como una más de la familia.

A mis queridas y más grandes amigas, mis "compinches" Juliana y Tufária. Sonrisas, pensamientos profundos y lágrimas son los que han

moldeado nuestra gran amistad, justamente como ocurre con los diamantes, que se forman en las condiciones más adversas.

Quisiera dar la gracias con un abrazo mayúsculo a las sonrisas más hermosas de CReSA, Rosa y Moni, tanta belleza junta en una sola persona pensé que no era posible, pero sí lo es y vosotras sois el mayor ejemplo. Gracias mayúsculas!

Amigos entrañables que siempre tendrán un espacio en mi corazón son Mario A, Maria J, Joseanne, Anna A, Pame, Júlia, Eli. Gracias por esos pequeños y grandes momentos!.

A los magníficos delegados de la cultura catalana, Mar, Joan y Kate, que hicieron y han hecho que muchos de los becarios foráneos aprendamos, comprendamos, respetemos y valoremos la cultura catalana...¡ Visca Catalunya!, i ¡visca totes les tres!. También agradezco a los demás becarios...porque en el ir y venir de las situaciones fue bueno sentir tanta complicidad...

Al grupo de investigación en influenza Aviar, especialmente Raquel, Núria, Toni, y otra vez a Rosa V y Júlia, por el apoyo y la compresión. Mis mayores buenos deseos y muchas bendiciones, que seguro compensarán tantas horas de arduo trabajo junto conmigo.

Gente maravillosa he conocido en el CReSA y AP de la UAB, gracias a todos por las atenciones y colaboración brindada durante estos cuatro años. Gracias por las sonrisas y sus saludos, que hacen que te sientas como en una gran familia.

Gracias a todos!

Abstract

Abstract

Influenza A virus infects a wide range of avian and mammalian species, including humans. In poultry species, two clinical presentations of the disease are recognized. The first one that do not cause clinical signs or produce only mild localised infections limited to the respiratory or gastrointestinal tracts is caused by low pathogenic avian influenza (LPAI) viruses. The second is caused by highly pathogenic avian influenza (HPAI) viruses which are able to produce a severe acute fatal disease as a consequence of systemic replication. Besides, HPAI viruses frequently induced central nervous system (CNS) lesions in birds. These CNS lesions observed in poultry species infected with HPAI viruses are thought to occur by haematogenous invasion of the virus into the CNS. However, the mechanism that leads to this clinical presentation has not been completely elucidated, neither have been evaluated the possible routes of entry of the virus into the brain. In this thesis, three studies were undertaken in order to provide knowledge about the mechanism of pathogenesis and the neurotropism of the H7N1 HPAI virus, as well as to establish the route and mechanism of entry into the CNS.

In the first study, the pathogenesis of the infection with a H7N1 HPAI virus strain in specific pathogen free (SPF) chickens intranasally inoculated with decreasing concentrations of virus: $10^{5.5}$ ELD_{50} (G1), $10^{3.5}$ ELD_{50} (G2) and $10^{1.5}$ ELD_{50} (G3) was carried out in order to establish the animal model. Disease progression was monitored over a period of 16 days and sequential necropsies and tissue samples were collected for histological and immunohistochemical (IHC) examination. Viral ribonucleic acid (RNA) loads were also quantified in different tissues, blood, oropharyngeal, and cloacal swabs using quantitative real-time reverse transcription-polymerase chain reaction (RT-qPCR). Clinical signs of depression, apathy, listlessness, huddling and ruffled feathers were recorded in G1 and few G2 birds, whilst neurological symptoms were only observed in chickens inoculated with the highest dose. Gross lesions of haemorrhages were observed in the unfeathered skin of the comb and legs, skeletal muscle, lung, pancreas and kidney of birds inoculated with $10^{5.5}$ ELD_{50}

and $10^{3.5}$ ELD_{50} doses. Microscopic lesions and influenza viral antigen was demonstrated in cells of the nasal cavity, lung, heart, skeletal muscle, brain, spinal cord, gastrointestinal tract, pancreas, liver, bone marrow, thymus, bursa of Fabricius, spleen, kidney, adrenal gland, and skin in G1 and some G2 birds. Besides, viral RNA was detected by RT-qPCR in kidney, lung, intestine, and brain samples of G1 and G2 birds. However, in birds infected with the lowest dose, viral RNA was detected only in brain and lung in low amounts at 5 and 7 days post-inoculation (dpi). These results demonstrate the high neurotropism of this virus because even in chickens infected with low doses, viral RNA is found in the brain. Viremia was detected at one dpi in animals of G1 suggesting that the bloodstream could be the pathway of viral entry and spreading to the brain. Additionally in this study, viral shedding was observed in oropharyngeal and cloacal swabs in correlation with the inoculation dose. It was concluded that although an adequate infectious dose is critical in reproducing the clinical infection, chickens exposed to lower doses can be infected and shed virus representing a risk for the dissemination of the viral agent. Besides, the chicken model was finally set up that correspond to SPF chickens inoculated with the $10^{5.5}$ ELD_{50} dose, which allow to reproduce the disease observed in the field and also experimentally with other HPAI viruses.

In the second study, the topographical distribution of the viral antigen was determined in the brain of chickens inoculated with the H7N1 HPAI virus (10^{6} ELD_{50} dose) during the first dpi. The main objective was to elucidate the pathway of viral entry into the brain. For this purpose, blood, cerebrospinal fluid (CSF), nasal cavity and brain tissue samples were obtained from 1 to 4 dpi from infected and control chickens. Viral antigen topographical distribution, presence of influenza A virus receptors in the brain, as well as, the role of the olfactory route in virus CNS invasion were studied using different IHC techniques. Besides, viral RNA load in CSF and blood was quantified by means of a RT-qPCR. Viral antigen was observed widely distributed in the CNS, showing bilateral and symmetrical distribution in the nuclei of the diencephalon, mesencephalon and rhombencephalon. Viral RNA was detected in blood and CSF at one dpi, indicating that the virus crosses the blood-CSF-barrier (BCSFB) early during infection. This early dissemination was possibly aided by the

presence of Siaα2,3Gal and Siaα2,6Gal receptors in brain vascular endothelial cells, and Siaα2,3Gal receptors in ependymal and choroid plexus (Chp) cells. No viral antigen was observed in olfactory sensory neurons (OSN), while the olfactory bulb (OB) showed only weak staining, suggesting that the virus did not use this pathway to enter into the brain. The sequence of virus appearance and the topographical distribution of this H7N1 HPAI virus indicate that the viral entry occurs via the haematogenous route, with early and generalized spreading through the CSF.

In the third study, the general mechanism of entry of the H7N1 HPAI virus to the CNS was determined, providing evidential support to the hypothesis of the blood brain barrier (BBB) disruption induced by HPAI viruses. Three different methods were used to determine the time course of BBB disruption in fifteen day-old chickens inoculated with a H7N1 HPAI virus (10^6 ELD_{50} dose). Basically, the permeability of the BBB was evaluated by means of the detection of Evans blue (EB) extravasation, determining the leakage of the serum protein immunoglobulin Y (IgY) and assessing the stability of the tight-junctions (TJs) proteins zonula occludens-1 (ZO-1) and claudin-1 at 6, 12, 18, 24, 36, and 48 hours post infection (hpi). Co-detection of EB and IgY extravasation with influenza viral antigen was evaluated using a double-staining immunofluorescence (IF). The onset of the viremia was evaluated in blood samples taken from all chickens at these same time points. Influenza A virus antigen was detected as early as 24 hpi in brain tissue samples, whereas, viral RNA copies were detected from 18 hpi onward in blood samples. EB extravasation was noted at 48 hpi, whereas IgY leakage was detected at 36 and 48 hpi. Both were observed as multiple foci mainly located in the *telencephalic pallium* (Pall) and *cerebellum* (Cb). Besides, viral antigen was observed in correlation with foci of EB extravasation and IgY leakage. Loss of integrity of the TJs was also observed at 36 and 48 hpi, which was evidenced by the disorganization or loss of the ZO-1 staining.

In conclusion, the H7N1 HPAI virus used in this study is able to infect the endothelial cells of the BBB at early time points (24hpi) and enter into the brain by disrupting the TJs of the BBB, as demonstrated by the detection of serum

proteins (IgY) leakage at 36 hpi. These data underlines the main function of the endothelial cells in the neuroinvasion by this H7N1 virus, however, more studies will be necessary to discern the molecular mechanism that lead to the damage in the TJ s of the BBB.

Resumen

Los virus de influenza tipo A infectan una gran variedad de especies de aves y mamíferos. En las aves de corral, es bien sabido que hay virus de influenza aviar de baja patogenicidad (IABP) que no causan signos clínicos o producen únicamente solo infecciones localizadas leves que se limita al aparato respiratorio o gastrointestinal. Pero también existen virus de influenza aviar de alta patogenicidad (IAAP), que son capaces de producir una enfermedad severa aguda y fatal como consecuencia de la replicación sistémica del virus. Además, estos virus de IAAP con frecuencia inducen lesiones en el sistema nervioso central (SNC) de las aves. Estas lesiones del SNC observadas en las aves infectadas, indican que posiblemente la invasión del virus ocurre desde el torrente sanguíneo. Sin embargo, el mecanismo que conduce a este cuadro clínico no se ha dilucidado, así como tampoco se han estudiado las posibles vías de entrada del virus en el cerebro de las aves. En esta tesis, se llevaron a cabo tres estudios con el fin de proporcionar conocimientos sobre el mecanismo de la patogénesis y neurotropismo del virus de IAAP H7N1, así como para establecer la ruta y mecanismo de entrada en el SNC.

En el primer estudio, la patogénesis inducida por una cepa de IAAP H7N1 fue estudiada en pollos libres de patógenos específicos (SPF, por sus siglas en inglés) con el fin adicional de establecer el modelo de infección en pollos para estudios subsiguientes. Con este fin, los pollos fueron inoculados por vía intranasal con concentraciones decrecientes de virus: $10^{5,5}$ ELD_{50} (G1), $10^{3,5}$ ELD_{50} (G2) y $10^{1,5}$ ELD_{50} (G3). La progresión de la enfermedad fue evaluada durante un período de 16 días, en los cuales se realizaron necropsias secuenciales y se tomaron muestras de tejido para su estudio histológico e inmunohistoquímico. La carga de ácido ribonucleico (ARN) viral se cuantificó en diferentes tejidos, sangre, hisopados de orofaringe, e hisopos cloacales utilizando una técnica de reacción en cadena de la polimerasa en tiempo real con transcriptasa inversa cuantitativa (RT-qPCR, por sus siglas en inglés). Los signos clínicos de depresión y apatía fueron registrados en algunas aves de los grupos G1 y G2, mientras que los síntomas neurológicos se observaron sólo en

los pollos inoculados con la dosis más alta. Lesiones graves de hemorragias fueron observadas en la piel sin plumas de la cresta y las patas, músculo esquelético, pulmón, páncreas y los riñones de las aves inoculadas con las dosis de $10^{5,5}$ y $10^{3,5}$ ELD_{50}. Las lesiones microscópicas y el antígeno viral fueron demostrados en las células de la cavidad nasal, pulmón, corazón, músculo esquelético, cerebro, médula espinal, tracto gastrointestinal, páncreas, hígado, médula ósea, el timo, bolsa de Fabricio, bazo, riñón, glándula adrenal, y la piel. Además, el ARN viral fue detectado por RT-qPCR en muestras de riñón, pulmón, intestino y cerebro de aves de los grupos G1 y G2. En las aves que recibieron la dosis más baja sólo se detectó el ARN viral en el cerebro y los pulmones en pequeñas cantidades a los 5 y 7 días post infección (dpi). Esto también demuestra que el virus de IAAP H7N1 tiene un alto neurotropismo, ya incluso en los pollos inoculados con dosis bajas, el ARN viral se encuentra en el cerebro. Adicionalmente, la viremia se detectó a un dpi, lo que sugiere que la sangre podría ser la vía de propagación de virus en el cerebro. Además, en este estudio, se observó excreción de ARN viral en hisopados orofaríngeos y cloacales y esta excreción disminuyó de manera proporcional a la dosis del inóculo. Finalmente, en este primer estudio se pudo concluir que a pesar de que la dosis infecciosa es de suma importancia para reproducir la infección clínica, los pollos expuestos a dosis más bajas pueden infectarse y eliminar virus representando un riesgo para la diseminación del agente viral. Además, se pudo instaurar el modelo de infección en pollo, utilizando el inóculo de $10^{5,5}$ ELD_{50}, el cual permite reproducir la enfermedad observada en el campo y también experimentalmente con otros virus de IAAP.

En el segundo estudio, la distribución topográfica del antígeno viral fue estudiada en el cerebro de los pollos inoculados con el virus de IAAP H7N1 durante los primeros dpi y utilizando una dosis de 10^6 ELD_{50}. El objetivo principal fue determinar la vía de entrada del virus en el cerebro. Con este objetivo, se obtuvieron muestras de sangre, líquido cefalorraquídeo (LCR), cavidad nasal y tejido cerebral de 1 a 4 dpi, en los pollos infectados y control. La distribución topográfica del antígeno viral, la presencia de receptores para el virus de influenza A en el cerebro, así como, el papel de la vía olfactoria en la invasión del SNC fueron estudiadas mediante diferentes técnicas de

inmunohistoquímica (IHC). Además, la carga viral de ARN en el LCR y sangre fue cuantificada por medio de una RT-qPCR. El antígeno viral se observó ampliamente distribuido en el SNC, donde mostraba una distribución bilateral y simétrica en los núcleos del diencéfalo, mesencéfalo y rombencéfalo. El ARN viral se detectó en la sangre y LCR a un dpi, lo que indica que el virus cruza la barrera sangre-LCR temprano durante la infección. Esta difusión temprana es posiblemente favorecida por la presencia de receptores virales de tipo Siaα2,3Gal y Siaα2,6Gal en las células endoteliales vasculares del cerebro y receptores Siaα2,3Gal en las células del plexo coroideo y ependimarias. No se observó antígeno viral en las neuronas sensoriales olfatorias, mientras que en el bulbo olfactorio sólo hubo una débil positividad, lo que sugiere que el virus no utiliza esta vía para entrar en el cerebro. La secuencia de aparición del antígeno viral y la distribución topográfica del virus de IAAP H7N1, indican que la entrada del virus se produce por vía hematógena, y rápidamente después se disemina de forma generalizada a través del LCR.

El objetivo del tercer estudio fue determinar el mecanismo general de entrada del virus de IAAP H7N1 en el SNC, y proveer soporte a la hipótesis de la disrupción de la barrera hematoencefálica (BHE) inducida por el virus. Tres métodos diferentes fueron utilizados para determinar el curso temporal de la disrupción de la BHE en pollos de 15 días de edad inoculados con el virus de IAAP H7N1 (dosis de 10^6 ELD_{50}). Básicamente, la permeabilidad de la BHE se evaluó por medio de la detección de la extravasación del azul de Evans (AE), la filtración de la proteína de suero inmunoglobulina Y (IgY) y la evaluación de la estabilidad de las uniones estrechas intercelulares (TJ_S, por sus siglas en inglés) utilizando marcadores para la proteína ZO-1 y claudina-1 a los 6, 12, 18, 24, 36 y 48 horas post-infección (hpi). La co-detección de AE y de la extravasación de IgY con el antígeno viral fue evaluada mediante una tinción de inmunofluorescencia (IF) doble. La aparición de la viremia se evaluó en muestras de sangre de todos los pollos a estas mismas hpi por medio de una RT-qPCR. El antígeno del virus de influenza se detectó a las 24 hpi en muestras de tejido cerebral, mientras que se detectaron copias de ARN viral a partir de 18 en muestras de sangre. La extravasación de AE se detectó a las 48 hpi y la difusión de IgY fue observada a las 36 y 48 hpi, ambas se detectaron

como múltiples focos principalmente en el pallium telencefálico y el cerebelo. El antígeno viral co-localizaba con los focos de extravasación de EB y IgY. También se observó pérdida de la integridad de las TJs a las 36 y 48 hpi, lo cual se evidenciaba por la desorganización y pérdida del marcaje para las TJs detectadas con un anticuerpo contra la proteína ZO-1.

En conclusión, el virus de IAAP H7N1 utilizado en este estudio es capaz de infectar a las células endoteliales de la BHE en fases tempranas de la infección (24hpi) y entrar en el cerebro por medio de la alteración de las TJs de la BHE, como se demuestra por la detección de la proteína sérica IgY a los 36 hpi. Estos datos ponen de relieve la función principal de las células endoteliales, durante el proceso de neuro-invasión por el virus de IAAP H7N1, sin embargo, serán necesarios más estudios para determinar el mecanismo molecular que conduce al daño de las TJs de la BHE por parte de los virus de influenza.

The results of the present Thesis have been published or submitted for publication in international scientific peer-reviewed journal:

Chaves, A.J, Busquets, N. Campos, N. Ramis, A. Dolz, R. Rivas, R. Valle. R. Abad, F.X. Darji, A. Majó, N. (2011). Pathogenesis of highly pathogenic avian influenza A virus (H7N1) infection in chickens inoculated with three different doses. *Avian Pathology*. Apr; 40 (2):163-72.

Chaves, A.J., Busquets, N., Valle, R., Rivas, R.,l Vergara-Alert, J., Dolz, R., Ramis, A., Darji, A., Majó, N. (2011). Neuropathogenesis of a highly pathogenic avian influenza virus (H7N1) in experimentally infected chickens. *Veterinary Research*. 42:106.

Chaves, A.J., Vergara-Alert, J., Valle, R., Rivas, R., Busquets, N., Ramis, A., Darji, A., Majó, N. (2011). Mechanism of disruption of the blood brain barrier (BBB) in chickens infected with a H7N1 highly pathogenic avian influenza (HPAI) virus. *In preparation*.

Index of contents

List of abbreviations

ABC	avidin-biotin-peroxidase complex
AGID	agar gel immunodiffusion
ANE	acute necrotizing encephalopathy
AP	*area postrema*
APT	*anterior pretectal nucleus*
BBB	blood brain barrier
BCSFB	blood cerebrospinal fluid barrier
BSA	bovine serum albumin
BSL-3	biosafety level 3
Cb	*cerebelum*
Chp	choroid plexus
CNS	central nervous system
CSF	cerebrospinal fluid
CVOs	circumventricular organs
DAB	3,3′-Diaminobenzidine tetrahydrochloride
dpi	days post-inoculation
DLA	*dorsolateral anterior nucleus*
DMA	*dorsomedial anterior nucleus of the thalamus*
DNA	*deoxiribonucleic acid*
DPall	*dorsal pallium*
EB	Evans blue
ELD_{50}	fifty percent embryo lethal dose
EID_{50}	fifty percent embryo infectious dose
FITC	fluorescein isothiocyanate
FIV	feline immunodeficiency virus
H	*hypothalamus*
HA	haemagglutinin
HAa	haemagglutination assay
HI	Haemagglutination inhibition assay
HIV	human immunodeficiency virus
HPAI	highly pathogenic avian influenza

HPNAI	highly pathogenic notifiable avian influenza
hpi	hours post-inoculation
HRP	horseradish peroxidase
Hp	Hippocampus
IAE	influenza associated encephalopathy
IF	immunofluorescense
Ig	immunoglobulin
IHC	immunohistochemistry
IPC	internal positive control
ISH	*in situ* hibridization technique
Ist	*isthmus*
IVPI	intravenous pathogenicity index
K	lysine
LH	*lateral hypothalamic area*
loD	limit of virus detection
LPAI	low pathogenic avian influenza
LPNAI	low pathogenic notifiable avian influenza
LPall	*lateral pallium*
LSO	*lateral septal organ*
lv	lateral ventricle
MAAII	*maackia amurensis leukoagglutinin*
M1	matrix protein
MDCK	Madin-Darby canine kidney
Med	*medial cerebellar nucleus*
ME	*median eminence*
M2	membrane ion channel
MG	*medial geniculate nucleus*
MPall	*medial pallium*
mSNC	*mesencephalic substancia nigra,* compact part
mRNA	messenger ribonucleic acid
NA	neuraminidase
NAI	notifiable avian influenza
NBT-BCIP	nitro blue tetrazolium chloride 5-bromo-4-chloro-3-indoxyl

NDS	normal donkey serum
NEP	nuclear export protein
Nhyp	neurohypophisis
NLSs	nuclear localization signals
NI	neuraminidase inhibition
NP	nucleoprotein
NS1	non-structural protein 1
NS2	non-structural protein 2
Och	optic area
OSN	olfactory sensory neurons
PA	polymerase acid protein
Pall	*telencephalic pallium*
PB1	polymerase basic protein 1
PB2	polymerase basic protein 2
PBS	phosphate buffered saline
PCR	polymerase chain reaction
PG	*pregeniculate nucleus*
PGP9.5	protein gene product
p2	*thalamus*
p3	*prethalamus*
2P	secondary prosencephalon
R	arginine
RMC	*red nucleus magnocellular part*
RNA	ribonucleic acid
RT-qPCR	quantitative real-time reverse transcription-polymerase chain reaction
Rot	*rotundus nucleus of the thalamus*
RT	room temperature
r2SuVe	*r2 superior vestibular nucleus*
r3LVeV	*r3 lateral vestibular nucleus,* ventral part
SNA	*sambucus nigrans*
Sia	sialic acid
Siaα2,3Gal	sialic acid (Sia) with α(2,3)-linkage to galactose (Gal)

Siaα2,6Gal	sialic acid (Sia) with α(2,6)-linkage to galactose (Gal)
SPF	specific pathogen free
Sp50	*spinal trigeminal nucleus* - oral part
SCO	*subcommisural organ*
SIV	simian immunodeficiency virus
SPall	*telencephalic subpallium*
SPF	specific pathogen free
SPO	*subseptal organ*
STh	*subthalamic nucleus*
TBS	tris-buffer saline solution
TNB	TNT plus blocking buffer
TNT	tris-HCl buffer
TGS	*tectal gray-superficial stratum*
TJs	tight-junctions
ToS	*torus semicircularis*
VI	virus isolation
VMH	*ventromedial hypothalamic nucleus*
VOLT	*vascular organ of the lamina terminalis*
VPall	*ventral pallium*
vRNP	viral ribonucleoprotein
vRNA	viral rinonucleic acid (negative sense RNA)
3v	third ventricle
4v	fourth ventricle
ZO	zonula occludens

1.General Introduction

1.1. Avian influenza

1.1.1. History of influenza

Influenza outbreaks have been described and recorded throughout history. The first epidemics consisting of rapidly disseminated acute catarrhal fevers in humans were described by Hippocrates in 412 BC [1]. However, the name of influenza was not coined until 1387 in Florence, when a severe epidemic affected the whole of Italy, who attributed the cause to some celestial influence, using the expression *"ex influential colesti"*. Later, the term was modified to influenza by Villaini and Segui. After that, many reports of influenza were made through the years in Europe and Asian countries [2].

In poultry species, avian influenza was first reported in Italy 1878, when Perroncito described the presence of a highly lethal systemic disease in birds, which was called "fowl plague" [3]. In 1880, as the disease was confused with the acute septicemic form of fowl cholera, Rivolto and Delprato could differentiate both diseases based on clinical and pathological features. In 1901, Centanni and Savonuzzi determined that the disease was caused by a filterable agent. By the mid-1930's , "fowl plague" was already an endemic problem in many parts of Europe [3,4]. Likewise, in the United States the disease was reported in 1924-1925 and 1929 [3].

Around the same time, in 1933, the agent causing the human influenza was discovered. This was achieved by Wilson Smith, Christopher Andrews, and Patrick Laidrow who indentified the virus thanks to the finding of a suitable host for propagation. This happened alongside the successful isolation of the swine influenza virus by Shope in 1931 [5,6]. Prior to that, there was one of the most devastating influenza pandemics in human history, the "Spanish Flu" (H1N1 subtype) which hit the population in 1918, causing thousands of deaths [2,7].

In 1955, the virus which caused “fowl plague” was also classified as influenza A virus [4]. Besides, the relationship between avian and mammalian influenza viruses was also demonstrated [8]. In fact, two of the most severe pandemics of influenza virus in humans were recorded in 1957 (H2N2) and 1968 (H3N2) [2] and emerged when the human influenza virus acquired a novel haemagglutinin molecule from an avian influenza virus, for which a significant number of the population was immunologically naïve [9]. This demonstrated the important role of the avian influenza viruses in the emergence of new reassortants or pandemic viruses in the human population [10].

Around the middle of the twentieth century, epidemiological studies in birds allowed the identification of a milder form of this viral infection. In fact, the first isolate of a low virulent influenza virus was obtained from a chicken in 1949 in Germany [11]. Based on epidemiological and virological studies, it was observed that all the pathogenic viruses were from the H5 and H7 subtypes [12]. Consequently, in 1981 in the “First International Symposium on Avian Influenza”, the most severe forms of disease were officially designated as “highly pathogenic avian influenza”. The milder forms were not designated as “low pathogenicity avian influenza” until 2002 [13,14].

More recently, the importance of the avian influenza virus has been highlighted with the emergence of the H5N1 in 1997, in Asia. This virus consisted of a complete avian influenza virus that can be directly transmitted from birds to people [15]. This outbreak produced much concern regarding the facility of interspecies transmission of the avian influenza virus and its adaptation to a new host [16].

1.1.2. Etiology

1.1.2.1. *Classification and nomenclature*

Avian influenza viruses belong to the *Orthomyxoviridae* family that includes RNA viruses with segmented negative-sense single stranded genome. Viruses of this family are divided into five different genera on the basis of the matrix and nucleocapsid antigens [8], including the type A, B, and C influenza viruses, Isavirus and Thogotovirus [12]. Avian influenza viruses are classified within the type A. This type affects a wide range of bird and mammal species, including humans [12]. Influenza B is related with epidemics of mild respiratory disease in humans, whereas, influenza C viruses cause slight respiratory symptoms in humans but do not produce epidemics. Sporadic cases of infection in animals have been reported for influenza B (seals and ferrets) [17,18] and C (pigs and dogs) [19,20,21].

Influenza A virus are further subtyped, according to the antigenic characteristics of the haemagglutinin (HA) and neuraminidase (NA) surface proteins. At present, 16 HA and 9 NA have been reported [8].

A standard international nomenclature for the designation of influenza virus strains has been established. The naming of the influenza virus includes: 1) antigenic type or genera, 2) host origin, 3) geographical location, 4) strain reference number, 5) year of isolation; and 6) the HA and NA subtypes [12]. For example: A/Chicken/Italy/5093/99 H7N1.

1.1.2.2. *Morphology and molecular organization*

All influenza A viruses are spherical to pleomorphic enveloped viruses of approximately 100nm in diameter that contain segmented, negative sense viral RNA genome (vRNA) [22]. Influenza A virus has eight different gene segments that encode for 11 viral proteins (Figure 1). Three of them, correspond to surface proteins that include the HA, NA, and the membrane ion channel (M2) protein. The internal proteins include the matrix protein (M1), and the core of

viral ribonucleoproteins (vRNP). The core consists of helical vRNP containing vRNA that is wrapped up around the nucleoprotein (NP), and the polymerase complex. This complex is composed of the polymerase acid protein (PA), the polymerase basic protein 1 (PB1), and the polymerase basic protein 2 (PB2). Additionally, some human and avian influenza A virus posses an extra protein, known as PB1-F2 [23]. There are two additional proteins forming the nuclear export protein (NEP). These include, the non-structural protein 1 (NS1) and non-structural protein 2 (NS2) [12,24].

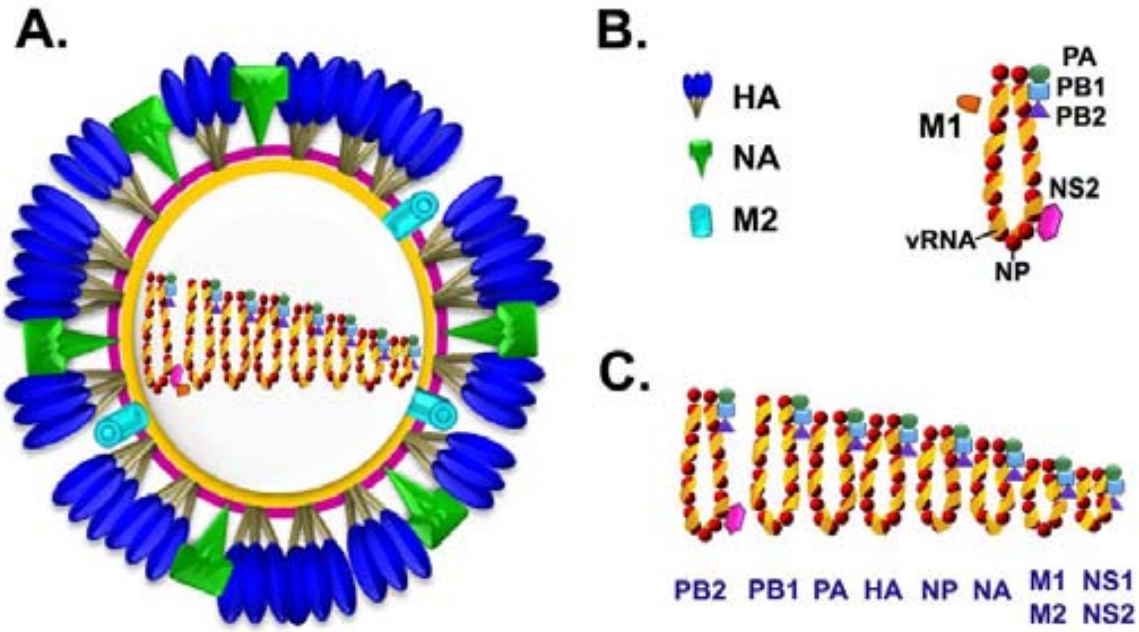

Figure 1. Schematic figure showing the structure of influenza A virus (A). Surface proteins are: the HA, consisting of trimers, NA which forms tetramers and the M2 protein (that is a tetramer which form ion-channels) (B). The M1 protein is found inside the viral membrane and the viral genome which consists of eight negative-stranded RNA segments are packaged into the viral particle as a vRNP in complex with NP and the viral polymerases PA, PB1 and PB2. The eight segments of influenza A virus codify by 11 proteins (B), that are: segment 1 (PB2), segment 2 (PB1 and PB1-F2), segment 3 (PA), segment 4 (HA), segment 5 (NP), segment 6 (NA), segment 7 (M1 and M2) and segment 8 (NS1 and NS2) (Illustration modified from reference [25]).

1.1.2.3. *Replication cycle*

Influenza virus binds to sialic acid (Sia) receptors found in the surface of host cells by means of the HA protein [26]. The Sia receptors are nine-carbon monosaccharides, consisting of *N*-acetylneuraminic (NeuAc) or *N*-glycolylneuraminic (NeuGc) types, and are bound to glycoproteins and glycolipids, by an α-2 linkage [27]. The conformation of this linkage determines the species affinity of the viruses. Thus, avian influenza A viruses show preference by the α-2,3 linkage, whereas, human viruses prefer the α-2,6 linkage [26,28,29]. Once attached, the viral HA has to be cleaved in order to be infectious. The HA cleavage into HA1 and HA2 subunits depends on the presence of host proteases, which allow the virus to enter into the cells by clathrin mediated endocytosis [30,31,32] or macropinocytosis [33]. The HA2 portion mediates the fusion of the virus envelope with the cell membrane, while the HA1 part contains the receptor binding and antigenic sites [34,35]. The cleavage of the HA is induced by the low pH of the endosome that is triggered by the activity of the M2 protein. This protein functions as an ion channel, enabling entry of hydrogen (H+) ions into the virion and consequently, the uncoating of the virus [35,36,37] (Figure 2).

Once the endosomal membrane has fused with the virus membrane, the vRNP can be released into the cytoplasm and transported to the nucleus where replication takes place [38]. This transport is mediated by viral protein's nuclear localization signals (NLSs), which import the vRNP and other viral proteins into the host cell nucleus [39]. In the nucleus, the vRNA is transcribed by the viral RNA-dependent RNA polymerase into two positive-sense RNA species: a messenger RNA (mRNA) and a complementary RNA (cRNA). The cRNA serves as template from which the polymerase transcribes more copies of negative sense, genomic vRNA that will form the virions [31]. Whereas, the mRNA has to be polyadenylated and capped in order to be translated into proteins, in a process knows as "cap snatching", where the virus PB1 and PB2 proteins "steal" 5'capped primers from host pre -mRNA transcripts [31,40]. After that, the mRNA migrates from the nucleus to the cytoplasm, where it

serves as a template for the synthesis of viral proteins using the host cell machinery. Here, the NS1 protein regulates this splicing and the nuclear export of the cellular mRNA, as well as, stimulates the translation [10]. A negative sense small vRNA is also produced which is thought to regulate the switch from transcription to replication [41,42]. Some of the newly synthesized viral proteins are transported to the nucleus where they bind to vRNA to form RNPs. Other newly synthesized viral proteins are processed in the endoplasmic reticulum and the Golgi apparatus where glycosylation occurs (HA, NA, M2). These modified proteins are transported to the cell membrane where they stick in the lipid bilayer. Part of the viral mRNA is spliced by cellular enzymes so that finally viral proteins, such as M1 and NS2, can be synthesized without any further cleavage [31]. At this point, the M1 protein together with the NS2, function as a bridge between the lipid membrane and the viral core of NP, vRNA and the polymerase complex [12,38]. Therefore, the nuclear localization of M1 and NS2 proteins is essential for the migration of the vRNP out of the nucleus and assembly into progeny viral particles in the cytoplasm [38]. Also, the integral membrane proteins HA, NA and M2 proteins are important for virus assembly [43].

Virus assembly is a highly inefficient process, where greater than 90% of the virus particles are non infectious with packing of too few or excessive viral gene segments [44,45]. In the end, the NA which holds a receptor's destroying activity, cleaves the terminal Sia residues of the cell surface glycotopes preventing aggregation and binding of the new viral particles in the cell surface [46,47].

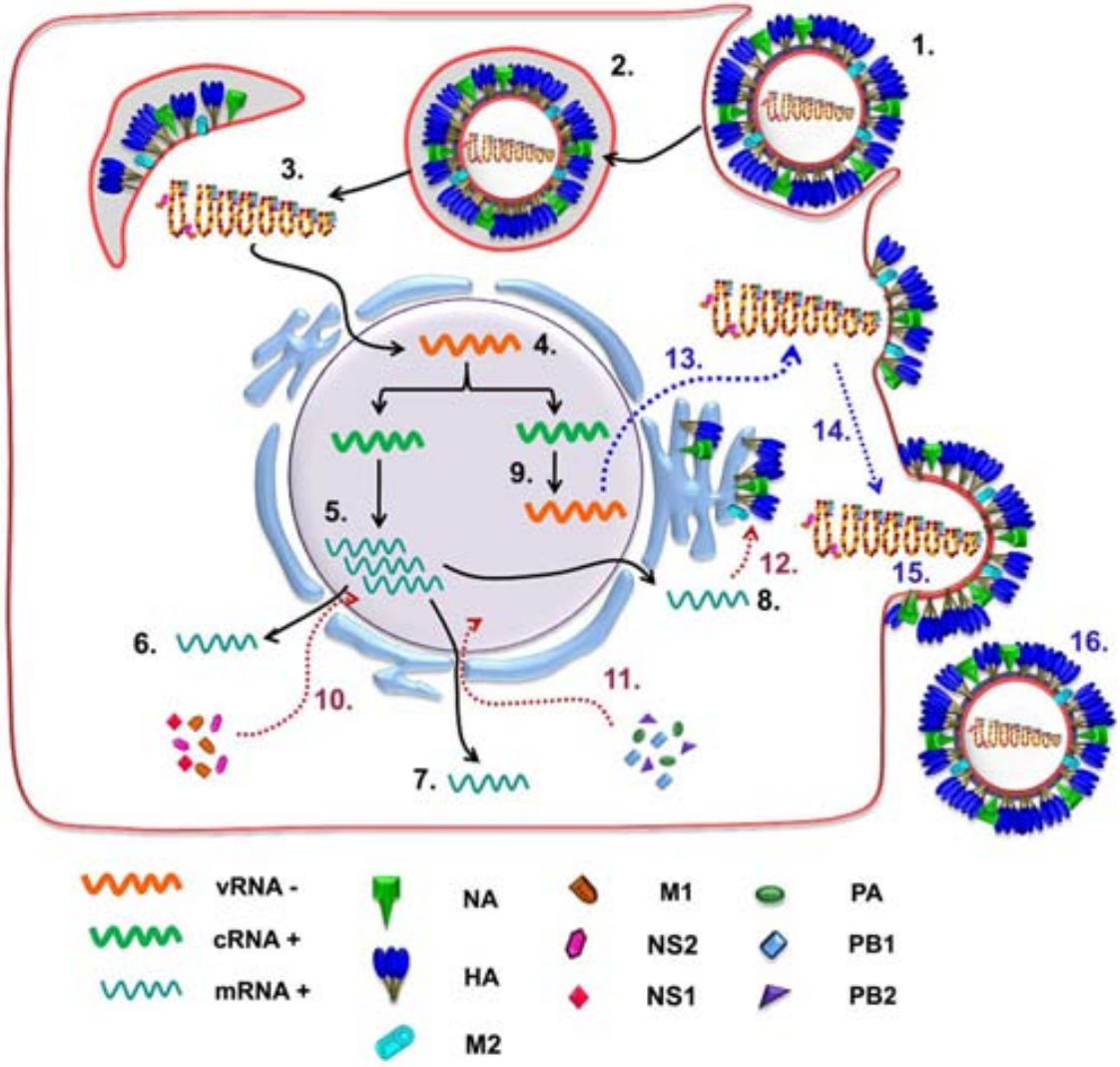

Figure 2. Influenza virus cycle: Binding to Sia receptors and entry into the host cell (1). Endocytosis (2). Fusion after acidification of the endocytic vesicle (3). Entry of vRNPs into the nucleus and release of vRNP complexes (4). The (-strand) vRNA is copied by virion RNA polymerase into mRNA (5). Export of mRNA from the nucleus to the cytoplasm for translation and production of viral proteins (6,7). The mRNA codifing for the viral surface proteins are translated by ribosomes bound to the endoplasmic reticulum (8), where they experience glycosylation (12). The PA, PB1, PB2 and NP proteins are imported into the nucleus (10), where they participate in the synthesis of full length (+) strand RNAs and (-strand) RNA (9). The M1 and NS2 are also transported to the nucleus (11). The M1 binds to the new synthesized (-strand) vRNA, shutting down the viral mRNA synthesis. M1 and NS2 induce the export of progeny nucleocapsids to the cytoplasm (13) and then to the cell surface in regions of the cell membrane containing NA and HA proteins (14, 15). When the assembly is complete, the new virions are bud from the plasma membrane (16) (Illustration modified from references [25,48]).

1.1.2.4. *Antigenic diversity of strains*

Due to the segmented genome of the influenza A virus and the lack of a proofreading mechanism of replication, influenza viruses may experience important changes in their genome giving rise to the vast viral diversity that characterizes this group of viruses. Basically, two mechanisms can provide diversity to the viral population: the changes can be gradually acquired by point mutations (antigenic drift) or they can be acquired by genetic reassortment (antigenic shift). These methods provide the opportunity for the virus to rapidly change and adapt, giving rise to new viruses which could re-infect the same host population or infect new host species [12].

Antigenic drift is mainly caused by the immunological pressure over the HA and NA, which produce great diversity on these genes [12]. The HA molecule is the most frequently affected with antigenic drift, specially the most antigenic sites which are exposed to the immunological pressure. The antigenic variation in a single gene codifying by the HA, cause changes in the structure of the glycoprotein [49,50,51], resulting in a virus strain that can no longer be neutralized by previous host antibodies [31]. This results in viruses which can replicate more efficiently and mutants that are transmitted more easily [12]. The antigenic drift is evidently observed in humans, as a result of the selective pressure imposed by the use of vaccines to protect the population [52]. For this reason, it is necessary to obtain sequence information of the circulating viruses every year to produce effective vaccines [12]. Another clear example of antigenic drift occurs in poultry species, in which viruses that are circulating for long time in the field, evolve increasing their adaption and virulence through mutations in the viral HA by mechanisms such as site mutations, nucleotide insertions and duplications. In the following table is provided a list of virulent viruses for which the mechanism of emergence from low virulent viruses is well documented (the proposed mutational changes in the HA are also given) (Table 1, was taken from Ref [53]).

Avian influenza virus strain: HPAI virus	LPAI virus precursor	Proposed genetic change in the HA cleavage site	Likely molecular mechanism
A/chicken/Pennsylvania/ 1370/83 H5N2	A/chicken/Pennsylvania/21 525/83 H5N2	(PQRETR*G)→PQRKKR*G (+loss of CHO)	Site mutation
A/turkey/Ontario/7732/ 66 H5N9	A/turkey/Ontario/6213/ 66 H5N9	(PQRETR*G)→ PQRRKKR*G	Accumulated single nucleotide insertions
A/chicken/Jalisco/14588-660/94 H5N2	A/chicken/Quetaro/7653/95 H5N2	(PQRETR*G)→ PQRKRKRKR*G	Tandem duplication/ insertion
A/chicken/Chile/176822/ 02 H7N3	A/chicken/Chile/4977/ 02 H7N3	(PEKPKTR*G)→ PEKPKTCSPLSRCRETR*G	RNA/RNA recombinant

Table1. Examples of antigenic drift events observed in poultry and proposed genetic changes in the HA cleavage site.

On the other hand, the **antigenic shift** is the reassortment of genes from two different influenza virus subtypes that infect a single cell or host, resulting in a virus with new antigenic proteins [31]. Also, the transfer of a whole virus from one host species to another and the reemergence of previously non circulating virus strain are considered an antigenic shift. Usually, when shifted viruses emerge, they rapidly spread among the population due to the lack of previous protective immunity, causing severe outbreaks or pandemics, such as the 1957 (H2N2) and 1968 (H3N2) pandemics in humans, caused by viruses that emerged by reassortment and acquisition of a new HA [12].

1.1.2.5. *Viral pathotypes*

The pathogenicity of all influenza virus depends of the presence of a precise combination of genes which provide to each virus strain with advantageous conditions in which to replicate, within a specific host [16]. In poultry species, the avian influenza viruses cause a range of clinical presentations that goes from asymptomatic to a severe acute systemic disease with mortality rates that can reach up to 100% [54].

Based on their ability to cause disease the avian influenza viruses can be classified into two groups: **low pathogenic avian influenza** (LPAI) and **high**

pathogenic avian influenza (HPAI) viruses. This difference is mainly determined by the mutations of the most variable region of the virus (HA gene), which allow the virus to have multiple replication cycles and produce infection. Specifically, the virulence is linked to the presence of multiple basic amino acids (arginine (R) or lysine (K)) in the HA cleavage site. As a result, most LPAI viruses show only a basic amino acid (monobasic) in its HA cleavage site, whereas, the HPAI viruses acquire an increased number of basic amino acids (R or K) in their proteolytic cleavage site [54] (see table above). As a consequence, the LPAI viruses can only be cleaved by trypsin-like proteases produced by the epithelial cell of the respiratory and gastrointestinal tract. Therefore, these viruses cause only mild symptoms restricted to these organs [55,56,57,58,59,60,61]. In contrast, the presence of multibasic cleavage sites in the HA of HPAI viruses make them more accessible to ubiquitous proteases of the furin enzyme family [34,58,62,63,64]. This differential cleavage of the HA in HPAI viruses allow their replication in a larger number of tissues, including brain, heart, pancreas, adrenal gland and kidney, among others [12], causing an extremely severe systemic disease with high fatality rates [12,14]. This characteristic is only present in viruses of H5 and H7 subtypes, although most of H5 and H7 subtype viruses are of low virulence [14].

It is also worth mentioning that viruses of these subtypes have been able to infect humans, causing severe and fatal infections such as the reported with the Asian HPAI virus H5N1, and flu-like symptoms and conjunctivitis as with H7 viruses [65].

In view of the fact that HPAI viruses emerge from LPAI viruses and their relevance in animal and human health, all HPAI viruses and LPAI viruses of H5 and H7 subtypes, have been classified as notifiable avian influenza (NAI) viruses by the World Organization for Animal Health (OIE) [13].

The OIE has dictated standard or official criteria to confirm the detection of these NAI viruses. This criteria is based on an *in-vivo* test and also on the molecular determination of the cleavage site of the HA. The *in-vivo* test involves

the inoculation of a minimum of eight susceptible 4- to 8-week-old chickens with an infectious virus. Strains are considered to be HPAI virus isolates if they cause more than 75% mortality within 10 days or have an intravenous pathogenicity index (IVPI) greater than 1.2. All HPAI virus isolates accomplishing this criteria, as well as, H5 or H7 viruses with an amino acid sequence in the HA cleavage site similar to any of those that have been observed in virulent viruses are identified as notifiable HPAI (HPNAI) viruses. H5 and H7 isolates that are not pathogenic for chickens and do not have multiple basic amino acids in the HA cleavage site are identified as notifiable LPAI (LPNAI) viruses [13].

1.1.3. Epidemiology

1.1.3.1. *Host range*

Influenza A virus infect a wide range of avian and mammal species, including humans [66] (Figure 3). Phylogenetic studies have made possible to identify lineages that are species-specific and others that are shared by different species. By means of these studies, it was possible to confirm that all influenza viruses come from aquatic birds, in which the viruses have achieved an evolutionary stasis and are optimally adapted, demonstrated by the low mutation rate [66,67,68]. In these birds it is possible to find all the 16 HA and 9 neuraminidase subtypes [69]. The range of wild birds infected is not completely known, but influenza A viruses have been reported in free-living birds from more than 100 species in 12 avian orders [68,70,71]. However, epidemiological studies indicate that the most consistently infected are birds from the Anseriformes and Charadriiformes orders. Anseriformes birds include ducks, geese, swans, although the most frequently infected are dabbling ducks, such as mallards, pintails, and teals. Charadriiformes birds, such as, shorebirds, terns and gulls, are less commonly infected [12,68]. In waterfowl, influenza viruses replicate preferentially in the intestinal tract, where high titers of virus are produced and disseminated in the environment [72,73,74].

In contrast, the number of virus subtypes found in mammals are limited [10]. This is mainly due to the requirement of long periods of time needed for host adaptation and to become endemic in the population. In general, influenza A viruses could cause infections in mammals in three situations: 1) endemic or enzootic infections caused by host adapted viruses, such as swine, equine and human influenza virus strains, and more recently the canine influenza A virus, 2) epizootic infections, such as the cases of infection with LPAI viruses of poultry origin which affected a large number of minks, seals, whales, and some pig and humans, and 3) sporadic infections, such as the recent cases of infection with the H5N1 HPAI virus, which promptly affected tigers, leopards, house cats, dogs, civets, stone martins, pigs and humans [75].

Endemic influenza A virus infections that have became established in humans, emerge from the reassortment of avian influenza viruses and host adapted influenza A viruses. At present, three HA and two NA subtypes are circulating in humans (H1, H2, H3, N1 and N2). Sporadically, avian influenza viruses of the H5, H7, and H9 subtype have been transmitted from birds to humans, causing disease and also mortality [15,65,76,77,78,79,80,81]. In horses, the classic influenza A virus strain is the H7N7 subtype, although the most common nowadays is the H3N8 subtype, which was first reported in the early 1950s [82,83]. In dogs, the H3N8 subtype has become the predominant after its first appearance in the early 2000s, when it was detected in racing greyhounds [84,85,86,87]. Regarding pigs, it was observed that under experimental conditions they can support the replication of all avian influenza virus subtypes. However, in nature, only the H1, H3, N1 and N2 subtypes, have been isolated [88]. Occasionally, self limiting infections with H1N7, H4N6, and H9N2 LPAI viruses have been reported in swine [89,90]. The possibility of direct contact with humans and birds, and their susceptibility to avian and human viruses have led to them being considered as “mixing vessels”, where genetic reassortment can take place [91]. Likewise, viruses genetically and antigenically related to avian viruses have been isolated from minks (H10N4 and H10N7) [92,93], seals (H7N7, H4N5, H3) [94,95,96,97] and whales (H1N1, H13N2, H13N9) [97,98].

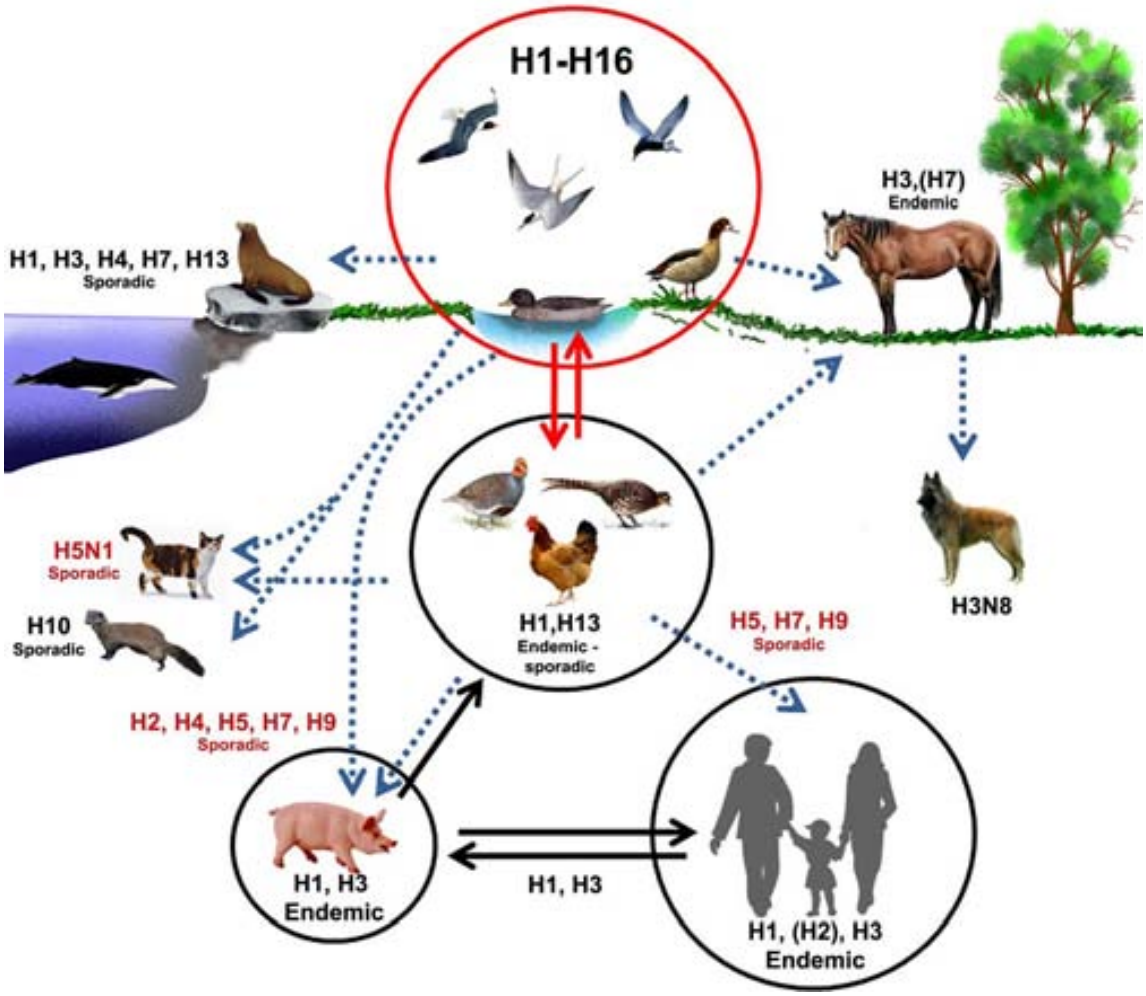

Figure 3. Host range. Wild aquatic birds are the reservoir for all influenza A virus, which are transmitted to poultry species, and occasionally to pigs, horses, sea mammals. Rarely, wild birds or poultry transmits influenza A viruses to cats or minks. Pig viruses could be transmitted to humans (and vice versa) and sporadically poultry species transmit influenza viruses to humans (Dashed lines indicate sporadic and rare transmission of influenza A virus between species) (Illustration modified from Ref [54])

Regarding poultry species, Influenza A virus can infect: chickens (*Gallus domesticus*), turkeys (*Meleagris gallopavo*), Japanese quails (*Coturnix coturnix japonicas*), Bobwhite quails (*Colinus virginianus*), pearl guineafowls (*Numida meleagris*), ring-neck pheasants (*Phasianus colchicus*), chukar partridges (*Alectoris chukar*) and zebra finches (*Taeniopygia guttata*). From these species, turkeys and chickens are the most frequently affected by disease outbreaks [10].

1.1.3.2. *Transmission and shedding*

Transmission of influenza A virus is a very complex process that depends on the virus strain, the species of bird, and environmental factors. The exact mechanism that allows an influenza virus to cross the interspecies barrier causing infection in another species is still poorly understood [99].

It is known that wild aquatic birds (waterfowl and shorebirds) are the reservoir of influenza A viruses, which is effectively disseminated through faecal/oral route [66,70,100]. As the virus mainly replicates in the intestinal tract, a high concentration of infectious virus could be excreted in their faeces which enable to perpetuate the influenza virus in their habitats and the nearest zones of poultry and swine production [74,101]. Experimentally, it has been observed that waterfowl birds, such as Muscovy ducks (*Cairina moschata*) can shed an estimated $1x10^{10}$ mean 50% embryo infectious doses (EID_{50}) of avian influenza viruses within a 24-hour period [101]. Besides, prolonged viral shedding has been demonstrated in some wild birds, such as Pekin ducks which are able to shed virus for more than 28 days [70]. Also, the ability of influenza virus to persist in water for long periods of time (6 months) provide an environmental reservoir [68,102,103], because, the contaminated water may result in faecal/oral or faecal/cloacal transmission. Then, it is thought that the virus is maintained in the wild bird population and is carried long distances by migratory movements of these birds which could be naturally resistant to disease [68,102,103]. How this virus is maintained in nature has still to be determined [103].

Transmission of avian influenza viruses from wild birds to poultry depends on several factors, being some of the most important the level of biosecurity and the concentration of poultry around the zone of initial outbreak [99]. The introduction of viruses to the poultry population can occur by five different means: 1) direct exposure to avian influenza infected wild birds, 2) exposure to equipment or materials that are contaminated with infectious respiratory secretions or faeces, 3) movement of people who carry the virus in

their shoes and clothes, 4) contaminated water and 5) windborne spreading of the virus [75]. The transmission of viruses from wild bird species to domestic birds was until recently sporadic. Also, the introduction of LPAI viruses of H5 and H7 subtype in poultry leading to mutations and emergence of more virulent viruses is occasional [99].

As it is difficult to determine when chickens infected naturally with LPAI and HPAI viruses start to shed the virus, most of the data regarding viral shedding comes from experimental infections [104]. Hence, chickens inoculated with LPAI viruses by intranasally, intraoral and intratracheal routes can shed virus in the faeces and respiratory secretions [105,106,107]. The onset of the detection of virus shedding depends mainly on the virus strain [108]. In this manner, the onset of the LPAI viral shedding in the faeces can be as early as day 2 dpi [105,106,107] and in respiratory secretions 1 dpi [106,109]. The virus strain also determines the site of replication and how the virus will be shed. Accordingly, most of the studies have found that at least occasionally, the LPAI viruses are shed by both routes [106,107,108,109,110]. LPAI viruses have not been detected in meat, and then the risk of dissemination from this source is considered minimum [104]. Likewise, LPAI viruses are rarely recovered from eggs in spite of the fact that some LPAI viruses replicate in reproductive organs, causing salpingitis and oophoritis [107,109,111,112,113,114]. However, it is considered that eggs can be contaminated with ovarian tissues and that also faecal contamination of the shell can occur in infected flocks [104].

HPAI viruses are shed by faeces and respiratory secretions in chickens, in which viruses can be detected at 1 and 2 dpi under experimental conditions [106,110,112,115,116,117,118]. Moreover, HPAI viruses cause systemic infections, and the virus can be detected in meat in the first or second dpi [106,116,118,119,120]. Although the isolation of HPAI viruses from meat in natural infections has not been reported in poultry species, the Asian HPAI virus H5N1 has been isolated from meat samples in naturally infected ducks [121,122]. HPAI viruses have been isolated at 3 dpi from egg yolk and albumin in birds intranasally inoculated with H5N2 HPAI viruses [123,124], however,

other HPAI viruses cannot be isolated from this sample or from dead embryos and live chicks that hatched [104]. Then, although viruses are found in gonads [125], it is considered that the main source of contamination of eggs are the infective faeces [104].

Once within the flock, the transmission of the virus will depends on several factors that include the bird's breed, age, presence of previous immunity to influenza viruses, concurrent infections and environmental factors such as the stocking density, size of the room, temperature, and airflow [110,126]. For example, it is known that the transmission of the virus occur more slowly in caged flocks (birds separated in cages) than in loose-housed flocks (flocks housed without barriers between birds) as demonstrated during H5N1 and H7 HPAI viruses outbreaks [111,127,128,129] and in experimental models of transmission [130,131]. Besides, some experimental studies indicated that certain viral strains need close contact of the naïve birds with infected birds or faeces for transmission [81,117]. In contrast, other viruses spread rapidly by contact or air borne transmission to the nearest cages [105,132]. For example, the Asian H5N1 HPAI viruses are preferentially transmitted from the respiratory route, requiring the direct contact among birds to be disseminated [133,134,135,136]. In general, as the HPAI viruses cause death rapidly after the infection in poultry species, it is considered that proportionally little quantities of virus particles could be excreted during the course of the infection [99,110,126,137]. For example, the Mexican H5N2 LPAI virus (A/chicken/Mexico/26654-1374/94) was not lethal for chickens and spread efficiently by contact and airborne transmission in caged flocks, whereas, the more virulent strains could not be isolated from uninoculated chickens sharing the same cage [105].

1.1.4. Clinical signs

In poultry species, **LPAI** viruses cause mild to inapparent clinical signs with high morbidity (50%) but low mortality (5%), which could increase in the case of secondary bacterial infections [54]. There are few studies in the literature describing the onset of clinical signs in chickens infected with LPAI viruses [104]. In experimental conditions, chickens inoculated intranasally with A/chicken/Pennsylvania/83 (H5N2) and A/chicken/Chile/176822/02 (H7N3) started to show clinical signs at 5 and 4 days post inoculation (dpi), respectively [118]. The signs of disease basically consisted of coughing, sneezing, rales and excessive lacrimation. Signs of decreased egg production and broodiness could be seen in infected active layers and breeders. Unspecific clinical signs of huddling, ruffled feather, listlessness, decreased activity, decreased feed and water consumption, and diarrhoea could also be distinguished [14,54].

Regarding **HPAI** viruses, its incubation period cannot be determined in the field, because chickens are frequently found dead during the outbreaks and show few preceding signs. Moreover, the clinical signs are unspecific and their frequency and type varies with the virus strain [12,104,138]. In experimental studies, chickens start to show clinical signs from 1 to 5 dpi [119,120,139].

HPAI virus infections cause high morbidity and mortality that can affect 100% of the flock. The clinical presentation mainly depends on the HPAI virus strain and species of bird affected. Generally speaking, there are two phases of infection: a peracute phase that is observed in the first hours post infection (hpi), when birds are found dead without showing clinical signs. Birds that survive for 3 to 7 dpi, experience a second or acute phase, when severe signs of central nervous dysfunction can be observed: tremors and incoordination, inability to stand, loss of balance and recumbency with pedaling movements, paresis, paralysis of the legs and wings, shaking of the head with abnormal gait, torticollis, opisthotonus, nystagmus, excitation, convulsions, rolling and circling movements, flapping movements of the wings and unusual position of the head and wings. However, not all HPAI virus strains produce neurological

signs. In this acute phase, it is also frequent to see less specific clinical signs, such as: listlessness, reduced activity, low feed and water intake, reduced sensitivity to stimuli and dehydration. Besides, infected birds can be found in recumbency or in a comatose state. Diarrhoea can also occur, as bile and urate loose droppings intermixed with mucus. Also, HPAI virus could cause respiratory signs such as rales, sneezing, coughing, and excessive lacrimation [54].

1.1.5. Gross and microscopic lesions

In poultry, **LPAI viruses** cause rhinitis and sinusitis that vary in character from catarrhal, fibrinous to fibrinopurulent. The presence of purulent exudates is associated with secondary bacterial infections [12]. The trachea usually show oedema, congestion, and occasionally haemorrhage and presence of serous to caseous exudates in the lumen. What's more, when associated with bacterial infection, fibrinopurulent bronchopneumonia could be present. Air sacculitis or coelomitis of catarrhal, fibrinous of fibrinopurulent character could be found. Lesions in the reproductive tract in adult birds include regression of the ovaries, with presence of haemorrhages in the large follicles progressing to colliquation and egg yolk peritonitis. Besides, catarrhal to fibrinous salpingitis can also be seen. The eggs are fragile, misshapened, and show loss of pigment. In turkeys, it is possible to observe fibrinous enteritis, typhlitis, proctitis, and paleness in the pancreas [54].

Regarding microscopic lesions, LPAI viruses produce heterophilic to lymphocytic tracheitis, bronchitis and ventromedial fibrinocellular to peribronchiolar lymphocytic pneumonia. Rarely, pancreatic acinar necrosis is observed, as reported in turkeys infected with a H7N1 LPAI virus in Italy during the 1999 outbreak [111,140,141]. Chickens that die from LPAI virus infections show lymphocyte depletion and necrosis of lymphocytes in the bursa of Fabricius, thymus, spleen and in lymphoid associated tissues [54]. Viral antigen is commonly detected in respiratory epithelium [14,142], renal tubule

epithelium, pancreatic parenchyma, intestinal epithelium [142] and rarely in lymphocytes [14].

Lesions observed in gallinaceous birds infected with **HPAI virus** reflect the clinical presentation of the disease. Consequently birds that die in the peracute phase may not show gross lesions. Whereas, birds in the acute stage generally show ruffled feathers, sinusitis, oedema of the head, face, upper neck, and legs, which may be associated with petechial to ecchymotic haemorrhages in the unfeathered skin of the comb, wattles and legs. The presence of cyanosis, petechial to ecchymotic haemorrhages and necrotic foci in the comb and wattles is considered syndromic of a HPAI virus infection. Lesions in internal organs vary with the strain, but generally include: haemorrhages in the coronary fat and epicardium, pectoral muscle, and on the serosa and mucosa of the proventriculus and ventriculus. More rarely, haemorrhages are found on the inner surface of the sternum, cecal tonsils, and Meckel's diverticulum [54]. The finding of multifocal areas of necrosis in the pancreas is common [12,108,118,119]. In layer hens, breeders and turkeys, the presence of free yolk in the coelomic cavity as a result of the rupture of ova has been reported [54,138]. Necrotic foci have been frequently reported in the heart, kidney and liver of chickens, pheasants, Chukar partridges, and turkeys [108,119]. Urate deposition in the kidneys is seen in association with kidney lesions. The lung may show congestion and haemorrhage [118,119,138]. In young birds, the thymus and the bursa of Fabricius may be atrophic and show haemorrhages [118]. Additionally, the spleen may become enlarged showing pale necrotic foci in the parenchyma [54].

Microscopic lesions in chickens infected with HPAI virus vary with individual virus strains, breed of the chicken, inoculum dose, route of inoculation, and passage history of the virus. In agreement with the clinical presentation and gross lesions, birds in the peracute stage may not show any microscopic lesion, and show only mild and multifocal presence of viral antigen in vascular endothelial cells and cardiac myocytes demonstrable by immunohistochemistry (IHC). On the contrary, birds in the acute phase show

lesions in multiple tissues and organs [54]: skin, brain, heart, pancreas, adrenal glands, lungs, and primary and secondary lymphoid organs [14,119,138,143] (Figure 4).

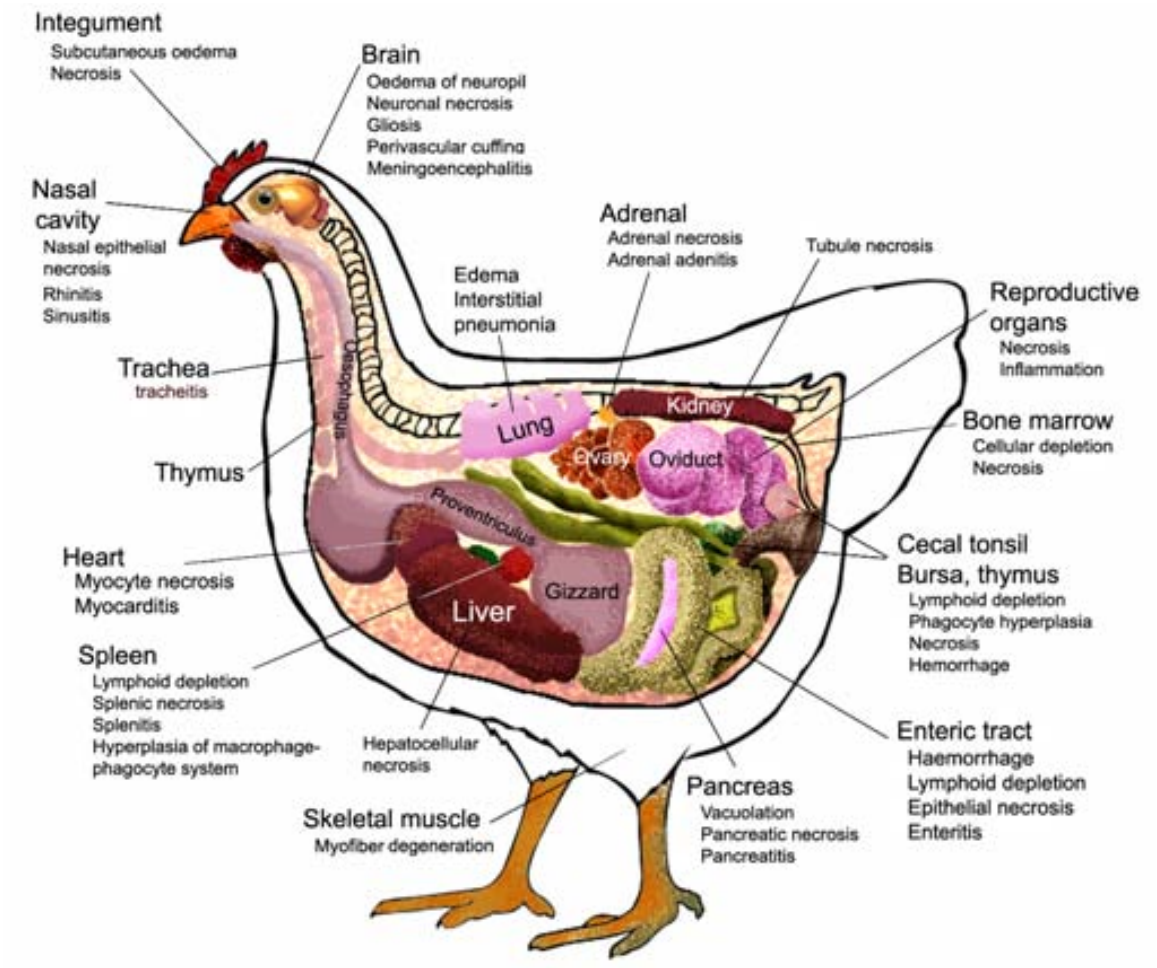

Figure 4. Schematic image summarizing the main histological lesions observed in HPAI virus infected birds (Information taken from Ref [54]).

Although the presence of microscopic lesions in the brain of HPAI virus infected birds is common [108,125,135,144,145,146,147,148,149,150], few studies have described in detail the neuropathogenesis of this infection. In general, the neuropathological lesions induced by HPAI viruses may be divided in two types or phases according to its presentation: 1) the acute necrotizing encephalopathy, or non-suppurative encephalitis that occurs within the first 3 dpi, characterized by disseminated vascular degeneration, microgliosis and

necrosis of the brain parenchyma, and 2) the ventriculitis and periventriculitis that occurs between 4 and 7 dpi, and involve degeneration, vasculitis and mild mononuclear infiltration around the brain vessels. Ventriculitis and periventricular inflammation with necrosis is also observed in this phase, but the mechanism through which it is developed has not been clarified [111,118,127,136,138,144,149,150,151,152,153,154]. Another form of HPAI virus infection in the CNS is observed in wild birds, in which there is no evidence of vascular damage, or viral antigen on endothelial cells either [155]. A summary of the wild bird species suffering CNS influenza virus-associated lesions is provided in annex 1.

1.1.6. Pathogenesis

To cause disease, influenza viruses have to be efficiently shed (by faeces and fomites), find the adequate attachment site and be able to replicate into the target cells of the new host. In poultry species, the nasal cavity is the main site of replication of the LPAI viruses. There, the virus replicates and is released, infecting other cells in the respiratory and intestinal tract [14,138]. Consequently, the signs observed in the affected birds are commonly associated with respiratory damage, especially when there are bacterial or viral concomitant infections. Occasionally, LPAI viruses spread systemically, replicating in tissues containing trypsin-like proteases, such as kidney tubules, pancreatic acinar epithelium, and other organs [14,138].

Regarding the HPAI viruses, the initial site of replication in poultry is also the epithelium of the nasal cavity, where it is possible to detect viral particles at 16 hours post exposure [138]. In the nasal cavity, the virus replicates in the epithelial cells causing ulceration and inflammation with presence of virus in submucosal macrophages, heterophils and capillary endothelial cells [14,138]. The macrophage and heterophil are important cells for the initial replication and dissemination of HPAI viruses [54]. The virus replicates in endothelial cells, spreads through the vascular system and infects a variety of cell types within

visceral organs, brain and skin. This initial visceral replication can be detected as early as 24 hpi, with the peak of virus load and lesions being at 48 hpi [54,138]. However, there are HPAI viruses which cause viraemia and extensive parenchymal damage with replication, without producing extensive replication in vascular endothelial cells. HPAI viruses produce damage by means of three possible mechanisms: 1) direct replication of the virus in cells, tissues and organs, 2) indirect production of cellular mediators, such as cytokines, and 3) ischemia from vascular thrombosis. Clinical signs and death are consequence of multiorgan failure [14].

1.1.7. Diagnosis

Several techniques have been developed to offer an accurate diagnose when infection with a LPAI or HPAI viruses is suspected. Besides these, there are a series of techniques used to characterize the virus and study the pathogenesis of the disease. Below is a list of well established methods for the purpose of diagnosis and study of the virus infection.

1. ***Virus isolation (VI):*** is the reference standard method to confirm the presence of avian influenza virus. The VI is performed in embryonated chicken eggs (9-11 days of incubation), and in culture cells of avian origin, Madin-Darby canine kidney (MDCK) cells, or other cell lines. This is considered the most sensitive method in the diagnosis of avian influenza viruses. However, their main inconvenience is that not all influenza viruses grow well in chicken eggs and other viruses, such as paramixoviruses, do grow. The VI is not commonly used for routine diagnosis because it is expensive and time-consuming [156]. The results of the VI have to be tested for the presence of haemagglutinating antigen and the result confirmed by molecular techniques, agar gel immunodiffusion (AGID) assay for detection of the nucleocapsid or matrix antigens or commercial immunoassay kits for detection of the nucleocapsid or neuraminidase of type A influenza [157].

2. ***Haemagglutination assay (HAa):*** is used to test the results obtained during the VI, however it is not an identification assay because other agents can produce haemagglutination. The assay is based on the ability of influenza virus to bind to Sia receptors found on erythrocytes, that when combined cause agglutination producing a diffuse lattice [158]. Due to the low sensitivity of this thechnique, it is generally used after passage of the virus into chicken eggs. Because, it is necessary 10^5-10^6 50% EID_{50}/mL for the detection of a virus by HAa [159]. Another disadvantage is that degraded and inactivated non-infectious virus particles are also detected with this test [158].

3. ***Agar immunodiffusion test (AGID):*** is used to confirm the results of the VI and HAa assays by means of the detection of the nucleocapsid-rich samples of type A influenza viruses, as well as, to detect the presence of antibodies. The first is performed using agar plates and a reference antiserum. The sample consists of antigen obtained from chorioallantoic membranes. The detection of antibodies is performed using the M1 or vRNP proteins as antigens. The main disadvantage of the AGID test is the low sensitivity [13].

4. ***Haemagglutination (HI) and neuraminidase inhibition (NI) assays for subtyping*****:** are quantitative methods used for classification and subtyping of the influenza A viruses. The HI is performed using subtype specific antibodies (polyclonal antisera) against the 16 HA subtypes [156,160]. Whereas, the NI assay is based in the inhibition of the viral enzymatic activity of the NA on the N-acetyl neuraminic acid (NANA) using specific antibodies against the 9 NA subtypes [160,161]. Both methods, the HI and NI assay or its modification, the micro-NI, are inexpensive and fast, however, requires an extensive number of reference reagents to identify antigenically all the distinct subtypes [160,162].

5. ***Immunohistochemistry (IHC) and immunofluorescence (IF) staining:*** are based in the demonstration of the presence of influenza A viral antigen

in tissue samples using labelled polyclonal and monoclonal antibodies. The reaction is visualized by the deposition of a chromogen or detecting the presence of fluorochrome in the nucleus or cytoplasm of infected cells. Both methods are used to study the pathogenesis of the avian influenza by allowing the identification of sites of replication in the infected tissues. Moreover, the IHC enable to make correlations between presence of virus and the histopathological lesions caused during the infection [163].

6. ***In situ hibridization technique (ISH):*** used to detect the sites of virus replication in tissues of infected birds using radiolabelled or non-radiolabelled probes. Similar to the IHC, the ISH is useful to study the mechanism of pathogenesis of influenza A virus [164,165]. The ISH is a time-consuming and expensive technique, that additionally require especial care because as the probes are basically labelled RNA [165], they are very prone to degradation [166].

7. ***Molecular techniques (multiplex-polymerase chain reaction (PCR), reverse-transcription-PCR (RT-PCR) and real-time RT-PCR):*** are based in the detection of the viral RNA from culture fluids, swabs or tissue specimens. To detect the viral RNA, first it has to be reversed transcribed to cDNA using a primer complementary to the 3'end of all influenza viral RNA or a sequence specific primer. In the multiplex PCR more than one primer is included in the amplification reaction, then more than one gene or genome segment of the virus is detected [167]. All these methods enable the rapid detection of viral genomic nucleic acid sequences in a short period of time, obtaining also highly sensitive and specific results [156,168,169,170], being comparable to virus isolation procedures. In particular, the *real-time RT-PCR* enables us to quantify the amount of viral RNA [170]. Furthermore, the *real-time RT-PCR* is also used to confirm the presence of H5 or H7 subtype influenza virus using H5- or H7-specific primers [171].

1.1.8. Control and prevention

The goals to control the emergence of avian influenza virus include measures at the following levels: 1) prevention, 2) management, and 3) eradication. To accomplish these objectives each individual country has developed a specific plan adapted to its actual conditions. The plan or strategy involved procedures at the level of: 1) education, 2) biosecurity, 3) diagnostics and surveillance, 4) elimination of infected poultry and 5) decrease the susceptibility of the host [172].

In developed countries, the development of rapid diagnostic test and the effective application of the five components of the control strategy above mentioned, usually enables a rapid response and control of outbreaks. In these countries, HPAI virus outbreaks can be erradicated within a period of few months to a year by means of stamping-out programs. Besides, it has also been possible to implement these types of measures for the eradication of LPAI H5 and H7 viruses, as a means to prevent the emergence of HPAI viruses. In contrast, in developing countries, the lack of indemnities, poor veterinary infrastructure, and high level of poultry production at a rural level, made the eradication unachievable in most cases [173].

Sporadically, vaccination has been used to contain the spread of HPAI viruses and H5/H7 LPAI virus outbreaks, mainly in developing countries [14,172,173], as the more realistic form to manage the disease. Vaccination is directed at decreasing the susceptibility of the host, preventing clinical signs and mortality or to protect from the infection. Protection conferred by the vaccine depends on: 1) the dose of challenge virus, 2) content of the target antigen in the vaccine (HA in the inactivated vaccines) or titer (high titer confers best protection), 3) adjuvants which help in the production of robust and long lasting immunes responses, 4) genetic similarity between the vaccine antigen (HA) and the field viruses, 5) length of protection which can be achieved with high doses of antigen or high titers or by multiple vaccinations, 6) route of administration (*in ovo*, drinking water, spray, topical or parenteral

administration) depends on the kind of vaccine and recommendations of the manufacturer, 7) species of birds and number of vaccinations, 8) age of vaccination (optimal age in most birds is after 2 weeks of age), 9) Field and farm conditions, which could reduce the effectiveness of the vaccine, such as presence of concomitant diseases, vaccine storage and transport problems, etc [174].

Multiple vaccines have been developed that include:

1. ***Live LPAI virus vaccines:*** have been experimentally used in poultry, and consist of LPAI viruses that are used to provide rapid protection against HPAI viruses of the same subtype. However, these are not recommended in field conditions because they may produce important economical losses associated with the induction of LPAI virus signs of infection. Besides, they can easily spread among birds and from farm to farm, and can also reverts to HPAI virus [174].

2. ***Inactivated whole avian virus vaccines:*** are the most widely used in humans and domestic animals. These vaccines consist of influenza viruses that are grown and later inactivated by chemical or physical methods [175]. The selection of the influenza vaccine strain in poultry species depend on the circulating field strain, and can be either from the same HA and NA that the field strain (homologous) or the same HA but different NA (heterologous). Both provide protection, nevertheless, the homologous vaccines are discouraged due concerns regarding biosecurity and biosafety. Disadvantages of this type of vaccines include the requirement of high antigen quantities and the necessity to use adjuvants to enhance the immunity [174,175,176].

3. ***Vaccines generated by reverse genetics:*** these are inactivated or live attenuated vaccines containing the HA and NA of circulating viruses from which the “dangerous part” has been removed [177]. These vaccines are produced by mixing the 6 plasmid DNA from a good-growing laboratory

strain with the HA and NA obtained by cloning relevant genes from currently circulating viruses. The main advantage of this type of technology is that allows us to convert HPAI virus into LPAI vaccines by mutating the HA cleavage site. However, the requirement of several doses and large quantities of nucleic acid per dose to produce immunity make the use of these vaccines non-viable in poultry [175].

4. ***Live vectored vaccines:*** are generated by recombinant DNA technologies to incorporate genetic material of an influenza virus into a viral backbone, such as poxvirus, adenovirus, herpesvirus, and paramyxovirus. These vaccines replicate in the host providing similar immune protection than a live vaccine, however, they can induce immunity against the vector itself and interfere with other vaccines [174].

5. ***DNA-based vaccines:*** consist of the inoculation of a plasmid DNA which confers protection by means of induction of the expression of an immunogen or proteins in the host, resulting in stimulation of both humoral and cellular immune responses. The DNA vaccines have the potential to protect against different antigenic variants and reduce divergence of mutants, also they are easy to manufacture. As it is a technology that is in development, several issues still have to be addressed, such as if the injected DNA may randomly integrate into the host genome, which is the immune response generated against the injected DNA and if there is induction of tolerance [178].

6. ***Synthetic peptide vaccines****:* consist of portions of influenza proteins that are chemically synthesized and formulated into a vaccine to stimulate a protective immune response in the host. The main advantage of this type of vaccine is that they are not growth in eggs or cell culture. The disadvantage of the vaccines produce with this technology is that the peptide alone stimulates a very weak immune response; however, this can be improved using adjuvants or another method of delivering the peptide to the immune cells.

1.2. Particularities of the central nervous system (CNS) in birds.

The general structure of the avian CNS and their functions show similarities to the mammalian brain, however they have differences that are important to know in order to understand the mechanism of neuroinvasion used by different infectious agents. As this knowledge is important to understand the neuropathogenesis and the mechanism of neuroinvasion of the H7N1 HPAI, in this section a brief description with the most relevant differences and the homologies between birds and mammals is provided.

The CNS of birds has essentially the same pattern of histogenetic parts observed in mammals. However, similarities between birds and mammals are not so manifest in the forebrain, particularly in the histological structure of telencephalon. In mammals, neural cells in the telencephalon are arranged in a particular disposition of six layers forming a laminar rind called neocortex [179,180]. In contrast, the avian telencephalon consists of uniformly distributed neurons whose dendritic trees are organized radially in nuclei. In spite of this, the avian *pallium* is as large as the mammalian *pallium* and most of its subcomponents are similar to neocortex with regards to their connectivity and histochemical characteristics [181]. For example, the prefrontal cortex of mammals which is associated with complex cognitive abilities has its homologous structure in the *nidopallium caudolaterale* of birds, as evidenced by the presence of dopaminergic innervations and the similarities in the interconnected pathways [182,183,184]. With respect to all other brain regions, both vertebrate classes demonstrate easily traceable homologies, but in some cases there are variations in proportions and location of brain structures, such as the “optic lobe” or *optic tectum* that has its homolog in the mammalial *superior colliculus*. However, as the *optic tectum* is larger than its equivalent in mammals, it modifies the shape of the ventricular cavity forming the lateral recess of the aqueduct [185] .

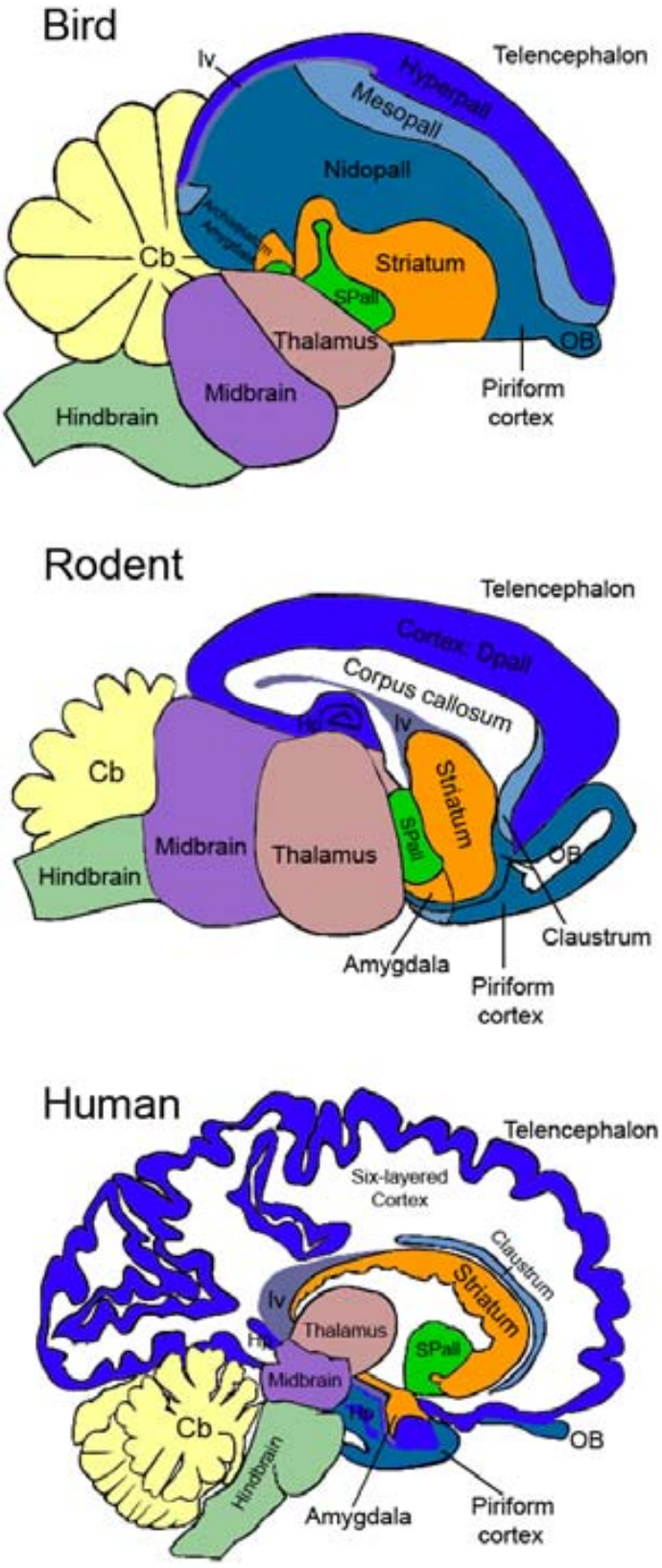

Figure 5. Schema representing the differences in structure and distribution of the different regions in the brain of birds, rodents and humans (Illustration modified from [186]).

In birds as in all other vertebrates, the blood brain barrier (BBB) is established at the level of microvascular endothelial cells (Figure 5A), which as the mammalial equivalent does not have fenestrations, contains sparse pinocytic vesicular transport, high density of mitochondrias and presence of more extensive tight junctions (TJs) [187]. The TJs consist of integral membrane proteins, namely, claudin, occludin, junction adhesion molecules, and adherens junctions. These are bound to a number of cytoplasmic accessory proteins including zonula occludens (ZO) proteins, cingulin, and AF-6 (Figure 5B). The cytoplasmic proteins help in the binding of membrane proteins to the cytoskeleton actin protein, forming a network which maintains the structural and functional integrity of the BBB [186,188]. However, the TJs in the chicken brain vascular cells differ from mammals in the morphology, molecular architecture and regulation. For example, the immunoreactivity of the TJs proteins claudin-1 and 5 is similar in rats, whereas in chickens, the claudin-1 show a more intense labelling, which is caused by differences in the protoplasmatic and extracellular association of the TJs with the cell membrane. Other TJs proteins which have been described in chickens and show similar expression in mammals are ZO-1 and occludin [189]. In contrast, claudin-3, and claudin 12, proteins also found in the mammalian BBB [190,191], have not been investigated in birds.

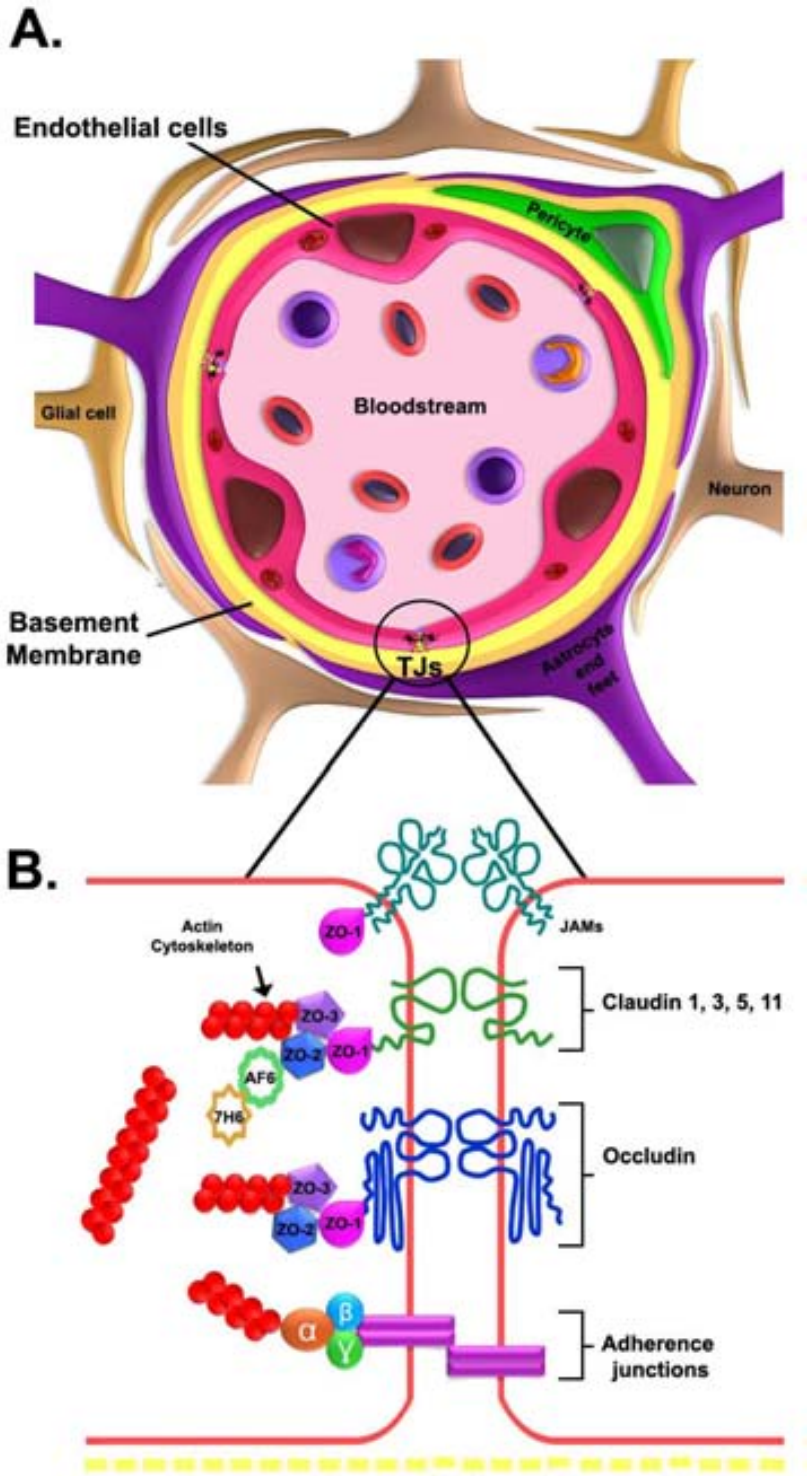

Figure 6. Schema representing the structure of the BBB and the TJs. (Illustration modified from [192]).

The choroid plexus (Chp) consists of epithelial cells, fenestrated blood vessels and the stroma. The presence of fenestrated blood vessels and TJs proteins among the epithelial cells serve as the site for major production of the

blood cerebrospinal fluid (CSF). The Chp in birds share many similarities with that of mammals, being found in the inner ventricular surface of the lateral ventricles, in the roof of the third ventricle and caudally and ventral to the cerebrum [193]. TJ proteins found in the Chp of mammals include: claudin-1, 2, 3, 11, and ZO-1 [194]. Investigations into the presence of these TJs proteins in the Chp of chickens and other bird species have not yet been performed.

Circumventricular organs (CVOs) are specialized tissues within the brain which carry out sensory and neuroendocrine functions, by means of the regulation of the autonomic nervous system and endocrine glands. Due to their specialized function, the CVOs occupy strategic positions along the surface of the brain ventricles, and are highly vascularized with fenestrated vessels, which allow the bidirectional movement of polar molecules between the hemal and neural environments of the CVOs [195,196,197]. Tissues within the CNS accomplishing with this definition in birds (Figure 6) are in the lateral ventricle: the *subseptal* organ (SPO) and the *lateral septal* organ (LSO). The former is analogous to the *subfornical* organ (SFO) of mammals. In the third ventricle, the neurohypophysis (Nhyp), the medial eminence (ME) the *vascular organ of the lamina terminalis* (VOLT) and the pineal gland (PG) are found, Whilst, lining the fourth ventricle, the *area postrema* (AP) is located [195,198,199]. Exceptionally, the *subcommisural organ* (SCO) that is located in the fourth ventricle and has no fenestrated capillaries is considered a CVO because of its endocrine function [200,201,202].

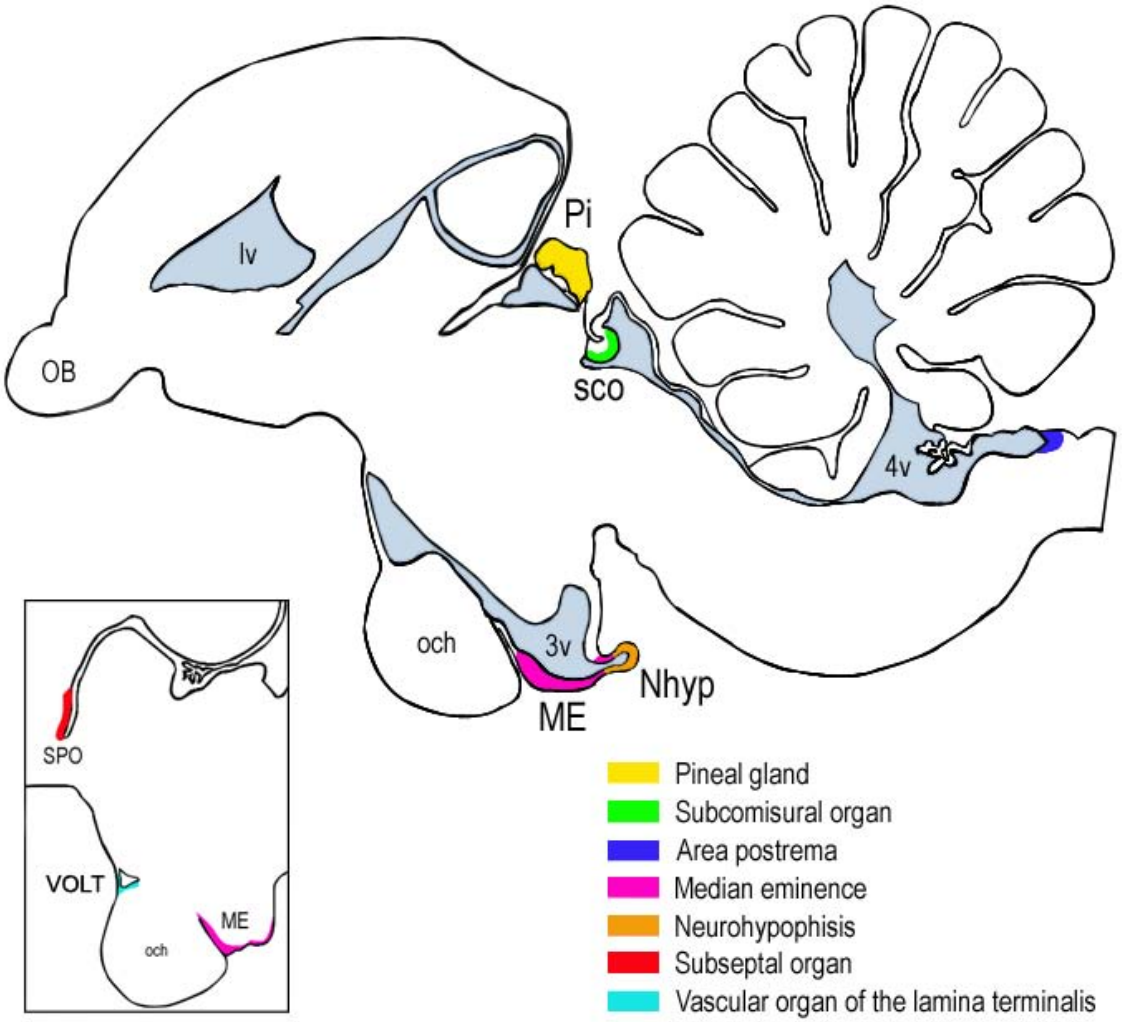

Figure 7. Schematic representation of the anatomical position of the CVOs in the chicken brain showed in a sagital section (lateral 0.24mm): pineal gland (Pi), Subcommisural organ (SCO), *area postrema* (AP), *Median eminence* (ME), Neurohypophisis (Nhyp). Inserted figure (sagital section: lateral 0.72mm) shows the position of the *subseptal organ* (SPO), the *vascular organ of the lamina terminalis* (VOLT) and the ME. (Illustration modified from Ref [185]).

2. Hypothesis and objectives

HPAI viruses cause viraemia and a multisystemic disease in chickens, which frequently induce CNS lesions [108,125,144,149]. It has been proven that influenza virus can use the nervous route to enter into the brain in mice [203,204,205,206], whereas, it has been hypothesized that in chickens the virus uses the haematogenous route, through disruption of the BBB [204,207,208,209,210]. However, the exact mechanism of HPAI virus entry into the CNS and the neuropathogenesis of this infection have not been determined.

Consequently, the general objective of this thesis was to establish a model of infection for a H7N1 HPAI virus and to study the pathogenesis, the neurotropism and the mechanism used by this virus to enter into the CNS.
Specific objectives of this thesis are:

- To set up the animal model for H7N1 HPAI infection in SPF chickens.
- To study the neuropathogenesis of the H7N1HPAI virus in chickens and to discern the possible route of entry of the virus into the brain.
- To determine the mechanism and time point of disruption of the BBB in chickens infected with H7N1 HPAI.

3. Study I: Pathogenesis of Highly Pathogenic Avian Influenza A Virus (H7N1) infection in chickens inoculated with three different doses

3.1. Introduction

HPAI viruses are able to produce clinical disease and death in poultry by a variety of mechanism including dysfunction of the nervous system, cardiovascular and endocrine systems [108]. Although, the mechanism of pathogenicity and tissue tropism of many HPAI virus strains show similar clinical presentations [144,149], a unique conclusion about the dynamics of the disease could not be generalized for all HPAI virus strains [211]. The aim of the present study was to assess the pathogenicity of the A/chicken/Italy/5093/99 H7N1 strain, which was associated with a serious epidemic in Italy [212]. To reproduce a natural infection, birds were inoculated by the intranasal route with one of three different doses ($10^{5.5}$, $10^{3.5}$ and $10^{1.5}$ ELD_{50}). Dynamics of infection, distribution of lesions and viral antigen, viraemia status and viral shedding was evaluated by means of IHC and RT-qPCR techniques.

3.2. Materials and methods

3.2.1. Virus

The avian influenza virus A/chicken/Italy/5093/99 H7N1 of fifth passage was kindly provided by Dr. Ana Moreno from the *Istituto Zooprofilattico Sperimentale della Lombardia e dell' Emilia Romagna* in Brescia, Italy. After its arrival at the *Centre de Recerca en Sanitat Animal* (CReSA), the virus was passaged once and propagated in 9 to 11-day-old specific pathogen free (SPF) embryonated fowls eggs. The fifty percent embryo lethal dose (ELD_{50}) was calculated as described previously [213]. The amino acid sequence at the HA0 cleavage site for the isolate used in the present experimental infection was PEIPKGSRVRR*GLF, that was identical to the cleavage site sequence of H7N1 HPAI virus strains isolated in Italy during the epidemic of 1999 and 2000 [214]. The IVPI was performed as described previously [171] obtaining a score of 2.8, thereby confirming the highly pathogenic phenotype of this isolate.

3.2.2. Experimental design

3.2.2.1. *Birds*

Eighty SPF chickens (Charles River, SPAFAS), were hatched and subsequently placed in negative pressure isolators under biosafety level 3 (BSL-3) containment conditions at the Centre de Recerca en Sanitat Animal (CReSA) for the duration of the experiment. Animal care and all procedures were performed in accordance with the regulations required by the Ethics Committee of Animal and Human Experimentation of the Universitat Autònoma de Barcelona.

3.2.2.2. *Infection*

Fifteen day-old SPF chickens were divided into four groups and placed in separate negative pressure isolators. Each group was infected with different doses of virus through the intranasal route. The first group (G1) was inoculated with $10^{5.5}$ ELD_{50} H7N1 HPAI virus in a final volume of 0.05 mL. The second group (G2) was inoculated with $10^{3.5}$ ELD_{50} and the third group (G3) received $10^{1.5}$ ELD_{50} of virus. The remaining chickens were inoculated with phosphate buffered saline (PBS) and served as sham- inoculated control group (G4). Clinical signs and mortality were monitored daily throughout the 16 days of the experiment. On days 1, 3, 5, 7, 10, and 16 post inoculation, three birds of the infected and control groups (G4) were selected for necropsy (birds were randomly selected at 1 dpi and later biased toward sick or apparently unhealthy birds). Birds found dead, as well as, those euthanized for ethical reasons were included in the study.

3.2.2.3. *Histology and immunohistochemistry*

Tissue samples from all necropsied birds in the four groups were collected and fixed by immersion in 10% buffered formalin for 24 hours. Samples selected included: nasal turbinates, trachea, oesophagus, gizzard, proventriculus, thymus, heart, lung, spleen, liver, small and large intestines (duodenum, jejunum, ileum, cecum/caecal tonsil, rectum), pancreas, adrenal gland, bursa of

Fabricius, bone marrow, skin, CNS that included brain and the thoracic spinal cord, myocardium, skeletal muscle (face, breast, and muscle of the lumbar areas), sciatic and *vagus* nerves. All tissues were embedded in paraffin and duplicate 4µm sections were cut for haematoxylin and eosin (HE) staining and IHC for the detection of the type A influenza virus NP. Procedures for the IHC followed those previously described [215,216]. Briefly, an antigen retrieval step was performed using protease XIV (Sigma-Aldrich, USA) for 10 minutes at 37ºC. Samples were then incubated with the primary antibody at a dilution of 1:250 at 4ºC overnight. The primary antibody used was a commercially available mouse-derived monoclonal antibody (ATCC, HB-65, H16L-10-4R5), followed by 1 hour incubation with biotinylated goat antimouse immunoglobulin (Ig) G secondary antibody (Dako, immunoglobulins AS, Denmark). Finally, an avidin-biotin-peroxidase complex (ABC) system (Thermo Fisher Scientific, Rockford, IL) was used and the antigen-antibody reaction was visualized with 3,3′-Diaminobenzidine tetrahydrochloride (DAB) as chromogen. Sections were counterstained with Mayer's Haematoxylin. Contribution of nonspecific staining of the primary antibody was evaluated by substitution of the primary antibody with PBS and by performing the standard method with tissues of non-infected SPF chicken embryos. Positive control consisted of formalin-fixed paraffin-embedded tissues of chicken embryos inoculated with the H7N1 virus and that were positive by RT- qPCR.

3.2.2.4. *Viral RNA quantitation in tissue samples, oropharyngeal and cloacal swabs and blood*

Blood samples were collected from G1 chickens at 1, 3 and 5 dpi with 1 mL Alsever solution (Sigma-Aldrich, USA). Oropharyngeal and cloacal swabs, as well as, brain, kidney, intestine and lung samples were collected from all birds and each placed in 500 µl of RNA later (Qiagen, Hilden, Germany). All samples were kept at 4ºC for 16 hours and then stored at -80ºC. Viral RNA was extracted from tissue samples, oropharyngeal and cloacal swabs using QIAamp viral mini kit (Qiagen, Hilden, Germany) and following the manufacturer's instructions. Viral RNA was extracted from 15 mg of tissue samples and from

140 µl of swab mixed with the RNA later, and RNA was eluted in 40 µl. The resulting viral RNA extracted were tested by one-step RT-qPCR for the detection of a highly conserved region of the M1 gene influenza A viruses using primers previously described [217], with the amplification conditions previously established [218]. This procedure uses an internal positive control (IPC) to avoid false negative results due to RT-qPCR inhibitors.

Viral RNA quantitation was carried out as described by Busquets *et al*., 2010 (251). Briefly, standard curves were achieved by prior amplification of 99 bp of the M1 gene using the H7N1 strain RNA as template. The amplified M1 gene fragment was cloned into the pGEM-T vector (Promega, USA) and transformed by heat shock into *Escherichia coli* competent cells (Invitrogen, USA). The recombinant plasmid was purified using a QIAprep Spin kit (Qiagen, Hilden, Germany) followed by digestion with SacI restriction enzyme (New England Biolabs, UK) to obtain overhanging ends, and then converted to blunt ends using DNA polymerase I large (Klenow) fragment (Promega, USA). In vitro-transcribed RNA was generated from the T7 promoter (RiboMax kit, Promega, USA). The residual template plasmid was removed by several RNase-free DNAse I (Roche, Switzerland) treatments. The RNA transcript obtained was quantified spectrophotometrically at 260 nm (Qubit, Invitrogen, USA). RNA copy numbers were calculated as described previously [219]. Tenfold RNA transcript dilutions, ranging from 6 to $6x10^7$ molecules, were used to obtain standard curves. The limit of virus detection (loD) for the one step RT-qPCR assay used in this study was 6 viral RNA copies per reaction, which is equivalent to 1 ELD_{50} per reaction. The loD obtained on this assay was equivalent to 1.46 $\log_{10}$ viral RNA copies per mL in case of swab and blood samples, and 2.28 $\log_{10}$ viral RNA copies per gram of tissue.

3.3. Results

3.3.1. Clinical signs, mortality and gross lesions

Clinical signs were limited to G1 and G2, and mortality was only seen in G1 group. Unspecific clinical signs consisting of moderate to severe depression, apathy, listlessness, huddling and ruffled feathers were first noted in 80% of birds from G1 at 2 dpi. More severe clinical signs of torticollis, lack of coordination and bilateral paralysis were observed at 6 dpi. Mortality was recorded at 3 (1 bird), 4 (1 bird), 5 (2 birds) and 6 (2 birds) dpi in this group, but two birds survived until day 10. Gross lesions were observed from 3 dpi and consisted of multifocal to diffuse haemorrhages and cyanosis of the comb and beak, mild diffuse oedema and multifocal haemorrhages in the unfeathered skin of the legs and slight mucous nasal discharge. At necropsy, petechial haemorrhages on leg skeletal muscles and serosal surfaces of proventriculum were also detected and lasted until 6 dpi. From 5 to 7 dpi, paleness in the liver, kidney swelling with prominent lobular pattern, splenomegaly and random multifocal areas of necrosis and haemorrhages in the pancreas were observed. In G2, one animal showed clinical signs and gross lesions similar to the G1 birds at 3 dpi while a second chicken showed necrosis in the comb, pulmonary congestion, kidney swelling and multifocal haemorrhages in the proventricular serosa at 5 dpi. The remaining chickens in the G2 group showed listlessness and ruffled feathers, from 3 to 6 dpi, and there was no mortality. In G3 and the sham infected group, no mortality, clinical signs or macroscopic lesions were observed.

3.3.2. Histology and immunohistochemistry

Histological lesions associated with the presence of viral antigen were observed in chickens from G1 and G2. In G1 chickens, lesions and specific immunostaining was observed from 3 dpi and persisted until 7 dpi in nearly all the tissues (Table 1). No lesions or immunostaining were detected in birds at 1 dpi or in those birds that survived until 10 dpi in the G1 group. In G2, lesions

and specific immunostaining were only detected in one animal on day 3 and another on day 5. In the first case, histological lesions and viral immunostaining were limited to the heart, pancreas and brain, whereas, samples collected from the animal at 5 dpi, showed lesions and distribution similar to what was observed in G1 chickens at 5 dpi. No histological lesions or antigen positive cells were observed in tissues from birds of the sham infected and G3 groups.

Table 1. Distribution of influenza A viral nucleoprotein antigen determined by immunohistochemistry in tissue samples from G1 chickens inoculated with H7N1 HPAI virus

Tissue	Days post infection							Positive cells
	1	3	4	5	6	7	10	
Nasal cavity	-	+	+	+	+	+	-	Salivary and nasal epithelial cells (3 to 6 dpi), olfactory and respiratory epithelial cells, Bowman gland (3-7 dpi), trigeminal nerve branches (day 7), macrophages, heterophils, EC[a] (3 to 7 dpi)
Trachea	-	-	-	-	-	-	-	-
Lung	-	+	+	+	+	+	-	Macrophages, EC
Heart	-	+	+	+	+	+	-	Myocytes, macrophages, EC
Skeletal muscle	-	+	+	+	-	-	-	Myocytes, EC
CNS	-	+	+	+	+	+	-	Neurons, glial cells, ependymal cells, epithelial cells of Chp, EC
Oesophagus	-	+	+	+	+	-	-	EC
Proventriculus	-	+	+	+	+	+	-	Macrophages, heterophils, EC
Gizzard	-	+	+	+	+	+		Mucosal epithelium, smooth muscle cells, macrophages, heterophils, EC
Intestine	-	+	+	+	+	-	-	EC
Caecal tonsil	-	+	+	+	+	+	-	Macrophages, heterophils, EC
Pancreas	-	+	+	+	+	+	-	Exocrine acinar cells, Langerhans islets cells, macrophages, EC
Liver	-	+	+	+	+	+	-	Kupffer's cells, EC
Bone Marrow	-	-	-	-	+	-	-	Myeloid cells
Thymus	-	+	+	+	+	-	-	Macrophages, EC
Bursa of Fabricius	-	+	+	+	+	-	-	Macrophages, EC
Spleen	-	+	+	+	+	-	-	Macrophages, EC
Kidney	-	+	+	+	+	+	-	Epithelial tubular cells, EC
Adrenal Gland	-	+	+	+	+	+	-	Corticotrophic and chromaffin cells, macrophages, EC
Skin	-	+	+	+	+	+	-	Keratinocytes, feather pulp inflammatory cells and follicular epithelial cells, macrophages, heterophils, EC

[a] EC: Endothelial cells.

Histological and immunohistochemical examination of G1 birds revealed severe morphological changes particularly in the respiratory tract, cardiovascular system, pancreas, kidney, adrenal glands and central nervous system. There was a strong correlation between the manifestation of viral antigen and the identification of histological lesions. Presence of viral antigen was not limited to the sites where the histopathologic alterations were visible by haematoxilin and eosin but was also distributed in the surrounding tissue. The brown antigenic staining was generally intense and compact in the nucleus, and, in some cells, it was also cytoplasmatic in distribution, although it was less intense and speckled.

In the respiratory tract, slight to moderate lymphoplasmacytic inflammation in the lamina propria of the nasal cavity, and multifocal areas of loss of cilia, vacuolar degeneration and necrosis of the respiratory epithelium was observed from 3 dpi to 7 dpi. Single cell necrosis was also observed in the olfactory epithelium of the posterior turbinate from 3 to 6 dpi. Influenza A virus antigen was demonstrated in individual cells in the respiratory and olfactory epithelium as well as in the Bowman's gland cells of the posterior turbinate (Figure 8). Endothelial cells and intravascular inflammatory cells in the nasal cavity were also positive from 3 to 6 dpi. Necrosis and positive immunostaining was also observed in the lateral nasal glands located in the nasal cavity and, sporadically, in salivary glands of the roof of the oral cavity. Interestingly, in one chicken sacrificed at 7 dpi, a focal area of nerve fibers degeneration and necrosis, associated with the presence of viral antigen, was observed in the ophthalmic medial branches of the trigeminal nerve located dorsally in the nasal cavity.

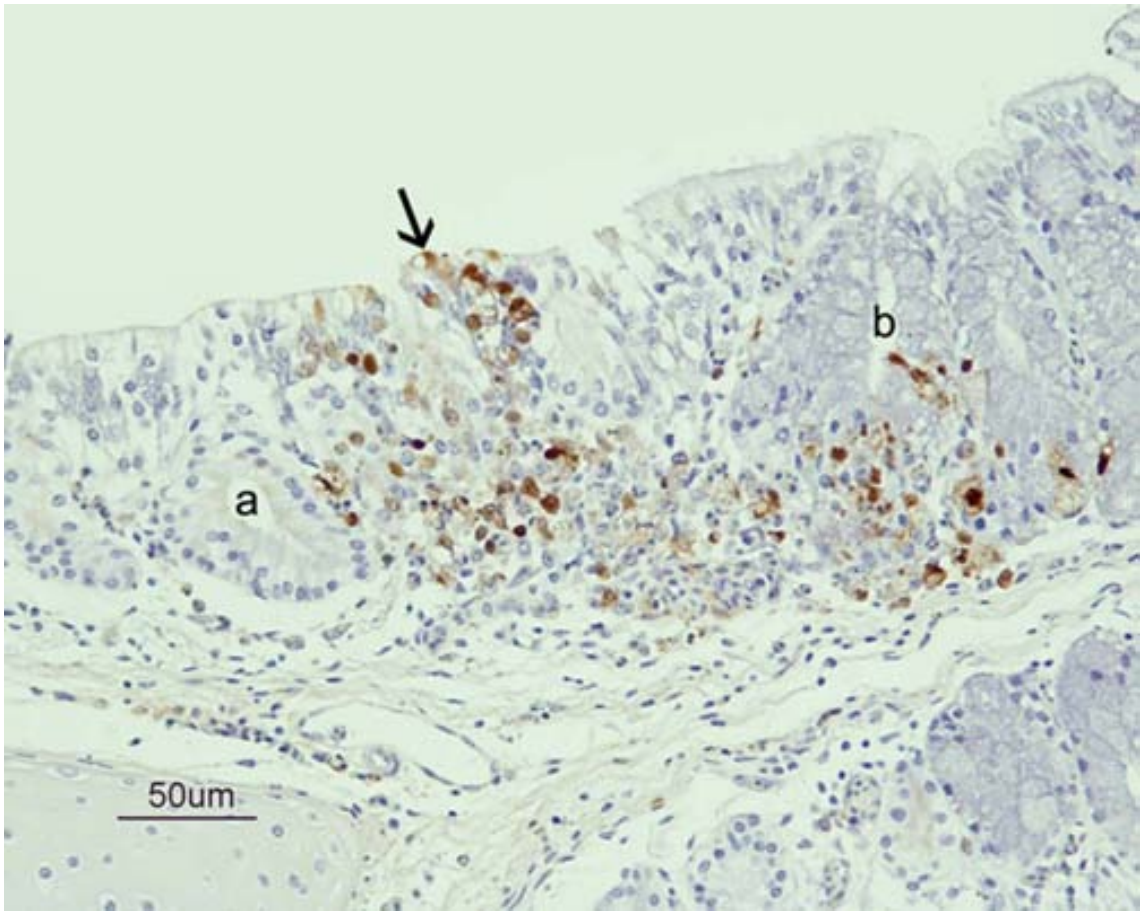

Figure 8. IHC detection of influenza A viral NP in the nasal cavity of SPF chickens inoculated intranasally with $10^{5.5}$ ELD_{50} of H7N1 A/Chicken/Italy/5093/99 at 7 dpi. Epithelial necrosis in the transition between respiratory and olfactory epithelium of the nasal cavity, associated with the presence of viral antigen (brown staining) in the olfactory (arrow), and respiratory epithelial cells, Bowman glands (a), mucous glands (b) and inflammatory cells in lamina propria from a G1 chicken at 7 dpi.

Lung lesions consisting of an increase of cellularity in the air capillaries of the parabronchi was evident from 3 to 7 dpi, mainly due to the presence of heterophils and most probably macrophages inside the capillaries or within the air capillaries interstitium. Microthrombosis of capillaries and scattered single cells necrosis were also seen at these days. Presence of viral antigen was only detected in scattered endothelial cells and macrophages in the air capillaries. No lesions or immunostaining was observed in the trachea of any of the birds evaluated.

Randomly distributed multifocal to coalescing areas of myocardial degeneration and necrosis, with fibre hyalinization and fragmentation associated with a slight infiltration of macrophages and heterophils were observed in birds from 3 dpi. Influenza A viral antigen was observed in myocytes in the necrotic areas as well as in the adjacent inflammatory cells and endothelial cells. Skeletal muscle lesions were slight and were only observed in sections taken from the face and lumbar area. They consisted of scattered areas of fiber degeneration and necrosis surrounded by infiltrated macrophages. Muscle cells and macrophages were positive for viral antigen. Breast muscle lesions were rare and slight.

Histological lesions in the alimentary tract (oesophagus, gizzard, proventriculus, duodenum, colon, caecum, caecal tonsil and cloacae) of lymphocyte depletion and infiltration with macrophages were confined to the submucosa and lymphoid-associated areas in the proventriculus and the caecal tonsils, where influenza A viral antigen was detected in endothelial cells and infiltrating macrophages and heterophils in the submucosa of the proventriculus, caecal tonsil and in the gizzard. Similarly, only slight lesions were observed in the liver that consisted of slight periportal lymphoplasmacytic infiltration and marked Kupffer cell hypertrophy. Erithrophagocytosis in Kuppfer cells and occasional fibrinous thrombi in the hepatic sinusoids were also observed from 3 to 5 dpi. Both, endothelial and Kupffer cells were positive for viral antigen, in addition to inflammatory cells in the portal vessels and periportal areas. No positivity was observed on hepatocytes or biliary duct epithelial cells (Figure 9).

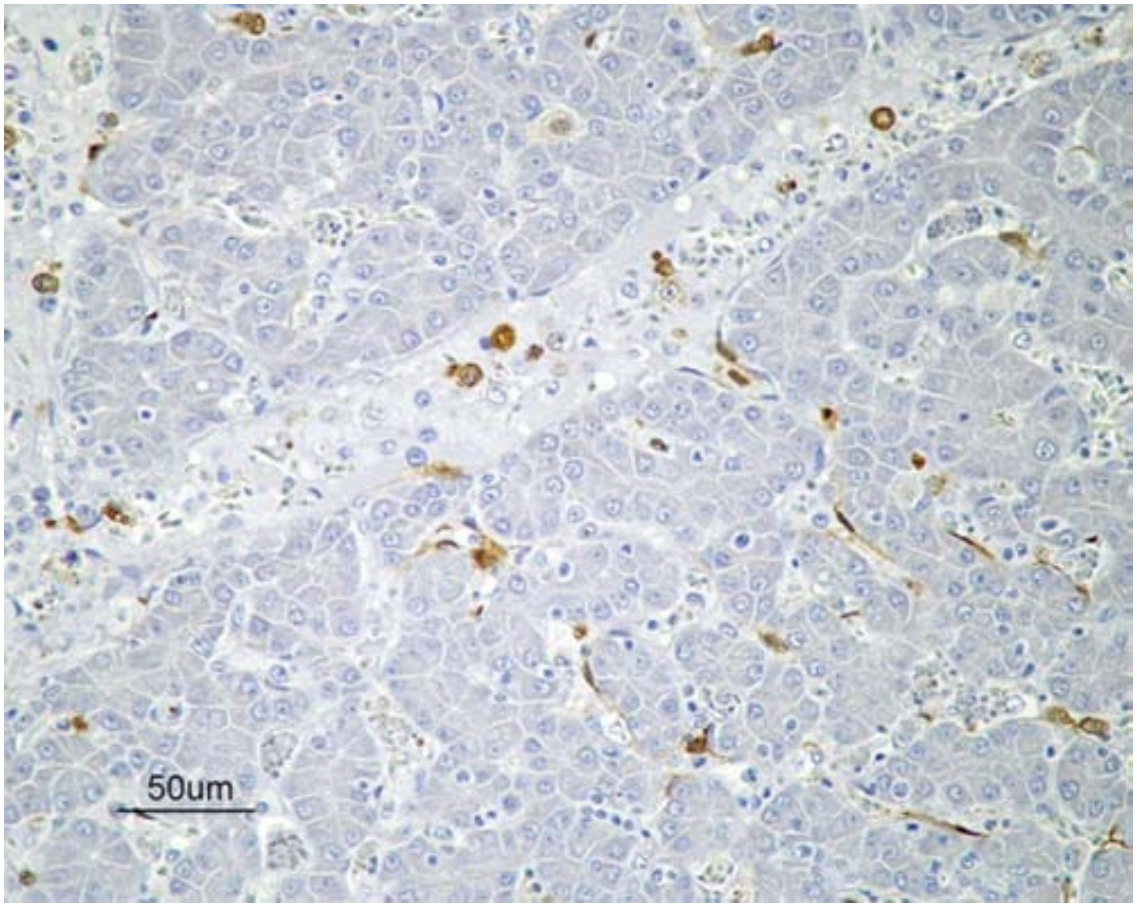

Figure 9. IHC detection of Influenza A viral NP in the liver of SPF chickens inoculated intranasally with $10^{5.5}$ ELD_{50} (G1) of H7N1 A/Chicken/Italy/5093/99 at 5 dpi. Influenza A viral antigen detected in Kupffer cells, endothelial cells and mononuclear intravascular cells in the liver.

More severe lesions were observed on pancreatic acinar cells, which showed focally extensive to diffuse areas of degeneration and necrosis of and stained strongly for the presence of associated viral antigen. Occasionally, there was inflammatory infiltrate associated with necrotic areas, which was also positive for viral antigen from 3 to 7 dpi.

Moderate lesions were observed in kidney, where proximal convoluted tubular epithelial cells showed multiple areas of tubular necrosis in association with the presence of viral antigen. Influenza A viral was also demonstrated on endothelial cells in the renal interstitium. Inflammatory infiltrate was rarely observed associated with necrotic areas. Severe lesions were detected in adrenal corticotrophic cells, and less frequently chromaffin cells, which showed disseminated vacuolar degeneration and necrosis associated with the presence

of influenza A viral antigen. Necrotic areas were infiltrated by macrophages and heterophils that were also positive.

In lymphohematopoietic organs, moderate erythroid and myeloid cellular depletion were noted in the bone marrow from 5 to 7 dpi. The spleen, thymus and bursa of Fabricius had slight to moderate lymphoid depletion of all histological compartments with apoptosis and/or necrosis of lymphocytes from 3 to 7 dpi. On these organs the antigen was restricted to endothelial cells and macrophages.

Skin lesions were confined to the face and comb samples, and consisted mainly in focal epidermal necrosis and diffuse oedema, hyperaemia and perivascular mixed inflammatory infiltrate (macrophages and heterophils) that was positive for viral antigen in the underlying dermis. There was microthrombosis and vasculitis affecting dermal vessels that caused focal areas of oedema, haemorrhage and necrosis. Positive staining was also observed in epidermal degenerated keratinocytes, dermal endothelial cells, follicular epithelial cells and endothelial and inflammatory cells in the follicular pulp.

Nervous system lesions were detected in the gray matter and, less frequently, in the white matter, and consisted of multifocal areas of malacia that were evident in all regions of the CNS (spinal cord, cerebellum, brain stem, cerebral hemispheres, and olfactory bulb (OB). These areas of malacia were characterized by neuropil vacuolation, neuronal central chromatolysis and neuronophagia, astro and microgliosis, and were associated with intranuclear and cytoplasmatic immunostaining on neurons and glial cells. Perivascular oedema was observed in capillaries near the affected areas, and endothelial cells as well as astrocytes of the glial limiting membrane were positive for influenza A viral antigen. Progressive coalescence of the areas of malacia was observed from 3 to 7 dpi. Ependimocytes showed degenerative changes and necrosis and were also positive for influenza A viral antigen from 3 dpi to 7 dpi. Slight inflammatory cell infiltration of the Chp that consisted basically of macrophages was detected at 5 and 6 dpi. Chp epithelial cells were also positive for viral antigen.

Thoracic sections of the spinal cord showed necrosis of ependymal cells in the central canal and neurons in the ventral or dorsal gray matter columns in chickens from 3 to 6 dpi (Figure 10). The peripheral nervous system did not show changes or presence of viral antigen in any bird.

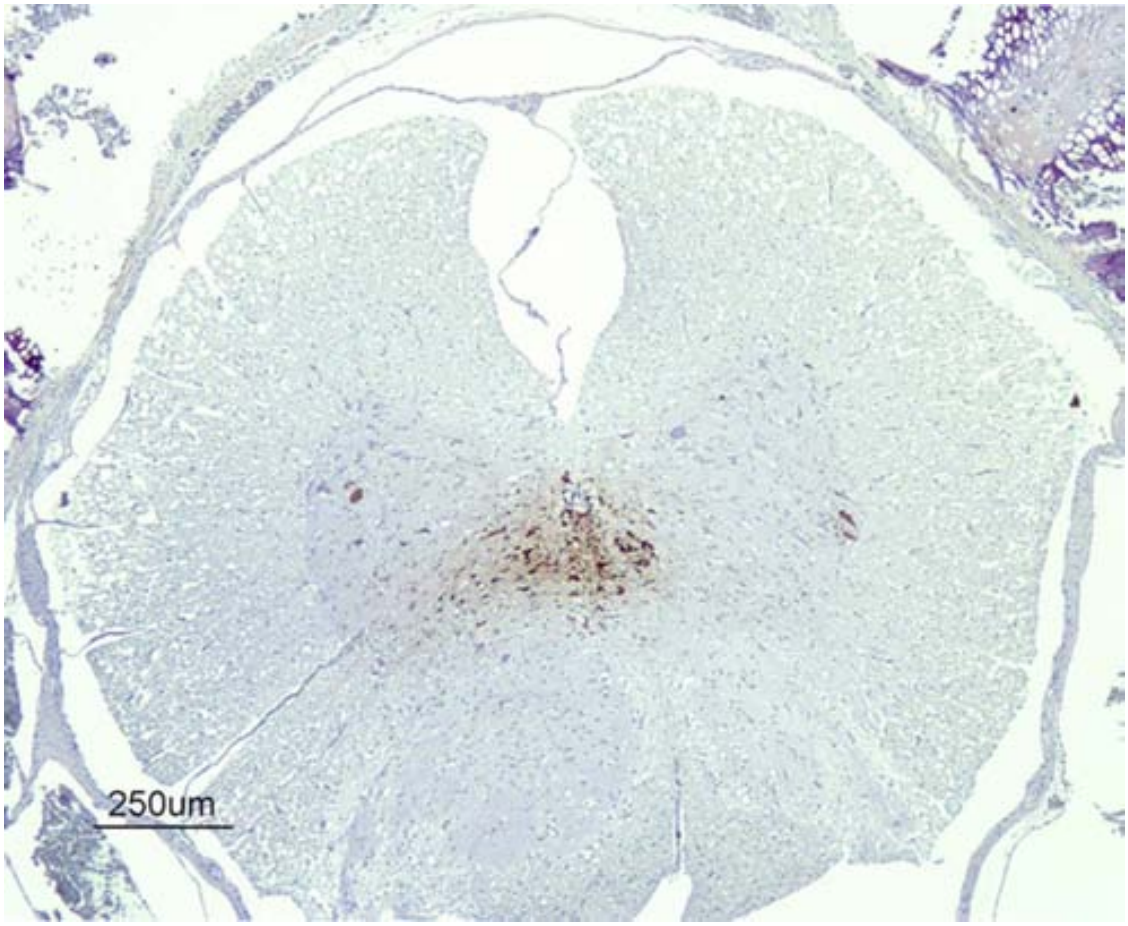

Figure 10. IHC detection of influenza A viral nucleoprotein in the spinal cord of SPF chickens inoculated intranasally with $10^{5.5}$ ELD_{50} (G1) of H7N1 A/Chicken/Italy/5093/99 at 3 dpi. Viral antigen was detected on ependymal cells surrounding the central canal and in the nearest glial cells and neurons in the gray matter from a G1 chicken at 3dpi.

3.3.3. Viral RNA quantitation in blood and tissue samples by RT-qPCR

In G1, viral RNA was detected in blood samples at 1 dpi (5.03 log_{10} viral RNA copies/mL) 3 dpi (9.21 log_{10} viral RNA copies/mL) and 5 dpi (7.70 log_{10} viral RNA copies/mL). Regarding the viral load in all the sampled tissues (CNS, lung, kidney and intestine) viral RNA copies could be detected in G1 birds, inoculated

with the highest ELD_{50}, as soon as 1 dpi in brain and kidney (Figure 11-A). In all the organs sampled viral RNA copies were found in birds euthanatized or found dead from 3-7 dpi. In birds from G1 sacrificed at 10 dpi no viral RNA load was detected. CNS and kidney were the tissues that showed the highest viral load during the whole experiment. In G2, viral RNA was detected from 3 dpi and lasted until 7 dpi in all tissues. At 10 dpi, viral RNA was detected in kidney (4.16 log_{10} viral RNA copies/gr) (Figure 11-B). High variability of the viral load was observed among individuals in this group. In G3, inoculated with the lowest ELD_{50}, low amounts of viral genome in CNS and lung at 5 and 7 dpi were detected (Figure 11-C). Viral RNA copies were not detected in blood and tissue samples of control birds.

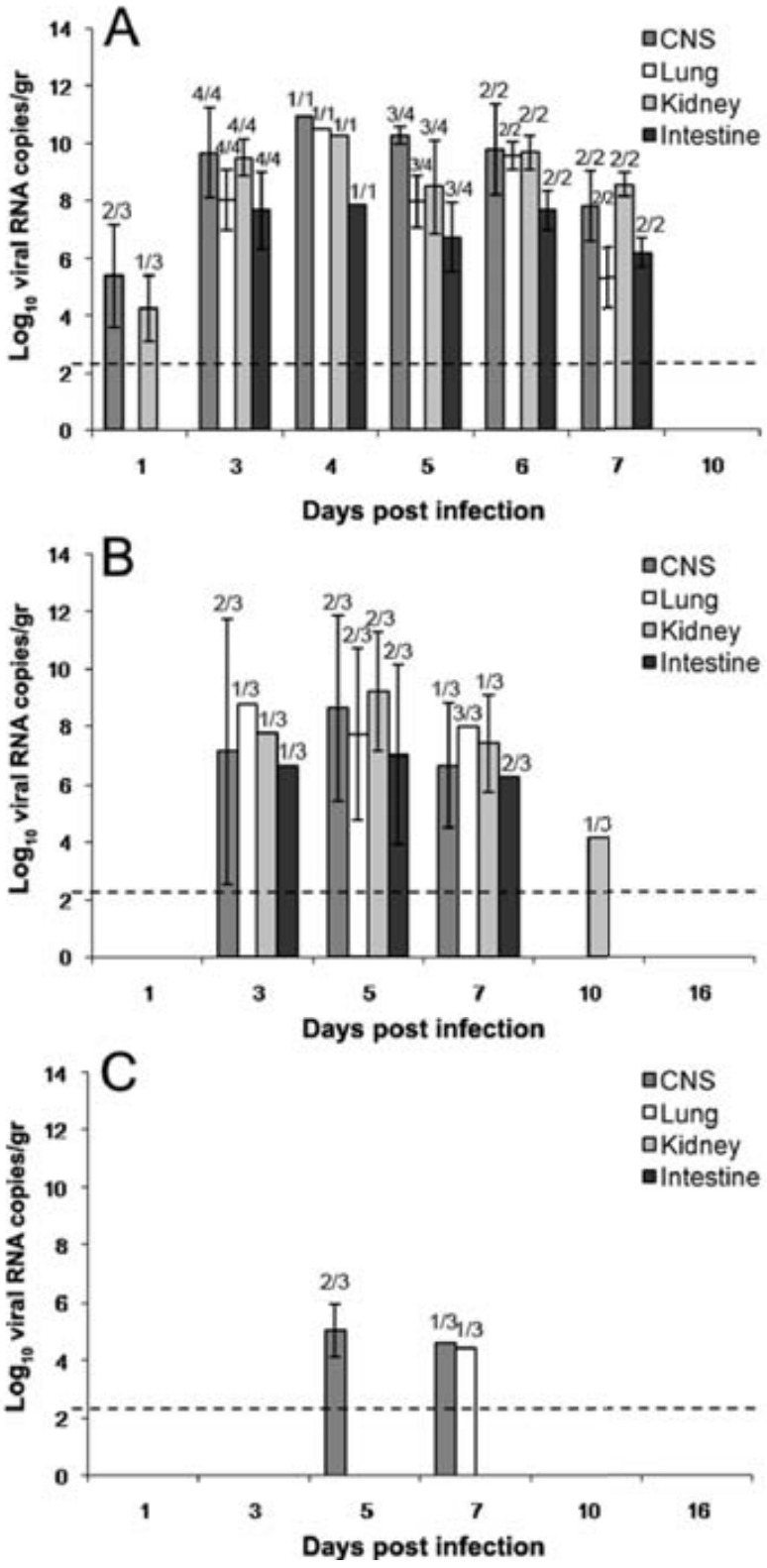

Figure. 11. Viral RNA detected by RT-qPCR expressed as log10 viral RNA copies per g of tissue in samples of CNS, lung, intestine, and kidney collected from day 1 to 10 in G1 (A) birds and from day 1 to 16 in group G2 (B) and G3 (C). Rates above the bars indicate the relation between positive birds and the total of animals examined. LoD is indicated by the dashed line (2.28 log_{10} viral RNA copies/gram of tissue).

3.3.4. Viral RNA quantitation in oropharyngeal and cloacal swabs by RT-qPCR

Viral RNA levels detected in oropharyngeal and cloacal swab samples were proportional to the inoculated ELD_{50} dose, being highest in G1, intermediate in G2 and low in G3. In G1, one animal showed cloacal shedding at 1 dpi, but the viral load levels in oropharyngeal and cloacal swabs were high and similar between 3 dpi and 7 dpi (Figure 12-G1). In G2, viral RNA copies were first detected on 3 dpi and gradually increased to peak levels for both samples (oropharyngeal and cloacal) on 5 dpi. Detection of viral RNA copies decreased on 7 dpi and reach the lowest level on 10 dpi in which oropharyngeal swabs were negative (Figure 12-G2). In G3, viral RNA copies were detected in cloacal and oropharyngeal swabs on 5 dpi and low levels could still be detected in cloacal swab samples on 7 dpi (Figure 12-G3). Viral genome was not detected in oropharyngeal and cloacal swabs of control birds.

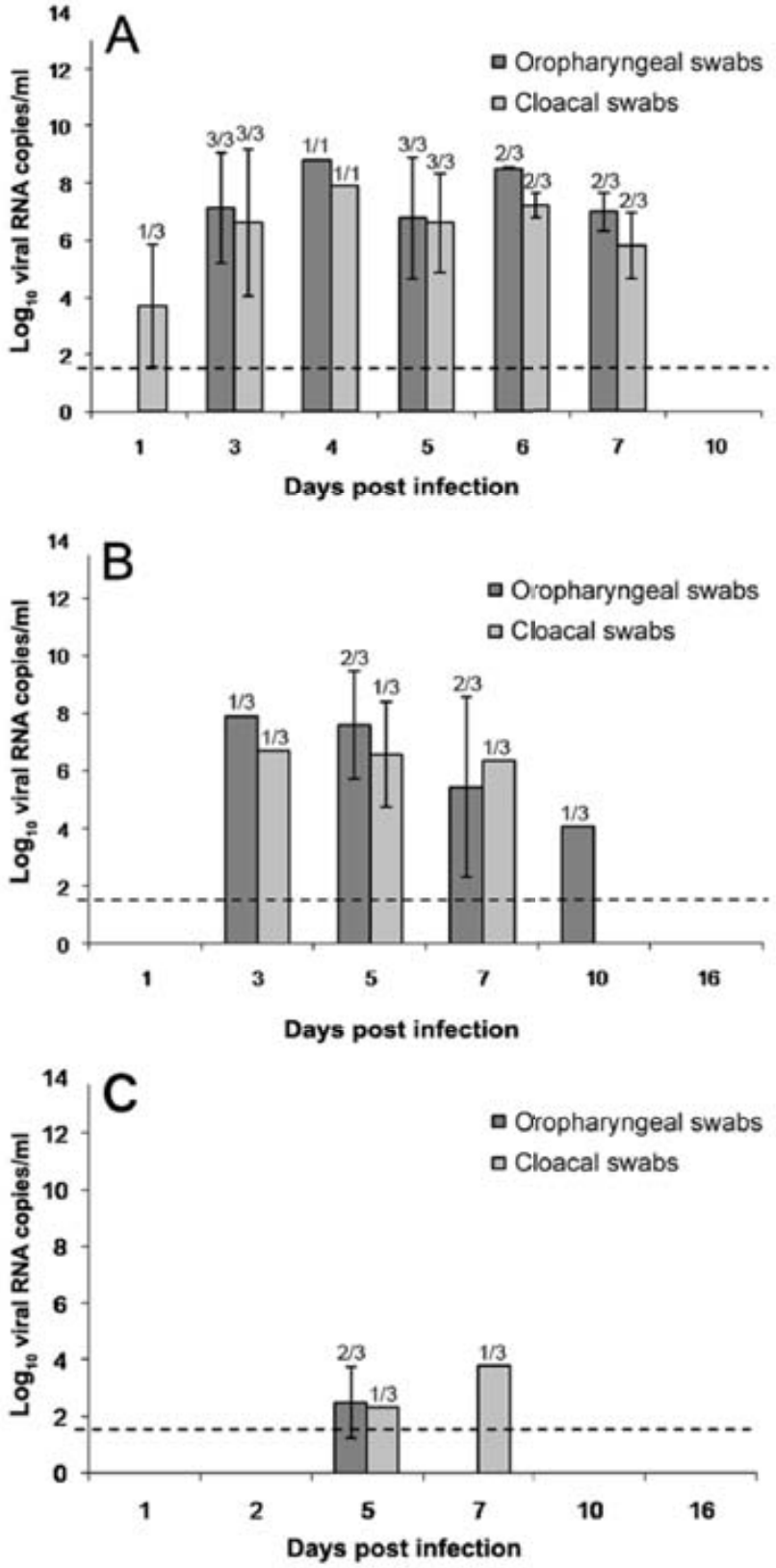

Figure 12. Viral RNA levels detected by RT-qPCR in 1 mL oropharyngeal and cloacal swabs obtained from day 1 to 10 in G1 (A) birds and from day 1 to 16 in group G2 (B) and G3 (C). The dotted line indicates the limit of the detection. Rates above the bars indicate the relation between positive birds and the total of animals examined. LoD is indicated by the dashed line (1.46 $\log_{10}$ viral RNA copies /mL).

3.4. Discussion

The H7N1 HPAI virus used in the present study caused an important HPAI outbreak affecting different bird species in the late nineties in Northern Italy [212]. A complete description of the clinical and pathological findings observed during the epidemic has already been published [111,212]. However, the pathogenic mechanisms and the dynamics of infection in chickens have not truly been studied. Here, a time course evaluation of the clinical presentation, lesions and infection/disease outcome and histopathological lesions, as well as, virus distribution, detection of viraemia and viral shedding was assessed in SPF chickens by using three different doses of this HPAI virus. Remarkable findings were observed that differed from the natural disease. Firstly, fibrinous peritonitis was a usual macroscopic lesion described during the H7N1 HPAI virus natural outbreak [111,212], but was not observed in the present experimental infection neither in other HPAI virus experimental infections [106,108,118,119,138]. Fibrinous peritonitis is a very common lesion in commercial birds, associated to secondary bacterial infections and its description in the natural outbreak can reflect a simultaneous viral-bacterial infection [14,220]. In the present study, evaluation of birds under experimental conditions allowed the identification of lesions only caused by H7N1 HPAI virus. On the other hand, during the outbreak only the pancreas, heart, and nervous tissues were positive for viral antigen by IHC in samples of chickens and turkeys [111,212]. By contrast, in the present study viral antigen was widely distributed in many tissues in chickens infected with the highest and middle doses. These differences in the extension of lesions and viral antigen distribution observed during the natural outbreak compared to the experimental infection can be attributed to the selection of a limited set of tissues (pancreas, kidney, spleen, brain and heart) during the natural outbreak for a rapid diagnosis of the disease. In addition, this extensive distribution of the virus is comparable to other reports of natural and experimental infections caused for H7 and H5 subtype HPAI viruses [108,118,119,148,149,221,222]. Lastly, it cannot be ruled out that the detection of a wider distribution of viral antigen can be attributed to differences in the IHC methodology used.

Most of the experimental infections with HPAI virus strains are carried out using high concentrations of virus to reproduce the early onset and rapid progress observed during the natural infection [106,126,221]. In the present study, we also evaluated the infectivity of this H7N1 HPAI virus strain using two lower doses ($10^{3.5}$ ELD_{50} and $10^{1.5}$ ELD_{50}). Our results revealed low morbidity and no mortality with the $10^{3.5}$ ELD_{50} and a subclinical infection with viral replication and shedding with the $10^{1.5}$ ELD_{50} doses. This strongly suggests that although an adequate, and usually high, infectious dose is critical in reproducing the clinical infection, chickens exposed to lower doses can be infected and shed virus representing a risk for the dissemination of the viral agent.

Viraemia has been observed at 1 dpi in chickens infected with H5 HPAI virus strains, such as the H5N3 (A/tern/South Africa/61) and H5N2 (A/chicken/Pennsylvania/1379/83), and also in Pekin ducks infected with H5N1 (A/duck/Vietnam/12/05) at 3 dpi [106,223,224]. Moreover, viraemia have detected from 1 to 4 dpi in turkeys infected with H7N1 HPAI virus [225]. The capacity of those HPAI viruses to produce viraemia may be attributed to the ability to infect endothelial cells, as demonstrated in chicken embryos infected with H7N1 HPAI virus A/Rostock/FVP/34 [211,226] or embryos of different avian species (chicken, turkey, Muscovy duck) infected with H7N1 HPAI virus A/ty/Italy/4580/99 [227]. HPAI viruses have been frequently reported on endothelial cells of poultry species naturally or experimentally infected [119,125,135,138,143,149,204,211,212,222,228,229,230,231,232]. A clear link between the degree of antigenic staining on endothelial cells and the severity of the disease in chickens has been reported [119]. In addition, HPAI virus antigen has also been demonstrated in leucocytes [135,211], heterophils [118,233], and monocytes and macrophages [118,230]. In our study, the presence of viral antigen in endothelial cells in venules, arterioles, and in capillary endothelial cells of many organs, in circulating mononuclear cells in association with the detection of viral RNA in blood samples from 1 dpi, provides evidence to indicate that this H7 subtype HPAI virus strain is able to produce viraemia early in the infection of chickens. This could explain the rapid dissemination of the virus in some tissues, i.e. brain and kidney did not show histological lesions or presence of viral antigen at 1 dpi, but virus was detected by RT-qPCR on this

day. Similarly, high levels of viral RNA copies were detected on the intestine and lung, although lesions were almost absent on these organs and few cells were positive for viral antigen. Therefore, the detection of virus on these samples could be attributed to the presence of viral RNA copies in the bloodstream.

As observed in this study and in agreement with previous studies of chickens, ducks, and herring gulls infected with HPAI viruses [106,153,234], oropharyngeal shedding was the principal route of excretion in birds from all groups. This could be explained by the detection of viral antigen in the respiratory and olfactory epithelial cells, as well as, salivary and lateral nasal glands in birds inoculated with the higher dose and some of the middle doses. With respect to the source for viral genetic material found in birds infected with HPAI virus in cloacal swab samples, previous studies have suggested the intestinal content, urine, bile and pancreatic excretions to be a source of the virus [222], as all these tracts empty into the cloaca. However, the IHC results obtained indicate that the most likely source of virus in the present experiment was the kidney, because no viral antigen was found in intestinal epithelial cells, hepatocytes or bile canaliculus. Viral detection in the pancreas was evident, but the volume of pancreatic secretion that emptied into the intestinal tract is very low in comparison with the urine.

The detection of high quantities of viral RNA in CNS of all inoculated groups, even in the birds inoculated with the lower dose was also an interesting finding. These results corroborate the strong neurotropism of this particular HPAI virus strain as reported during the Italian outbreak in different poultry species but also experimentally demonstrated in mice [212,235].

Involvement of CNS in HPAI virus infection has been widely described [108,125,144,146,149,150,153,236]. However, our study shows that, not only the encephalus, but also the spinal cord is consistently affected early in the infection with this H7 subtype HPAI, which has been previously reported in chickens and mice infected with different HPAI virus subtypes [144,204,232,237]. Viral antigen detection was also described in ependymal

cells lining the spinal canal of mute swan (*Cygnus olor*) and whooper swan (*Cygnus cygnus*) naturally infected with H5N1 HPAI virus [147]. Viral antigen has been also demonstrated in peripheral autonomic ganglia, plexi of the enteric tract and nerve in the skeletal muscle of turkeys, Japanese quail, Bobquail, pheasants and partridges infected with HPAI viruses [119]. Moreover, it has been detected in peripheral ganglia that provides innervation to the heart, adrenal gland and gastrointestinal tract of house sparrows [153], in the myenteric plexus of Pekin ducks [150,169,238] and peripheral nerves and ganglia of domestic ducks [116]. However, in this study we did not detect virus in nerves or ganglia of the peripheral nervous system.

The presence and distribution of the viral antigen in the CNS of chickens infected with H7N1 HPAI virus is of particular interest and different viral pathways have been hypothesized: the influenza A virus can reach the CNS through the olfactory nerves [239], through the peripheral nervous system [203,240] or through the bloodstream [241]. In our study, viral antigen was detected in the olfactory epithelium of birds inoculated with a higher dose during the first days post infection, but location of the viral antigen in the CNS at 3 dpi was widespread and did not correspond with an entry by the olfactory route; further studies aimed to determine whether the cells that support viral replication in the olfactory mucosa are neurons or supporting stromal cells would clarify this point. The viral entrance to the brain could be via the peripheral nervous system, especially the *vagus* nerve as demonstrated in mice infected with H5N3 HPAI [240] but this seems also unlikely since the presence of virus in the *vagus* nerve was not detected. Therefore, based on our results, we suggest that virus dissemination to different organs and tissues and its entry to brain in chicken is most probably through the blood stream. This assumption is further supported by the finding that astrocytes of the glial limiting membrane were conspicuously positive to viral antigen detection by IHC. Migration of the virus across the BBB may occur directly from the blood through opening of endothelial cell junctional complexes (para-cellular route) [242] or using vesiculo-tubular structures (trans-cellular route) [242,243]. Another possibility is the “Trojan horse mechanism” where viral particles are transported through the BBB using leukocytes and/or mononuclear cells [244]. If influenza virus uses

any of these routes, they have not been investigated. Therefore, more studies must be conducted to discern the underlying mechanism of BBB disruption that leads to the severe necrotizing encephalopathy and death of the birds.

4. Study II: Neuropathogenesis of highly pathogenic avian influenza virus (H7N1) infection in chickens.

4.1. Introduction

HPAI viruses cause a generalized infection in which oedema, haemorrhages, and multiple organ failure are common findings [138]. Besides, a large amount of the reported natural and experimental HPAI virus infections in birds describes CNS as one of the main target organs affected during the infection [138,143,144]. Different pathways for influenza A virus to reach the CNS have been hypothesized such as through the peripheral nervous system [203,245], via the olfactory nerves [204], or through the bloodstream [246]. In the mouse model, the virus reaches the brain through trans-synaptic invasion via cranial nerves [204,246]. In chickens, the lesion profile reported in the literature points to viraemia and alterations of the vascular endothelium as the mechanism by which the virus disseminates and cause damage to the CNS [144,226,247]. In fact, previous studies in natural and experimental HPAI virus infections have demonstrated the association between the severity of the lesions and the affinity of the virus for endothelial cells in specific tissues, indicating that the endothelial tropism has a central role in the pathogenesis [118,138,143,144,248].

The aim of this study was to elucidate the entry point of a H7N1 HPAI virus into the CNS of chickens and to define factors determining cell tropism within the brain. For that reason, the chronological and topographical distribution of viral antigen, as well as the presence and distribution of influenza A viral receptors in the CNS of infected chickens were established. A double immunostaining was employed to determine the role of the olfactory sensory neurons (OSN) in the neuropathogenesis as an initial target of influenza A virus entry into the CNS. Finally, the presence of haematogenous dissemination was determined by means of viral RNA detection in the blood and CSF using a RT-qPCR.

4.2. Material and Methods

4.2.1. Virus

The avian influenza virus used in this study consisted of a sixth passage A/chicken/Italy/5093/99 H7N1, kindly provided by Dr Ana Moreno from the Istituto Zooprofilattico Sperimentale della Lombardia e dell' Emilia Romagna in Brescia, Italy. The IVPI of this virus was 2.8, indicating that it is a highly pathogenic strain. This virus was propagated in 9 to 11-day-old SPF embryonated chicken eggs. The determination of the ELD_{50} was carried out in SPF embryonated eggs and was determined as described previously [213].

4.2.2. Chickens and experimental infection

Twenty-nine SPF chickens (Charles River, SPAFAS, MA, USA), were hatched and subsequently placed in negative pressure isolators under BSL-3 containment conditions at the Centre de Recerca en Sanitat Animal (CReSA). At 15 days of age, chickens were randomly divided into two groups. The first group consisted of 17 chickens that were inoculated intranasally with 50 μL diluted infectious allantoic fluid containing 10^6 ELD_{50} H7N1 HPAIV. The second group consisted of 12 chickens that were inoculated with PBS and used as negative controls. Chickens were monitored daily by visual observation for clinical signs. At 1, 2, 3, and 4 dpi, 3 chickens from each group were randomly selected for necropsy and sampled. In addition, chickens found dead on these same days were necropsied and included in the study, obtaining 4 and 1 additional chickens at 3 and 4 dpi, respectively. Blood samples were only taken from 3 chickens from each group at 1 and 3 dpi in 1 mL Alsever's solution (Sigma-Aldrich, Madrid, Spain) to determine the presence of viral RNA in the bloodstream by RT-qPCR. All chickens were kept and managed according to procedures reviewed and approved by the Ethics Committee for Animal and Human Experimentation of the Universitat Autònoma de Barcelona.

4.2.3. Post-mortem sampling

CSF samples were collected from 3 euthanized chickens from each group at 1 and 3 dpi. Briefly, the skin and muscle over the atlanto-occipital joint were carefully removed. Later, the skull and the duramater over the brain and spinal cord were separated in anterior direction. After that, roughly 1 μL of CSF was collected from the *cisterna magna* using a micropipette. These samples were used to detect the presence of viral RNA by RT-qPCR.

Samples of the nasal cavity and brain tissues were taken from all dead and euthanized chickens and immediately fixed in 10% buffered formalin for 24 hours. Formalin-fixed nasal cavity samples were sectioned at the level of the olfactory epithelium and brain samples were cut at six different coronal levels and embedded in paraffin wax. Later, sequential 3 μm microtome sections corresponding to the following interaurals: a: 9.04mm, b: 6.64mm, c: 3.04mm, d: 1.60mm, e: -0.56mm, and f: -3.68mm (Figure 13) [185], were made from each paraffin block and used to perform all the IHC studies.

4.2.4. IHC to detect viral antigen in the nasal cavity and brain tissues and study its topographical distribution into the brain

An IHC for the detection of influenza A viral NP was performed in sections of the brain and nasal cavity from all euthanized and dead chickens in accordance with procedures previously described [216]. Briefly, paraffin-embedded samples were sectioned at 3 μm thick, dewaxed and treated with 3% H_2O_2 in methanol to eliminate the endogenous peroxidase. Then, sections were treated with protease at 37 ºC for 10 minutes and incubated with the primary monoclonal antibody (ATCC, HB-65, H16L-10-4R5) diluted 1:250, at 4 ºC overnight. After being rinsed, the samples were incubated with biotinylated goat anti-mouse IgG secondary antibody (Dako, immunoglobulins AS, Glostrup, Denmark), followed by incubation with ABC (Thermo Fisher Scientific, Rockford, IL, USA). The reaction was developed with DAB (brown colour) (Sigma-Aldrich, Madrid, Spain) at RT, followed by counterstaining with Mayer's haematoxylin. Sections from positive-control tissue blocks belonging to chicken embryos infected with

the same H7N1 virus strain were included in each IHC run. Negative controls consisted of substitution of the primary antibody with PBS.

The distribution, intensity and pattern of H7N1 viral antigen staining in the CNS of chickens at each dpi were examined in different brain regions, including: OB, *telencephalic pallium* (Pall), *telencephalic subpallium* (SPall) (that contains the *striatum* (St)), *hypothalamus* (H), optic area (Och), diencephalon (that contains the *prethalamus* (p3), *thalamus* (p2), *pretectum* (p1), and the secondary prosencephalon (2P)), midbrain or mesencephalon, hindbrain (that contains the *isthmus* (Ist) and rhombencephalon (r1-6)), and the *cerebellum* (Cb).

In the six coronal sections, the intensity and extent of viral antigen staining were visually determined using a scoring system, which assesses the number of positive cells including the following: neurons, glial cells (astrocytes, oligodendrocytes, microglial cells) and endothelial cells in a 10x field. To graphically represent the pattern of staining, we proceeded to quantify in each animal the number of positive cells in a variable number of 10x fields (the number of fields was variable from one to six depending on its extension) in each region described above. The following scale was used to rank the intensity of staining in each region: nil (0: no labelling detected); scarce (1: less than 20 nuclei of cells positive for viral antigen on average), slight (2: more than 20 but less than 100 positive cells on average); moderate (3: focal area of more than 100 but less than 500 positive cells on average); intense (4: focus of more than 500 positive cells on average). In a third step, we determined the arithmetic mean for each brain region and dpi, considering that we evaluated at least three birds per day. Finally, in brain regions (*hypothalamus* (H), diencephalon, mesencephalon, and hindbrain) where viral antigen was found in specific neural nuclei and symmetrically distributed, we evaluated the neural nuclei separately from the rest of the area, in order to represent the viral antigen distribution more clearly. Then, the intensity of staining was represented using a heap of points labeling each specific neural nucleus. Finally, the topographical distribution of the viral antigen staining was graphically represented in the six coronal sections, using the Adobe Photoshop CS2 program.

The staining of ependymal cells was considered as a separate entity, and represented with different colours according to the intensity of viral antigen staining. In that way, the absence of viral antigen was not denoted, yellow was used to indicate a scarce number of positive cells (1-10 out of 100 positive cells), green for slight staining (10-30 out of 100 positive cells), blue for moderate staining (31-50 out of 100 positive cells) and red for intense staining (51-100 out of 100 cells positive).

4.2.5. Lectin histochemistry for the detection of influenza virus receptors in the CNS of chickens

Lectin histochemistry was carried out on brain samples from all euthanized and dead infected and control chickens according to the protocol described by Yao *et al*., [249] with minor modifications. Briefly, paraffin embedded samples were sectioned at 3 μm thick, dewaxed and treated with 3% H_2O_2 in methanol to eliminate the endogenous peroxidase activity. Duplicated samples were rinsed with Tris-HCl buffer (TNT) and then blocked for non-specific binding with TNT plus blocking reagent (TNB) (Perkin Elmer, Madrid, Spain) for 30 minutes. Samples were incubated with the biotinylated lectins *Sambucus nigrans* (SNA) (10 μg/mL) or *Maackia amurensis leukoagglutinin* (MAAII) (15 μg/mL) (Vector laboratories Inc, CA, USA) in TNB at 4 °C, overnight. The MAAII lectin that preferentially binds to the Siaα2-3Gal linkage was used to detect the avian type receptor, whereas, the SNA lectin that shows preference towards the Siaα2-6Gal linkage was used to identify the human type receptor [250]. After washing with TNT, sections were incubated with horseradish peroxidase (HRP) 1:100 for 30 minutes, followed by incubation with Tyramide Signal Amplification (TSA™ Biotin System, Perkin Elmer) diluted 1:50 in buffer for 10 minutes and again incubated with HRP for 30 minutes at RT. The reaction was developed with DAB (brown colour) (Sigma-Aldrich) at RT for 30 seconds followed by counterstaining with Mayer's haematoxylin.

Positive controls consisted of sections of tissues where the distribution of influenza A virus receptors has already been determined (human lungs, pig

trachea, and duck lungs and intestines). Negative controls consisted of sequential tissue sections treated for 24 hours with 12.5 U/μL of neuraminidase from *Clostridium perfringes* at 37 °C (P0720L, New England Biolabs, MA, USA). Besides, an additional negative control consisted of substitution of the lectin by TNB buffer.

4.2.6. Double IHC for the codetection of HPAI virus antigen and OSN in the nasal cavity of chickens

Nasal cavity samples from 2 chickens euthanized at 2 dpi, 3 from 3 dpi and 2 from 4 dpi were double stained for the codetection of viral antigen and OSN. Briefly, paraffin-embedded tissue samples were dewaxed, cut at 3 μm thick, and blocked to eliminate the endogenous peroxidase activity using 3% H_2O_2 in methanol. Antigen retrieval was carried out for 30 minutes with proteinase K diluted 1:50 in Tris-HCl 0.05 M, pH 7.6 (S3004, Dako) at RT, and later permeabilized using triton 0.5% in PBS for 10 minutes. Slides were blocked with 2% bovine serum albumin (BSA) (Sigma-Aldrich) diluted in 0.5% triton in PBS for 1 hour at RT. The primary staining corresponded to the incubation with the antibody against influenza A viral NP (ATCC, HB-65, H16L-10-4R5) diluted in blocking buffer and incubated overnight at 4 °C. Later, tissue samples were washed three times with PBS and incubated for 1 h with alkaline phosphatase conjugate goat anti-mouse Ig (H+L) secondary antibody (1010-04, Southern Biotechnology, AL, USA), diluted in PBS. The presence of viral antigen was visualized in blue using nitro blue tetrazolium chloride 5-bromo-4-chloro-3-indoxyl (NBT-BCIP) (11 681 451 001, Roche, IN, USA).

For the second staining, samples were rinsed three times with PBS, and incubated for 1 h with the polyclonal antibody rabbit anti-human protein gene product (PGP9.5) (RA 95101, Ultraclone, Isle of Wight, UK) diluted 1:200 in PBS at RT. After that, tissue sections were incubated for 1 hour with the biotinylated secondary antibody, followed by incubation with ABC and visualization of the reaction using DAB (Thermo Fisher Scientific, Rockford, IL, USA), obtaining a brown staining where OSN were detected. Samples were not

counterstained. Negative controls consisted of incubation of a sequential sample with PBS instead of the primary antibodies. Unspecific binding of both secondary antibodies was discarded, incubating them with the contrary primary antibody.

4.2.7. Combined lectin and IHC staining for the codetection of influenza viral antigen and Siaα2-6Gal receptors in the CNS of chickens

Brain sections of two infected and euthanized chickens obtained for each dpi and an equal number of sections of sham-inoculated control tissues were double stained for the detection of Siaα2-6Gal receptors and influenza A viral nucleoprotein. To that end, SNA lectin staining was performed as previously described and visualized in brown colour using DAB. Later, samples were rinsed three times with tris-buffer saline solution (TBS), treated with proteinase K (Dako) and blocked with 2% BSA diluted in TBS (Sigma-Aldrich). Samples were incubated with the antibody against influenza A viral antigen (ATCC, HB-65, H16L-10-4R5) diluted 1:1000, overnight at 4 °C and visualized by incubation with goat anti-mouse Ig (H+L)-PA (1010-04, AL, Southern Biotechnology) for 1 hour at RT and NBT-BCIP for 10 minutes (11 681 451 001, Roche). The positive reaction was visualized in blue colour. Samples were not counterstained. Negative controls included substitution of the influenza viral antigen antibody or the lectin per PBS and incubation of the lectin with the biotinylated anti-mouse antibody.

4.2.8. RT-qPCR for the detection of viral RNA in CSF and blood

The RT-qPCR technique used to quantify the viral RNA copies have been thoroughly described previously [251]. Briefly, viral RNA was extracted from each sample using QIAamp viral mini kit (Qiagen, Hilden, Germany). The RNA was eluted in 40 µL and amplified by one-step RT-qPCR for the detection of a highly conserved region of the M1 gene of influenza A virus using the previously

described primers [252]. This procedure uses an IPC to avoid false negative results due to RT-qPCR inhibitors.

4.3. Results

4.3.1. Clinical signs, mortality and gross lesions

No clinical signs and gross lesions were observed at one dpi. Eight out of 14 infected chickens showed depression, prostration, ruffled feathers and respiratory distress at 2 dpi. Conjunctivitis was noted in one out of 14 chickens on this day. At necropsy, only pulmonary congestion was observed in 2 out of 3 chickens at 2 dpi. At 3 dpi, 4 chickens were found dead, whilst, severe depression, inactivity and neurological signs were additionally observed in 3 out of 11 chickens. Macroscopic lesions of petechial haemorrhages in the unfeathered skin of the leg and comb, as well as in skeletal muscles and pancreas were also recorded in 2 out of the 3 euthanized chickens and in all chickens found dead. At 4 dpi one chicken was found dead, whereas, similar clinical presentation with prostration, dyspnoea and neurological signs of profound depression, tremors and loss of balance were observed in the rest of the chickens. Gross lesions also consisted of petechial to ecchymotic haemorrhages in the comb and legs, pallor of the kidney with accentuated lobular surface, atrophy of the bursa of Fabricius, petechial haemorrhages in the serosa on the proventricular serosa, and multiple petechial to ecchymotic haemorrhages in the pancreas. There were no clinical signs, mortality or gross lesions in the control non-infected chickens.

4.3.2. Histological lesions and pattern of H7N1 HPAI virus staining and topographical distribution in the CNS of infected chickens

No viral antigen was detectable in any region of the brain of infected chickens at 1 dpi. Microscopic lesions of perivascular oedema, endothelial cell hypertrophy,

focal and focus of malacia associated to moderate gliosis were mainly seen in the gray matter of the brain at 2 dpi. Additionally, at 3 and 4 dpi, focal haemorrhages and coalescent foci of malacia were observed. Viral antigen was detected from 2 to 4 dpi in all 6 chicken brain coronal sections, albeit with different intensities. Euthanized and dead chickens showed similar patterns and intensities of staining. Viral antigen staining was detected as dark brown chromogen deposition predominantly in the nuclei of neurons, glial cells, endothelial and ependymal cells, and less commonly, as granular cytoplasmatic staining in neurons, endothelial and ependymal cells. In addition, granular or linear brown staining in the neuropil was observed and interpreted as positive neuronal axons and dendrites, and cytoplasmatic prolongations of glial cells. Overall, positive viral antigen staining was found mainly in the gray matter but there were small sporadic positive foci in the white matter. Altogether, viral antigen positive cells and neuropil staining was found in isolated or multiple foci that in severe cases coalesced in large round to irregular foci. These foci were randomly distributed in the *telencephalic pallium* (medial, dorsal, lateral, and *ventral pallium* - MPall, DPall, LPall and VPall, respectively), *subpallium* (Spall), and *striatum* (St), and their location varied among chickens (Figure 13). In contrast, symmetrical and bilateral viral antigen distribution was observed in the mesencephalon, *hypothalamus* (H), diencephalon, and r1-6, where the staining was restricted to particular neural nuclei. Staining in the Chp was scarce and mainly noticed in the nuclei of epithelial Chp cells, although cytoplasmatic staining was also observed.

Figure 13. Schematic drawing to show the topographical distribution of influenza A virus antigen in chickens infected with H7N1 HPAI virus at 2, 3 and 4 dpi. A. Schematic view of a chicken's brain showing the rostro-caudal levels depicted in the coronal diagrams below. The diagram on the left shows the brain regions evaluated in each section and on sections c, d, e, and f, the neural nuclei where viral antigen was found bilaterally and symmetrically were represented and labelled. The severity of viral antigen immunostaining in cells of the central nervous system (neurons, endothelial cells and microglia) was represented using different density of dots, as follows: null, scarce, slight, moderate and severe. The intensity of viral antigen staining of the ependymal cells was scored using different colours as follows: null (no colour), scarce (yellow), slight (green), moderate (blue), intense (red). (Illustration modified and reproduced with permission from Ref. [185]).

The topographical distribution and intensity of viral antigen staining, thoroughly examined, quantified and represented in Figure 13, shows how the virus spreads into the CNS of chickens. According to the viral antigen neuroanatomical distribution, the most rostral sections of the brain displayed less antigen staining in comparison with the most caudal sections, with the exception of the rhombencephalon where the staining was weak. The intensity of the staining increased with time, reaching a maximum at 4 dpi. In particular, viral antigen staining was scarcely detected in cells of the OB at 2 and 3 dpi, whereas, a slight increase was observed at 4 dpi. Likewise, weak viral antigen staining was observed in the *telencephalic pallium* (DPall, LPall, and VPall) and *subpallium* (Spall) of the most rostral regions at 2 dpi. At 3 dpi, moderate staining was observed in the LPall and VPall, while at 4 dpi the viral antigen staining was intense in the *pallium* (DPall, LPall and VPall) and *subpallium* (Spall). Furthermore, the most rostral periventricular regions and ependymal cells showed scarce to minor staining (labelled in yellow) at 2 and 3 dpi, whereas, at 4 dpi, moderate staining was observed in these most rostral periventricular regions and on ependymal cells (labelled in blue).

Viral antigen staining in the intermediate section of the *telencephalic pallium*, essentially in the MPall, DPall, LPall, and *striatum* (St), was very weak at 2 dpi, and moderate at 3 dpi. However, the VPall showed little increase in viral antigen staining at 2 dpi and intense staining at 3 dpi. The most caudal section of the *telencephalic pallium* showed high viral antigen staining, being moderate at 2 dpi and intense at 3 dpi. At 4 dpi, the amount of viral antigen staining on the intermediate and caudal sections of the *telencephalic pallium* was intense, with formation of large coalescent positive viral antigen areas. Slight to moderate viral antigen staining was observed in the *hypothalamus* (H), *thalamus* (p2), *prethalamus* (p3), and secondary prosencephalon (2P) at 2 and 3 dpi, respectively. Furthermore, it was almost restricted to the following neural nuclei: *dorsolateral nucleus of the thalamus* (DLA), *pregeniculate nucleus* (PG), *medial geniculate nucleus* (MG), the *rotundus nucleus of the thalamus* (Rot), *anterior pretectal nucleus* (APT) and *tectal gray-superficial stratum* (TGS). On these nuclei, the viral antigen was also found bilaterally and symmetrically (Figure 14).

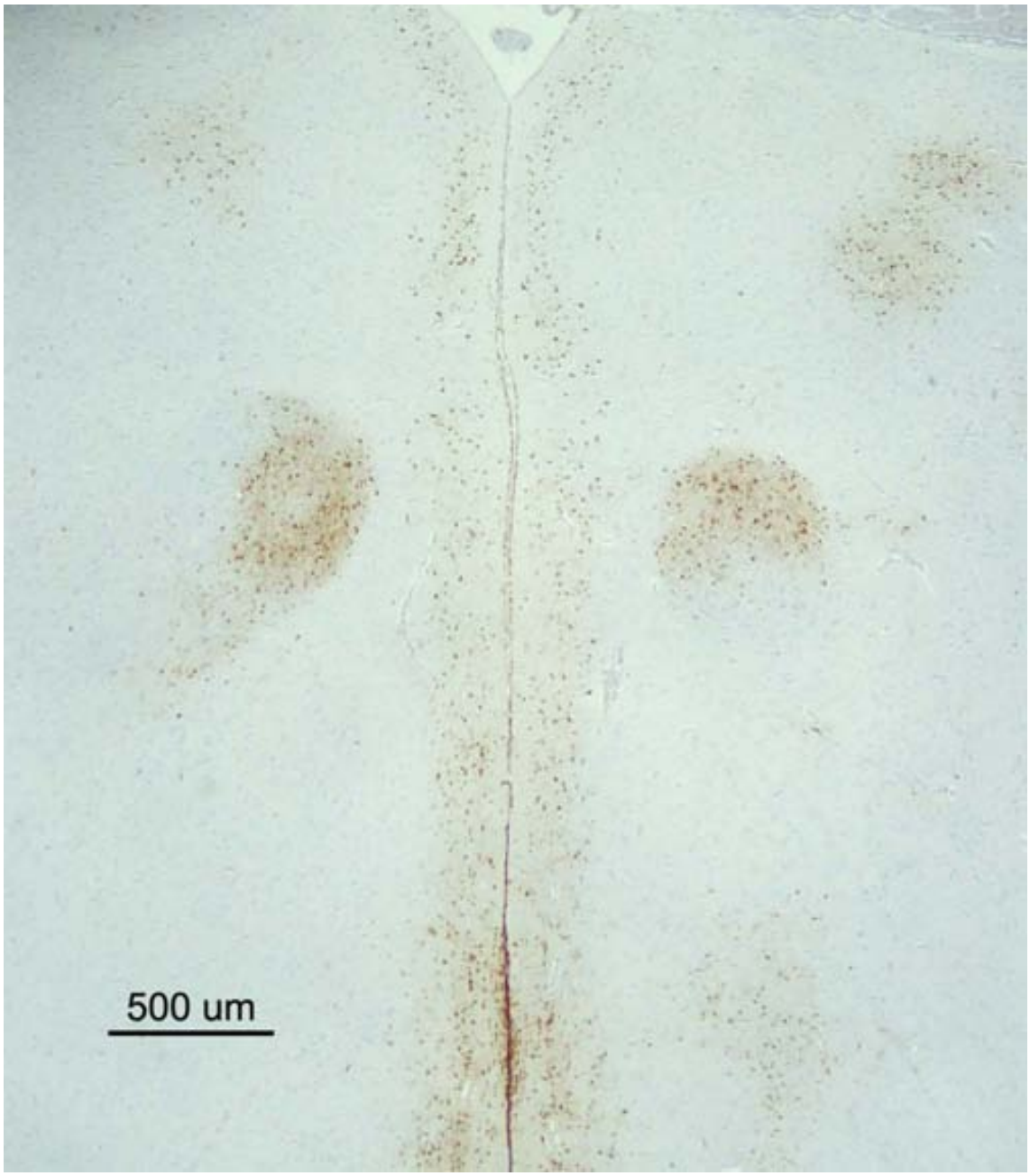

Figure 14. Symmetrical and bilateral distribution of H7N1 HPAI virus antigen in the brain of an infected chicken at 2 dpi. Microphotograhy showing the presence of bilateral and symmetrical viral antigen staining in the MG (*nucleo ovoidalis*) of the *thalamus*. (bar = 500 μm).

Similar intensity of staining was observed on ependymal cells, being slight at 2 dpi (labelled in green) and moderate at 3 dpi (labelled in blue). At 4 dpi, bilateral and symmetrical viral antigen staining was found in the same neural nuclei observed at 2 and 3 dpi, with an evident increase in the intensity of the staining. Additionally, at 4 dpi viral antigen staining was also detected in

the following neural nuclei: the *lateral hypothalamic area* (LH), the *dorsomedial anterior nucleus of the thalamus* (DMA), the *subthalamic nucleus* (STh) in the mammilary region, the *ventromedial hypothalamic nucleus* (VMH) and the *r3 lateral vestibular nucleus*, ventral part (r3LVeV). Viral antigen positive staining was scored as moderate for the periventricular regions and ependymal cells at 4 dpi (labelled in blue).

In the mesencephalon, slight staining was observed at 2 and 3 dpi, whereas moderate staining was found at 4 dpi. In these regions, the viral antigen staining was also found bilateral and symmetrically and almost restricted to the following nuclei: the *torus semicircularis* (ToS), the red nucleus, magnocellular part (RMC), and the *mesencephalic substancia nigra*, compact part (mSNC). The intensity of staining in the mesencephalic periventricular zone and ependymal cells increased in severity from slight (labelled in green) to intense (red) from 2 to 4 dpi, respectively.

In the cerebellum, high virus affinity was noted for the Purkinje cells and their cytoplasmic processes in the molecular layer. Less intensity of staining was observed in the granular layer. The viral antigen staining in the cerebellum was scored as intense at 2, 3 and 4 dpi, but their distribution varied, being found as single individual foci at 2 dpi and large coalescent viral antigen positive areas at 3 and 4 dpi. Moderate to intense bilateral staining was observed in the rhombencephalon from 2 to 4 dpi, respectively. Bilateral and symmetrical distribution was observed in the following rhombencephalic nuclei: the *medial cerebellar nucleus* (Med), the *r2 superior vestibular nucleus* (r2SuVe), the oral part of the *spinal trigeminal nucleus* (Sp50). In the rhombencephalon, the viral antigen staining on ependymal cells was weak at 2 dpi (labelled in green) and increased on severity at 3 and 4 dpi, where moderate staining was found (blue). Epithelial cells of the Chp in the lateral, third and fourth ventricles showed less intensity of viral antigen staining in comparison with the ependymal cells, being scarce at 2 dpi and slight at 3 and 4 dpi. In the same way, although cells of the leptomeninges were negative, subpial astrocytes in the glial limitants in the intermediate and caudal sections of the brain showed positivity in each dpi, but particularly at 4 dpi.

In general, the most commonly affected neural nuclei were the following: the PG (found positive in 12 out of 14 chickens) and the Rot in the *thalamus* (11 out of 14 chickens), the ToS in the mesencephalon (9 out of 14 chickens), and the APT in the *pretectum (*8 out of 14 chickens).

It was not possible to evaluate all CVOs in each chicken every dpi. However, at 2 dpi, slight viral antigen staining was observed in the SPO (4 out of 4 chickens), AP (in one chicken), VOLT (in one chicken) and *the* LSO (one chicken).The SCO was found negative in one chicken. Whereas at 3 dpi, the SPO (4 out of 5 chickens), SCO (3 out of 3 chickens), AP (one chicken), ME (2 chickens) and the VOLT (one chicken) and the LSO (one chicken) showed moderate staining. Moderate to intense viral antigen staining was observed in SCO, ME and SPO at 4 dpi (one chicken).

4.3.3. Distribution of influenza virus receptors in the CNS of control and infected chickens

Siaα2-3Gal receptors were detected in the apical surface of Chp cells and the ependymal cells of the lateral and fourth ventricle, whereas only slight staining was detected on endothelial cells (Figure 15 a, c). There were no differences in the pattern and intensity of staining with the MAAII lectin between healthy and infected chickens, also among different dpi. Neither were there any differences in staining pattern observed with both lectins between dead and euthanized chickens. Siaα2-6Gal receptors were observed in the luminal border of endothelial cells distributed throughout the brain parenchyma, Chp, and meninges (Figure 15b, d). Differences in the pattern of staining with this lectin (SNA) were detected between healthy and HPAI virus infected chickens. In infected chickens, foci of granular SNA positive staining in the neuropil were observed adjacent to SNA-positive endothelial cells. These foci were found randomly distributed in all regions of the brain of infected chickens at 3 and 4 dpi, and more frequently in those chickens most affected.

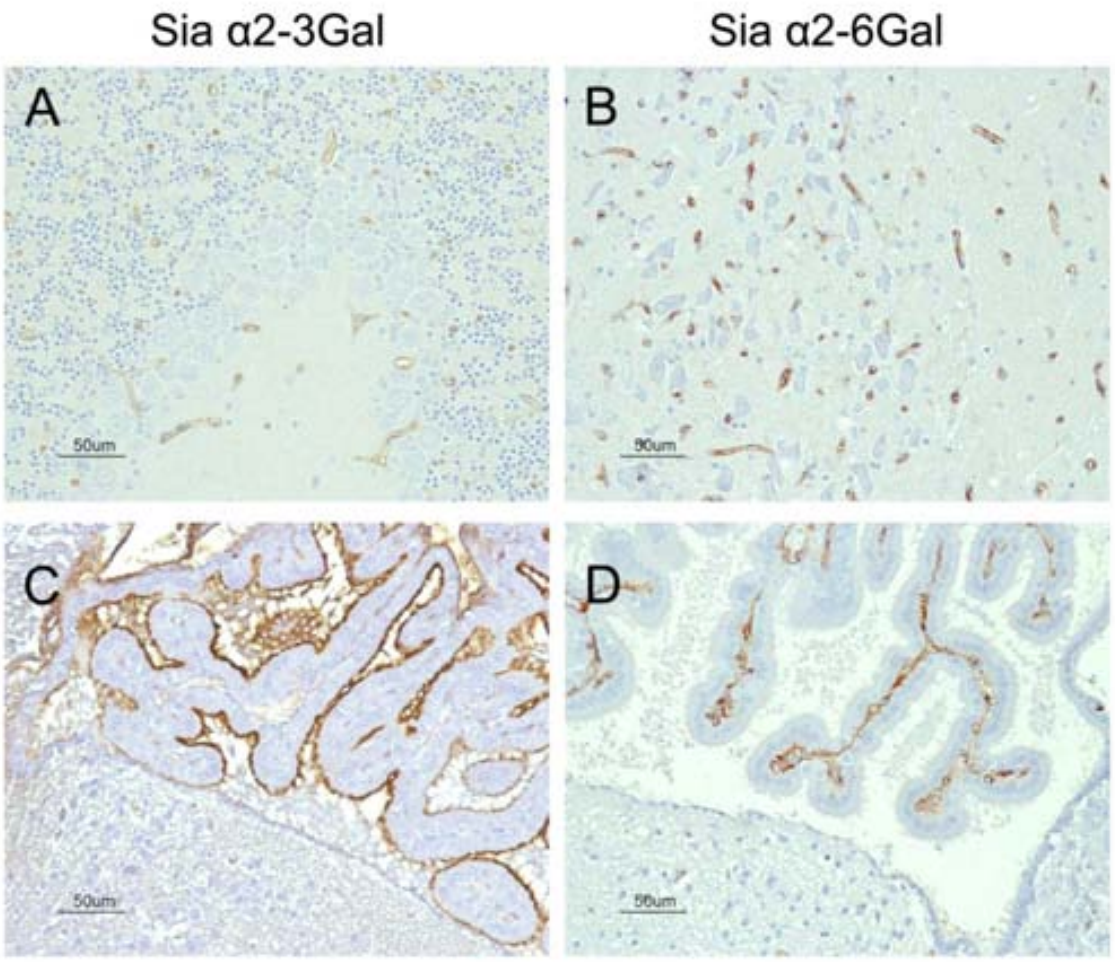

Figure 15. Detection of Siaα2-3Gal and Siaα2-6Gal influenza A virus receptors in the brain of chickens using the lectins MAAII and SNA, respectively. Slight staining for Siaα2-3Gal receptors was found on endothelial cells (A) and ependymal cells, whereas the apical membrane of Chp cells showed abundant presence of Siaα2-3Gal receptors (C). Intense staining for Siaα2-6Gal receptors was observed on endothelial cells in the brain and Chp cells. (bar = 50 μm).

4.3.4. Co-detection of Siaα2-6Gal receptors and HPAI virus in the CNS of infected chickens

In order to understand the nature of the granular focus of SNA staining observed in the brains of chickens infected with this HPAI virus, a double IHC was performed in sections of HPAI virus infected and control chickens. Interestingly, the foci of granular SNA lectin deposition were frequently observed as closely associated with the presence of viral antigen staining and malacia at 3 and 4 dpi (Figure 16). However, granular SNA lectin deposition was not found in all viral antigen positive areas.

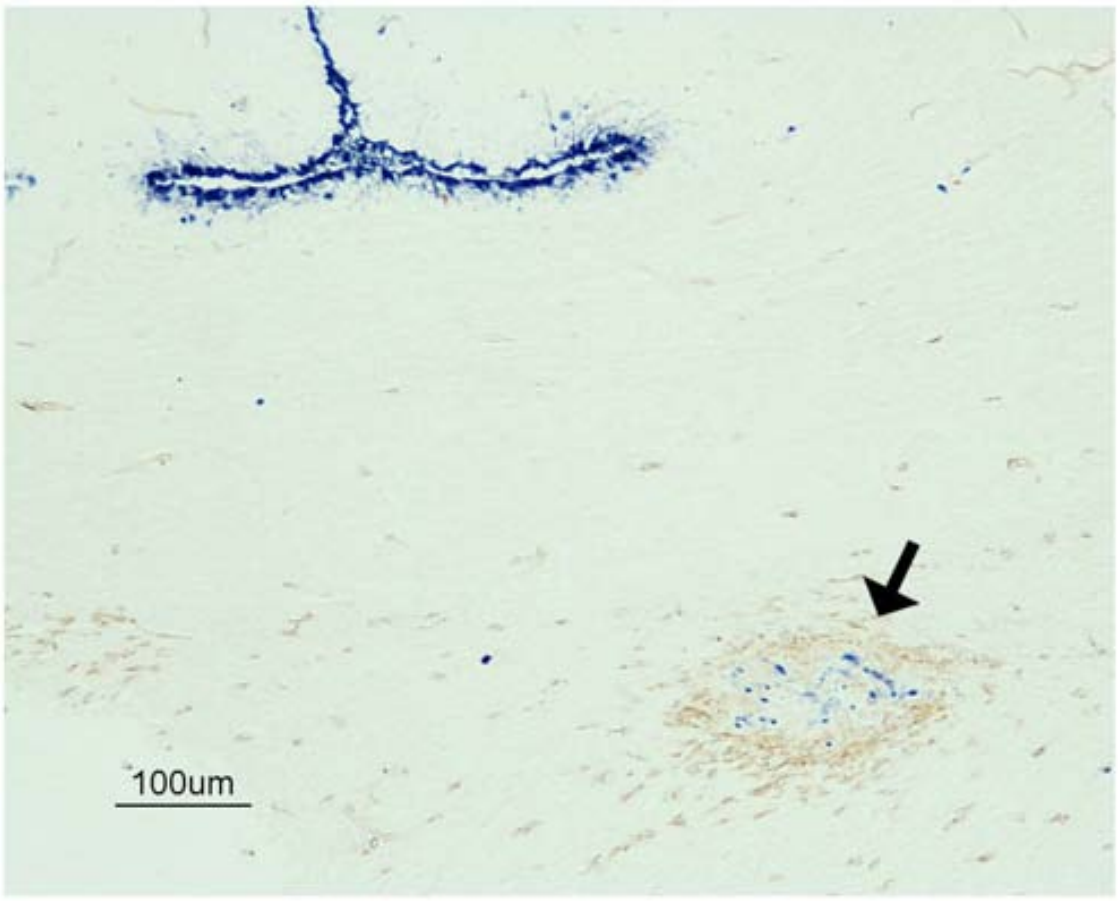

Figure 16. Codetection of viral antigen and Siaα2-6Gal receptors in the brain of an H7N1 HPAI virus infected chicken at 3 dpi. Double immunohistochemistry showing the focus of SNA granular staining (arrow) in correlation with the presence of influenza virus antigen detected in the optic chiasm of infected chicken. Influenza virus antigen was abundant also on ependymal cells (bar = 100 μm).

4.3.5. Codetection of avian influenza virus antigen and OSN in the nasal cavity of infected chickens

PGP9.5 antigen was detected in the nucleus and cytoplasm of olfactory neurons in all chickens. Viral antigen staining was sporadically observed in the nuclei of cells of the olfactory epithelium of chickens infected with H7N1 HPAI virus from 2 to 4 dpi. Viral antigen staining did not colocalize with the PGP9.5 antigen in any chicken (Figure 17).

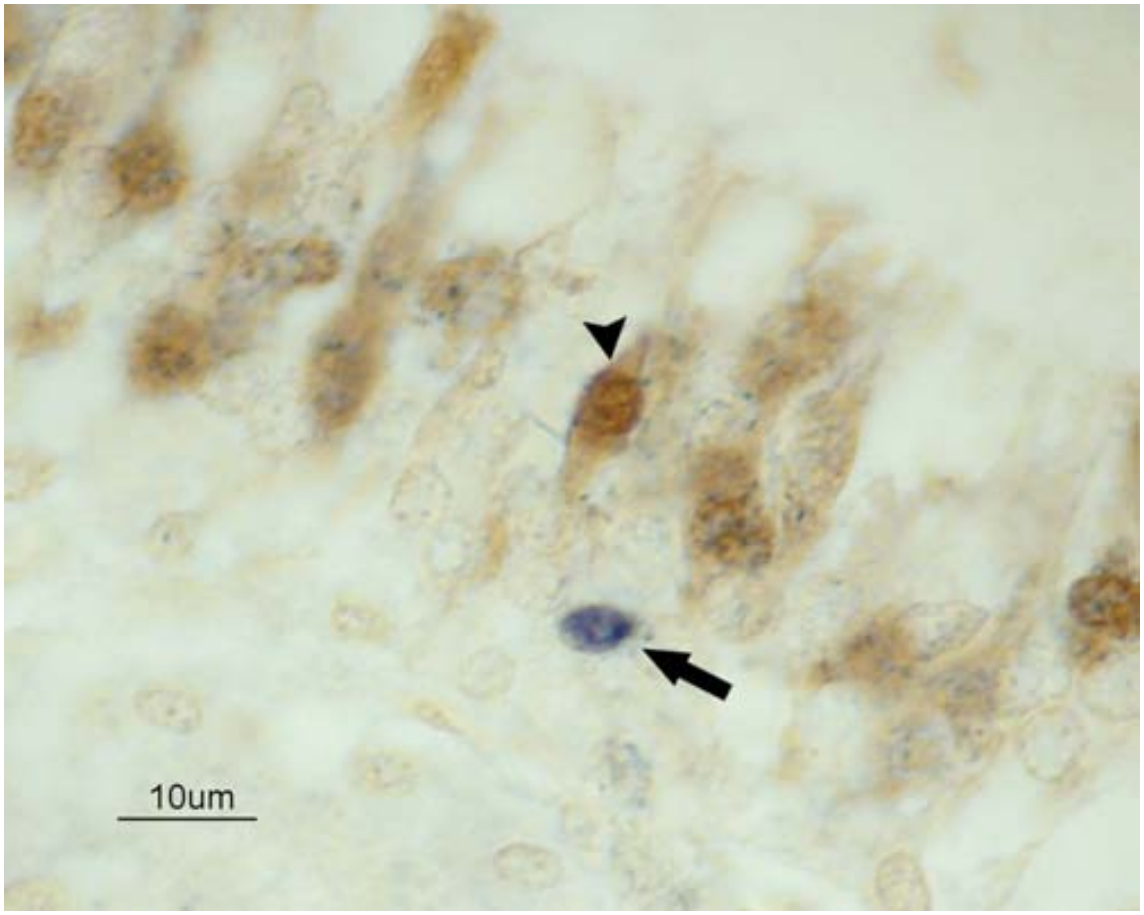

Figure 17. Codetection of influenza viral antigen in OSN of the nasal cavity in a chicken infected with H7N1 HPAIV, at 3 dpi. Double immunohistochemistry showing OSN labelled with PGP9.5 (arrowhead). Viral antigen was found in supporting (arrow) and basal cells of the nonsensory epithelium (not stained), but not in OSN. (bar= 10μm).

4.3.6. Detection of viral RNA in blood and CSF

Viral RNA was detectable in the blood and the CSF as early as 1 dpi. On this day, 5.03 $\log_{10}$ viral RNA copies per mL in the blood and 1.36 $\log_{10}$ viral RNA copies per μL in the CSF were reported. At 3 dpi, the viral load increased to 9.21 $\log_{10}$ viral RNA copies per mL in blood and 5.39 $\log_{10}$ viral RNA copies per μL in CSF.

4.4. Discussion

Although HPAI virus neuroinvasiveness and neurovirulence are considered to be one of the main factors leading to the fatal course of infection in birds [144,154], few detailed studies on viral neuropathogenesis have been conducted in chickens. Previous experimental studies carried out on different species have suggested that influenza A virus could enter into the CNS through one or more of these three pathways: haematogenous [144,253], olfactory [239,254] and neural routes [204,245].

In the first study, we reported sparse detection of H7N1 HPAI virus in the chicken olfactory epithelium from 3 to 6 dpi [255]. Therefore, we were interested in elucidating whether the OSN could provide free access to the virus to enter the CNS. Several neurotropic viruses, such as herpes simplex virus, Borna disease virus, rabies virus, vesicular stomatitis virus, parainfluenza virus, mouse hepatitis virus, and Venezuelan equine encephalitis virus have been proven to use the olfactory pathway to enter into the CNS [254 4,256,257,258]. However, in the present study, the OSN were negative for viral antigen during the first four days of evaluation, confirming that these cells are not a major target for the virus. Viral antigen positive cells in the olfactory epithelium corresponded to basal or supporting cells. In addition, according to the topographical distribution of the viral antigen, the relevance of the olfactory pathway for virus invasion into the CNS could be considered as negligible or absent, because scarce to slight staining was found in the OB and the most cranial regions of the brain at 2 dpi.

Influenza A virus antigen has also been detected in peripheral nerves, plexus and ganglia of thoracic and enteric tissues in turkeys, Japanese quails, pheasants, partridges, domestic ducks and house sparrows infected with HPAI virus [119,150,169,238,259]. In a previous work, we reported the presence of H7N1 HPAI virus antigen in branches of the trigeminal nerve of chickens at 7 dpi [255]. However, based on the present results, the neural pathway does not seem to play an important role in influenza A virus neuropathogenesis in birds, because neural nuclei associated with cranial nerves, such as the vestibular nerve (r2SuVe, r3LVeD, r4LVeD) or the trigeminal nerve (Sp50) were only

sporadically positive at early stages of infection, nor was there caudal to cranial increase in viral antigen staining observed in any of the chicken brains examined.

Early endothelial infection and viraemia are key events during HPAI virus infection in birds [144,225]. The viraemia determines the spreading of this H7N1 HPAI virus to different organs and the final entrance into the CNS [135,138], similarly to other viral infections, such as canine distemper virus [260] and human immunodeficiency virus (HIV-1) [256]. Several results obtained in this study support the hypothesis that the bloodstream is the main route of entry and early dissemination of HPAI virus into the brain. Firstly, the detection of viral RNA in the blood at one dpi confirms the capacity of this virus to induce viraemia very early during the course of the infection. Secondly, the detection of Siaα2-3Gal and Siaα2-6Gal receptors on CNS endothelial cells and, moreover, the finding of viral antigen in the brain capillary endothelial cells and the surrounding nervous parenchyma as early as 2 dpi, corroborates the permissiveness of this cell type for HPAI virus entrance and replication and further support the haematogenous neuroinvasion hypothesis. In addition, the widespread distribution of the viral antigen in the CNS during the early stages of infection follows a pattern consistent with a haematogenous viral spreading [261].

Neuroinvasion through the haematogenous pathway implies that the virus could cross the BBB localized in the brain endothelial cell and the blood-CSF barrier, confined to the Chp [262]. To overcome these barriers and disseminate into the CNS, viruses and other infectious agents must disrupt the BBB in the brain parenchyma and meninges or cross the fenestrated endothelium located in the Chp and CVOs [263]. Detection of abundant and widespread viral antigen in brain capillary endothelial cells and astrocytes forming the *glia limitants* suggest this H7N1 HPAI virus could be able to disrupt the BBB and infect the brain parenchyma. However, the detection of viral RNA in the CSF of chickens at one dpi, indicates that disruption of the BCSFB occurs subsequently to the establishment of viraemia, as has also been demonstrated

for other neurotropic viruses (HIV, simian (SIV) and feline immunodeficiency viruses (FIV)) [264,265,266,267]. Epithelial and endothelial cells of the Chp as well as ependymal cells expressed Siaα2-3Gal receptors, therefore it is not surprising to detect viral antigen as early as 2 dpi, on these cells. It has to be pointed out that the viral antigen was very abundant in ependymal cells, which could be a consequence of further replication of H7N1 HPAI virus, amplification and dissemination of the virus by means of the CSF along the ventricular system and in the subpial parenchymal areas.

The CVOs can be portals of entry of infectious pathogens, such as *trypanosoma brucei*., bovine spongiform encephalopathy (BSE) and Scrapie, into the CNS [268,269]. Similarly, in this study we observed viral antigen in CVOs (SPO, AP, VOLT, LSO) early during the infection, which is in agreement with the expected facility of a virus that causes viraemia to enter into brain areas lacking a real BBB. However, we did not observe dissemination of the viral antigen from CVOs to the surrounding brain regions. Instead, the staining was almost restricted to these brain areas, indicating that these organs might contribute to virus entry and spreading in the CNS, but they are not the main route of entry.

Interestingly, bilateral and symmetrical areas of positive viral detection were observed in the diencephalon, mesencephalon, and rhombencephalon, especially in the Rot (p2), PG (p3), ToS (mesencephalon), and APT nuclei (p1). Detection of bilateral and symmetrical lesions in the brain has also been described in humans suffering from influenza-associated encephalopathies (IAE) [270,271]. In these conditions, it has been suggested that regional differences in blood flow and myelinisation could determine the distribution of lesions [272]. Based on our results, the symmetrical and bilateral distribution of the viral antigen in the CNS of chickens could be explained by the distribution of the blood vessels in the brain and the direct infection of selected periventricular nuclei.

Few studies have been conducted to investigate the presence of influenza virus receptors in the brain of chickens and other species. In spite of

that, both receptors have been reported on endothelial cells of humans, pigs, rats and chicken embryos; however, they are not specific to the brain [226,249,273,274]. In chickens, previous investigations have failed to detect avian influenza receptors in brain endothelial cells [275], which could be explained by differences in the sensitivity between the histochemical techniques and specially due to the signal amplification system used for the IHC in the present study.

Similarly, there are no studies comparing the presence of both receptors in infected and healthy chickens, which as demonstrated in this study was altered. Increased detection of SNA staining in association with the presence of necrotic foci and viral antigen was observed in infected chickens. Local up-regulation of Siaα2-6Gal glycotopes has been reported under different experimental inflammatory conditions [276,277,278]. For example, increase Siaα2-6 and Siaα2-3 glycotopes have been detected in respiratory cells of ferrets infected with H1N1 influenza virus [277], mice affected with asthma [276] and in serum of mice injected with turpentine oil to induce inflammation [278]. Similarly, an increased expression of mRNA of α2-6 and α2-3 sialyltransferases have been observed in rat liver after inflammation [279], and human tracheal cells and bronchial mucosa stimulated with tumour necrosis factor-α (TNFα) [280]. However, considering that most acute-phase proteins and other inflammation-sensitive glycoproteins contain sialic acids [278,281,282], the increased expression of Siaα2-6Gal observed in the brain of infected chickens needs careful interpretation and further investigation to understand its role in influenza A virus neuropathogenicity.

In summary, the results obtained in this study indicate that the most likely pathway for entry of the H7N1 HPAI virus into the chicken brain is the haematogenous route. This is supported by the fact that brain endothelial cells, Chp and ependymal cells hold large numbers of influenza A virus receptors in their surface, which could play an important role, together with the CSF, in the entry and early dissemination of the virus. Further studies are needed to explain the exact mechanism leading to the disruption of the BBB by influenza A virus.

5. Study III: Mechanism of disruption of the Blood brain barrier (BBB) in chickens infected with a highly pathogenic avian influenza A virus (H7N1).

5.1. Introduction

HPAI viruses cause a very severe and acute disease that usually induces high mortality and CNS lesions in poultry species [108,125,135,144,149]. CNS lesions induced by influenza viruses have also been described in a number of animal species, including: wild birds, cats, horses and laboratory animals [205,206,210,235,237,240,283,284,285,286]. In fact, recent studies in ducks and mice show that the capacity of some HPAI virus strains, such as H5N1, to cause systemic illness and produce CNS lesions have increased with the years [287]. Also, CNS lesions induced by influenza have been sporadically reported in humans infected with different influenza virus strains (mainly of H1N1 and H3N2 subtypes) [288,289,290,291,292,293].

Most of the studies on influenza virus neuropathogenicity have been conducted on mice, as this model is characterized by the induction of CNS lesions and entry of the virus into the CNS using nervous routes [203,204,205,206,210,294,295]. The mouse model has been useful to study the non-purulent encephalopathies observed in humans associated to influenza virus infection, that included the von Economo's encephalitis or encephalitis lethargica and the post-encephalitic Parkinsonism [296] which are hypothesized to occur by virus invasion of the brain using a nervous route. On the other hand, there are a second group of human influenza-associated encephalopathies that are characterized by the induction of necrotizing encephalopathy and include the acute necrotizing encephalopathy (ANE) of childhoods [272,297], the hemorrhagic shock and encephalopathy [298], and the Reye's syndrome [299]. This group of encephalopathies are believed to occur through disruption of the BBB [204]. In the previous study, the topographical distribution of a HPAI virus H7N1 in the CNS at early stages of infection was described. It was concluded that the virus spreads to the CNS by the haematogenous route and it likely, enters the brain after disruption of the BBB [255]. Thus, our previous findings also indicated that the chicken model could be a good animal model to understand the mechanism of this second group of influenza-associated

encephalopathies; nevertheless, the mechanism of disruption of the BBB in chickens has still to be elucidated.

The BBB is a neurovascular filtering system that also serves as diffusion selective barrier and mechanism of protection for the brain, avoiding the entry of potentially toxic molecules and infectious agents. The BBB is composed of endothelial cells that are firmly sealed with TJs, and supporting cells. The last ones include astrocytes, microglia, pericytes, and neurons, which together with the endothelial cells form the neurovascular unit [300]. TJs are considered the truly structural and anatomical BBB [244] and consist of a network of transmembrane, cytoplasmatic and accessory proteins, that include: occludin, claudin (1, 3, 5, and 11), JAMs, ZO-1, 2, 3, and the accessory proteins cingulin, AF-6, and 7H6 [301,302]. The TJs form a seal between endothelial cells and provide to the brain with a high transendothelial electrical resistance that limits the movement of solutes [303]. However, this barrier can be crossed by different pathogens, such as HIV, SIV, measles virus, human cytomegalovirus (HCMV), human T-cell leukemia virus (HTLV) and West Nile virus, which have developed different strategies that include: 1) the passage of cell-free virus into the brain using paracellular or transcellular routes, 2) transversal of the BBB inside infected leucocytes or “Trojan horse” mechanism, and 3) direct replication of the virus on endothelial cells or astrocytes causing BBB breakdown and entry of the virus to the brain parenchyma [244,304,305,306,307].

Then, the main objective of this study was to demonstrate that the HPAI virus H7N1 (A/Chicken/Italy/5093/99) invades the CNS through the disrupted BBB in chickens. Moreover, the general mechanism used by this HPAI virus to damage the BBB was investigated in experimentally infected chickens. Also, the first cells affected by the virus as it enters the brain, and time of entry, were determined.

5.2. Material and Methods

5.2.1. Virus inoculums

The influenza virus used on this study corresponds to a fifth passage H7N1 HPAI virus strain A/Ck/It/5093/99 that possesses an intravenous pathogenicity index of 2.8. To prepare the virus for the study, it was propagated once in 10-day-old embryonated SPF chicken eggs. Allantoic fluid was titrated according to the method of Reed and Muench [213] and later diluted in PBS to obtain a dose of 10^6 ELD_{50} in 0.05mL (50µL).

5.2.2. Experimental design

In order to determine the mechanism and time of disruption of the BBB, sixty four fifteen day old SPF chickens were divided into two groups. The first group consisted of 46 chickens that were intranasally inoculated with 10^6 EI of H7N1 A/Chicken/Italy/5093/99, HPAI virus, and a second group of 18 chickens that were used as uninfected control chickens. The 46 infected chickens of the first group were further subdivided in three sampling groups (A, B, C). At the same time, the 18 uninfected chickens were used as control for the sampling group A (six chickens) and B (12 chickens) groups. Blood samples were taken from all animals in order to determine the presence of viraemia (Figure 18).

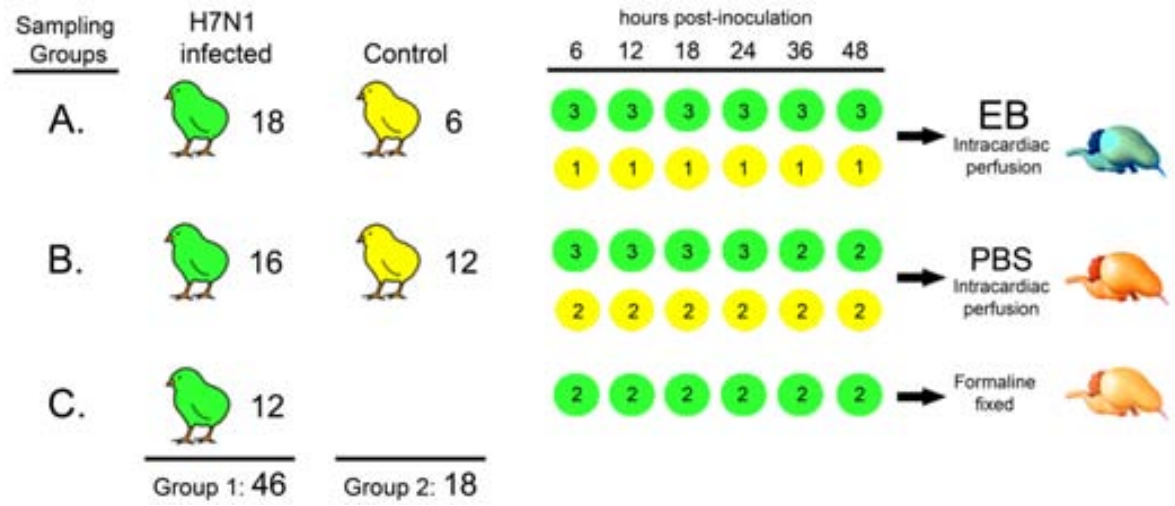

Figure 18. Experimental design: distribution of chickens and procedures performed in each group.

The sampling group A consisted of 18 infected chickens that were used to evaluate the BBB stability by means of the intracardial perfusion of the IF tracer Evans blue (EB) at 6, 12, 18, 24, 36 and 48 hpi (3 chickens each hpi). Additionally, one uninfected chicken was used as control, and also perfused and sampled at the same hpi. The perfusion was performed using first 50 mL of PBS and later 50 mL of a “cocktail” containing EB and paraformaldehyde diluted in PBS pH 7.2, prepared as previously described [308]. To perfuse the chickens, they were deeply anesthetized with 50 mg/kg of sodium pentobarbital intravenously. Once the chickens were unresponsive to stimulus, the coelomic cavity was immediately opened. Later, a polished 21-gauge needle was inserted through the left ventricle into the ascending aorta and rapidly a gravity-dependent perfusion system was connected to the needle. Then, an incision was made into the right atria to drain incoming venous blood and the perfusion solution that was allowed to enter into the left ventricle. The mean flux rate was 2 mL/minute. Brain samples of these chickens were carefully collected and used to determine the presence of EB and IgY extravasation.

The sampling group B consisted of sixteen infected chickens that were perfused only with PBS. Similar to the previous group, perfused brain samples of three chickens were collected at 6, 12, 18, 24 hpi, whereas at 36 and 48 hpi, two infected chickens were evaluated. Perfused brain samples of two control

uninfected chickens were examined at the same hpi. Brain samples obtained from these chickens were cut in five coronal sections and immediately embedded in (OCT-Fast Frozen compound) (Tissue-Tek, Torrance, CA), fast frozen in isopentane (M32631, Sigma-Aldrich Química, S.A.) on liquid nitrogen, and stored at -80C until use. On these samples, the presence of IgY extravasation and influenza A virus antigen was assessed, as well as, the pattern of staining for ZO-1 and claudin-1 proteins.

The third sampling group (C) included 12 infected non-perfused chickens, which brains were sampled at 6, 12, 18, 24, 36 and 48 hpi (two at each hpi), and fixed in 10% buffered formalin. These chicken brains were used to determine the distribution of the influenza A virus antigen at the first hpi.

5.2.3. Processing of EB perfused chicken brain samples and analysis

EB perfused brain samples obtained from the sample group A, were postfixed in 4% paraformadehyde (15714, Electron Microscopy Science) for 12 hours and cryoprotected by immersion in 30% sucrose (84097, Sigma-Aldrich Química, S.A.) for 24 hours. Afterwards, brains were cut in six gross coronal sections embedded in cryostat-embedding compound (OCT-Fast Frozen compound) (Tissue-Tek, Torrance, CA), and fast frozen using isopentane (M32631, Sigma-Aldrich Química, S.A.) chilled in liquid nitrogen. Samples were stored at -80°C until they were used. Later, ten µm thick cryostat sections were obtained at −22 °C (Leyca Microsystems, Germany), mounted on SuperFrost plus glass slides (631-9483, VWR International Eurolab, S.L) and stored, until further use at−20 °C. To directly evaluate the disruption of the BBB, slides of the six coronal sections from perfused infected and control chickens were fixed with acetone for five minutes, washed three times for five minutes with PBS pH 7.4, and directly cover-slipped using Vectashield mounting media (H-1000, Vector Labs, Burlingame, CA). Images from these samples were captured with a spot digital camera (Nikon DXM1200F) coupled to a Nikon microscope (Nikon eclipse 90i) and using the software Nikon ACT-1.

5.2.4. IF staining for the detection of influenza A virus antigen in perfused and fresh frozen brain sections

Sequential brain sections from all infected EB and PBS perfused chickens, as well as brain sections from control chickens collected at 6, 12, 18, 24, 36 and 48 hpi, were cut to a 10μm thickness, mounted on SuperFrost plus and stored at -20°C until they were used. Later, sections were allowed to thaw for 30 minutes at RT and later fixed using 95% ethanol at 4°C for 15 minutes and acetone for one minute at RT. Samples were then rinsed three times with PBS pH 7.4 and blocked with 2% BSA (85040C, Sigma-Aldrich Química, S.A.) in PBS pH 7.4, containing 0.1% triton X-100 (T8787, Sigma-Aldrich Química, S.A.), one hour at RT. After that, brain sections were incubated overnight with the anti-NP monoclonal antibody (ATCC, HB-65, H16L-10-4R5) diluted 1:100 in blocking buffer, at 4°C, overnight. The second day, samples were rinsed with PBS and incubated with the secondary antibody DyLight488 goat anti-mouse IgG (115-485-166, Jackson ImmunoResearch Lab, USA), diluted 1:200 in PBS for 1hour, at RT. Nuclear counterstaining was performed using Hoechst 33258 (Sigma-Aldrich Química, S.A.), diluted 1:500 in PBS for 10 minutes, at RT. Samples were rinsed with PBS and cover sliped with anti-fade Vectashield mounting medium. Negative controls consisted of sequential samples of the same tissue incubated with blocking buffer instead the primary antibody. A positive control was also included with each batch and consisted of tissues of chicken embryos inoculated with the same H7N1 HPAI virus strain. EB extravasation zones were visualized in red colour, whereas, influenza A virus antigen was seen in green colour. Photographs were merged using Adobe Photoshop CS2 (Adobe System Inc., San Jose, CA).

5.2.5. IF staining for the detection of IgY extravasation in perfused brain sections

The breakdown of the BBB was also evaluated by means of the detection of increase in the vascular permeability to the endogenous protein IgY. To do that, ten μm thick cryostat brain sections from two infected chickens perfused

with EB and three perfused with PBS as well as control uninfected chickens were processed as described above for the detection of the influenza A virus antigen, with some modifications. Briefly, tissue sections were blocked using 5% normal donkey serum (NDS) (D9663, Sigma-Aldrich Química, S.A), 1% BSA, and 0.2% triton diluted in PBS pH 7.4 (5% NDS/1% BSA/0.1% triton). Later, they were incubated with fluorescein isothiocyanate (FITC)-conjugated donkey anti-chicken IgY (H+L) (DAIgY-F, Gallus immunotech, Inc, Canada) diluted 1:50 in the same blocking buffer. IgY extravasation was observed in green around the vessels. Brain sections of mice were used as a negative control to evaluate the specificity of the antibody, considering that the primary antibody was directed against the chicken IgY which differed antigenically from the mammalian IgG [309,310,311].

5.2.6. Double IF staining for codetection of IgY leakage and influenza A virus antigen in fresh frozen brain sections

With the aim to determine the presence of IgY extravasation in influenza A virus positive zones, fresh frozen brain sections from infected and control chickens collected at 18, 24, 36 and 48 hpi, were processed as previously described for the detection of IgY, with some modifications. Briefly, ten μm brain sections were incubated with a mix of FITC-conjugated donkey anti-chicken IgY (H+L) (1:50) and anti-NP monoclonal antibody (ATCC, HB-65, H16L-10-4R5) (1:100) diluted 1:100 in 5% NDS/1% BSA/0.1% triton in a total of 200 μm per section, and incubated at 4°C, overnight. Later, the samples were incubated with Cy3 goat anti-mouse IgG (H+L) (115-165-003, Jackson ImmunoResearch Lab, USA) diluted 1:200 in PBS, for 1 hour at RT. The unspecific binding of the Cy3 secondary antibody to the IgY antibody, was tested incubating sequential brain slides of the same chickens with the FITC donkey anti-chicken IgY antibody alone, followed by 1 hour of incubation with the secondary antibody Cy3 goat anti-mouse IgG.

5.2.7. IF staining for the detection of the TJs proteins Claudin-1 and ZO-1 in perfused brain sections

In order to evaluate the effect of the virus over the BBB, the presence, distribution and pattern of staining of the BBB proteins ZO-1 and Claudin-1, were tested in brain sections from all chickens perfused with PBS and control chickens subjected to the same process and obtained in the same sampling hours. To do that, the same protocol used for the detection of the influenza A virus nucleoprotein was used to detect the ZO-1 and claudin-1, with some modifications. Briefly, ten μm cryostat brain sections were incubated with the primary antibodies: anti-ZO-1 rat monoclonal antibody (Clone R40.76, Chemicon, Tamecula, CA. USA) or the anti-claudin-1 rabbit antibody (51-9000, Invitrogen, S.A.) diluted 1:50 in PBS containing 1% BSA and 0.1% triton, at 4°C overnight. The ZO-1 signal was visualized using the secondary antibody DyLight 488 rabbit-anti-rat IgG (312-485-003, Jackson ImmunoResearch Lab, USA), whereas the claudin-1 was detected using a goat–anti-rabbit FITC (F9887, Sigma-Aldrich Química, S.A.). Both secondary antibodies were diluted 1:200 in PBS, for 1 hour at RT. Positive controls for the detection of Claudin-1 were brain samples from a rat, whereas the specificity of the ZO-1 was tested in brain samples of mice. Negative controls consisted of sequential sections of the same brain samples evaluated, but incubated with blocking buffer instead of the corresponding primary antibody. Both signals were observed in green.

5.2.8. Double IF staining for the codetection of ZO-1 and influenza A virus antigen in fresh frozen brains sections

Fresh frozen brain sections of two infected and one control chickens collected at 6, 12, 18, 24, 36 and 48 hpi were processed for the codetection of ZO-1 and influenza A virus antigen. To do that, 10μm cryostat sections were incubated first with the anti-ZO-1 rat monoclonal antibody diluted 1:50 in blocking buffer prepared as already described for the detection of influenza A virus antigen and incubated at 4°C overnight. Afterwards, they were incubated with the secondary antibody Cy3-goat anti-rat IgG (H+L) (112-165-062, Jackson ImmunoResearch

Lab, USA) diluted 1:200 in 1% BSA PBS pH 7.4, for 1 hr at RT. After that, samples were blocked using 2% BSA in PBS, for 1 hr and incubated with anti-influenza virus nucleoprotein monoclonal antibody (ATCC, HB-65, H16L-10-4R5) diluted 1:100 in same blocking buffer, at 4°C, overnight. The third day, samples were incubated with Cy2-goat anti-mouse IgG, subclass 2a (115-225-206, Jackson ImmunoResearch Lab, USA) diluted 1:100 in PBS pH 7.4, for 1 hr at RT. In this case, the ZO-1 staining was visualized in red and the influenza A virus antigen was seen in green. Negative controls consisted of incubation of a sequential sample with 2% BSA in PBS instead of each primary antibody. Unspecific binding of both secondary antibodies were discarded by incubating them with the contrary primary antibody.

5.2.9. IHC staining to determine the topographical distribution of the viral antigen and initial target cells in the brain of chickens during the first hpi.

Formalin-fixed brain samples were cut in six different coronal sections and later embedded in paraffin. The immunohistochemistry technique used for the detection of influenza A virus NP was performed as previously described [216]. Briefly, brain sections (3 μm thick) were dewaxed and treated with 3% H_2O_2 in methanol to eliminate the endogenous peroxidase. Later, antigen retrieval was performed using protease at 37ºC for 10 minutes followed by incubation with the primary monoclonal antibody (ATCC, HB-65, H16L-10-4R5) diluted 1:250, at 4ºC overnight. On the second day, samples were incubated with biotinylated goat anti-mouse IgG secondary antibody (Dako, immunoglobulins AS, Denmark), and the ABC complex (Thermo Fisher Scientific, Rockford, IL, USA). The reaction was developed with DAB (Sigma-Aldrich, MO, USA) at RT, and counterstained with Mayer's haematoxylin.

The distribution, intensity and pattern of viral antigen staining in the CNS of chickens at each hpi was evaluated and later scored as described in the third study. In brief, of the six different coronal sections the following regions were evaluated: the OB, *telencephalic pallium* (Pall), *subpallium* (Spall) (that contains

the *striatum* (St)), *hypothalamus* (H), optic area (Och), diencephalon (that contains the *prethalamus* (p3), *thalamus* (p2), *pretectum* (p1), and secondary prosencephalon (2P)), midbrain or mesencephalon, hindbrain (that contains the *isthmus* (Ist) and rhombencephalon (r1-6)), and the *cerebellum* (Cb). In these regions, the number of viral antigen positive cells in 10x fields was counted. As the extension of each region was variable, an average was calculated for each region. At the same time, at 36 and 48 hpi, an arithmetic mean for each region was obtain for the two animals evaluated. The scoring system used to evaluate the intensity of the staining was as follows: nil (0: no labelling detected); scarce (1: less than 20 nuclei of cells positive for viral antigen on average), slight (2: more than 20 but less than 100 positive cells on average). We did not use the rank of moderate and intense viral antigen staining, because in comparison with the study II the number of positive cells was low (less than 100 positive cell per 10x field [216]. Finally, the topographical distribution of the viral antigen staining was graphically represented in the six coronal sections, using the Adobe Photoshop CS2 program.

5.2.10. Quantification of viral RNA by RT-qPCR in the blood of chickens

The RT-qPCR technique used to quantify the viral RNA copies in blood and brain tissue samples have been thoroughly described previously [251]. Briefly, viral RNA was extracted from each sample using a QIAamp viral mini kit (Qiagen, Hilden, Germany). To do that the RNA was eluted in 40 µl and tested by one-step RT-qPCR for the detection of a highly conserved region of the M1 gene of H7N1 influenza A viruses using primers [252] and the amplification conditions previously described [251]. This procedure uses an IPC to avoid false negative results due to RT-PCR inhibitors.

5.3. Results

5.3.1. Clinical evaluation

No clinical signs compatible with HPAI virus infection, such as, depression, ruffled feathers, prostration or skin haemorrhages were observed on the infected and control chickens. Neither were gross lesions observed at any hpi.

5.3.2. EB extravasation in brains of control and H7N1 inoculated chickens

EB extravasation on infected animals was not detected until 48 hpi, when multiple foci of intense and bright red staining were observed. These foci corresponded to blood microvessels of different calibre which usually showed a rim of EB leakiness or vessels showing a fan shape of EB extravasation (Figure 19-C1, C4). In such areas of EB extravasation, the neuropil and neural cells were intensely stained. These foci were found widely distributed in the brain of infected chickens, but they were especially frequent in the *telencephalic pallium* and *cerebellum* (Cb), followed by the *thalamus* (p2), *subpallium* (Spall) and brain stem. In the OB, diencephalon, mesencephalon and rhombencephalon less foci of EB extravasation were observed. No evidence of EB leakage was observed in the brain of control chickens at any hpi. In the control chickens, the EB staining was imperceptible and restricted to the lumen of some vessels along the brain and in the meninges (Figure 19-A1, A4). Also, the endothelial cells in the Chp showed EB staining, furthermore, some epithelial cells of the Chp have weak EB staining. The CVOs which are brain areas normally lacking a BBB, including the ME and AP showed light staining. Similarly, the brain of chickens perfused a 6 hpi, 12, 18, and 24 hpi showed only weak EB staining in blood vessels, but not diffusion to the surrounding brain tissue.

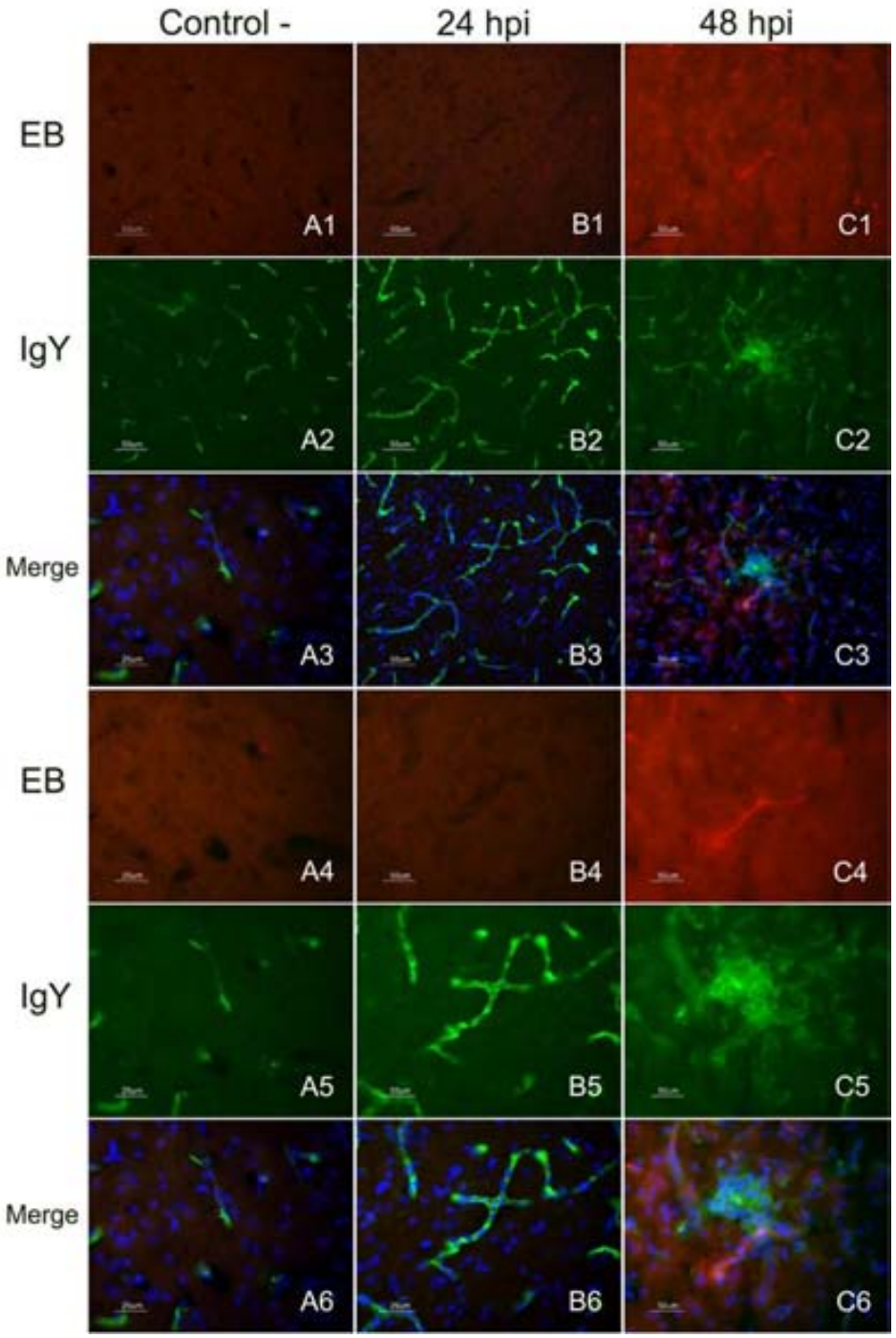

Figure 19. Representative images from EB perfused brains obtained at the level of the *telencephalic pallium* (Pall) and double staining with IgY in control and infected chickens. EB extravasion was only observed in brain samples of chickens evaluated at 48hpi. Images at two different magnifications showing a microvessel with a fan-like area of EB leakage (red colour) (C1,C4). No EB extravasation was observed in the control and infected chickens at 24hpi, perfused with EB (A1, A4 in control chickens and B1, B4 in infected chickens at 24 hpi). Leakage of the serum protein IgY (C2, C5) was observed in the lumen of the vessel and the nearest brain cells in infected chickens perfused at 48 hpi. IgY staining in control (A2, A5) and infected chickens at 24 hpi (B2, B5) was limited to the lumen of the vessels. Double staining allowed demonstrating the presence of colocalization of IgY leakage in areas of EB extravasation in chickens evaluated at 48 hpi (C3, C6). Controls and infected chickens evaluated at 24 hpi did not show EB leakage and the IgY staining was limited to the lumen of the vessels.

5.3.3. IF staining for the detection of influenza A virus antigen in perfused and fresh frozen brain sections

Influenza A virus antigen was detected in zones of EB extravasation at 48 hpi, but regularly the influenza A virus positive zones were more extensive than the EB diffusion ratio (Figure 20). It was also common to see brain microvessels showing extravasion of EB without presence of viral antigen. These areas of EB and viral antigen co-localization were commonly observed multifocally in the telencephalon and *cerebellum* (Cb). They were observed less frequently in the diencephalon, mesencephalon and rhombencephalon. In these areas, the presence of viral antigen and EB extravasation was multifocal and exceptionally in the Rot nucleus was located bilaterally in the vessels surrounding this nuclei. Influenza A virus antigen was also observed in tissue of PBS perfused-infected chickens at 24, 36 and 48 hpi. At 24 hpi, the staining was restricted to endothelial cells of blood vessels. On this day, the influenza A virus antigen was observed mainly in the nucleus but also in the cytoplasm of few endothelial cells. At 36 and 48 hpi, positive parenchymal cells (glial cells and neurons) were found forming foci or as individual positive cells. Besides, influenza A virus antigen was detected in ependymal cells lining the lateral, third and fourth ventricles, as well as in the meninges at these same hpi. The presence of viral antigen was mainly observed in the nucleus neural and glial cells, but also it was detected in the cytoplasmic prolongation of these cells, as well as the neuropil.

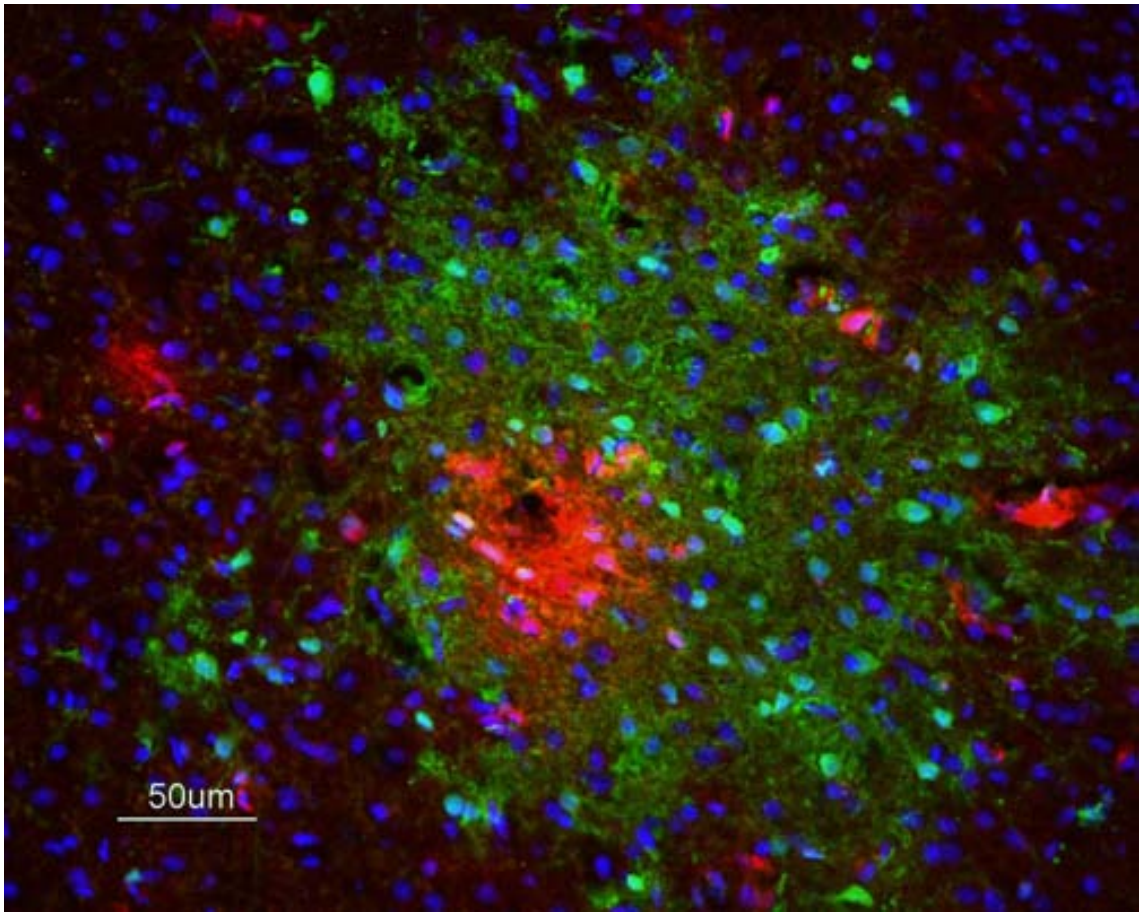

Figure 20. IF image showing EB extravasation (red) and influenza viral antigen (green) forming a large halo surrounding the area of EB leakage.

5.3.4. IF staining for the detection of IgY extravasation in perfused brain sections

The detection of IgY was used to determine the limits of the brain microvessels and the extravasation of this endogenous protein toward the extravascular space [312,313,314]. IgY staining was observed restricted to the lumen of blood microvessels in the parenchyma of the brain, meninges and Chp of control chickens (Figure 19-A2, A5), as well as, in samples of infected chickens from 6 to 24 hpi (Figure 19-B2, B5). CVOs were diffusely immunostained, showing IgY widely distributed in the vessels, ependymal cells and parenchyma in healthy and infected chickens. IgY leakage was seen in infected chickens at 36 and 48 hpi. The most affected brain regions were the *telencephalic pallium* (Pall) and *cerebellum* (Cb) where the IgY extravasation was multifocal. In these

regions, IgY extravasation was observed as a slightly stained, green rim around the vessels and as focal zones of diffusion where the neuropil and nearest glial and neural cells showed green staining (Figure 19-C2, C5). The IgY extravasation increased with time, being at its most severe at 48 hpi. Other brain regions, such as the diencephalon and mesencephalon showed zones of IgY extravasation, however, there they were less severe and frequent.

5.3.5. Codetection of IgY extravasation and viral antigen in fresh frozen brain samples

Colocalization of IgY extravasation zones and presence of influenza virus antigen was observed in infected chickens at 36 and 48 hpi (Figure 21). This codetection was most evident in sites where the IgY leakage formed large foci (Figure 21, B1). In general, the diameter of the IgY extravasation staining was equal in extension with respect to the diameter of the positive influenza virus antigen foci.

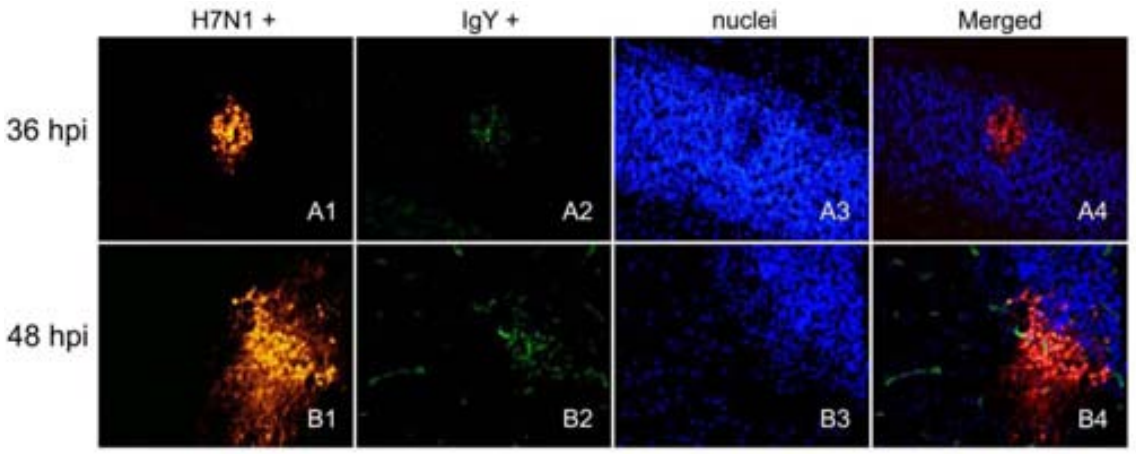

Figure 21. Representative images showing the codetection of influenza viral antigen and IgY extravasation in the cerebellum of infected chickens at 36 and 48 hpi. Influenza virall antigen was found focally infecting the endothelium and a group of neural cells between the Purkinje and granular layer of the *cerebellum* (Cb) (A1, B1) at 36 and 48 hpi, but with evident increase in intensity at 48 hpi (B1). IgY extravasation was found in the same focus (A2, B2), staining the neuropil and brain cells surrounding the affected vessel. The superimposed image (A4, B4) showed that the IgY extravasation foci corresponded to an area where there was influenza viral antigen.

5.3.6. IF staining for the detection of the TJs proteins Claudin-1 and ZO-1 in the brain of chickens

ZO-1 staining was observed as a continuous line externally bordering the endothelial cells in the brain parenchyma (Figure 22-A, C), meninges, Chp and the CVOs (AP and ME). In the arterioles, the ZO-1 staining showed a transverse line joining the cells. ZO-1 was also found between epithelial of the Chp, where the protein outlined the perimeter of the cells giving a honeycomb appearance. A similar pattern was observed in the CVOs but it was denser than in the Chp. Claudin-1 staining was only observed in the CVOs (AP) and the Chp, where the same pattern of staining as for ZO-1 was seen. Neither of the TJs proteins were detected between the ependymal cells. The intensity and pattern of staining for Claudin-1 did not show differences between control and infected chickens at any hpi. In contrast, the pattern of staining for ZO-1 showed changes in infected chickens evaluated at 36 and 48 hpi in comparison with the negative controls. These alterations consisted mainly of focal loss of the characteristic structure of the blood vessels, which seemed discontinuous or with granular appearance (Figure 22, B). Besides this, at 48 hpi, there were foci where the ZO-1 staining was totally absent (Figure 22, D). The pattern and intensity of staining for ZO-1 and claudin-1 in the CVOs and Chp did not show visible alterations in the infected animals at any hpi.

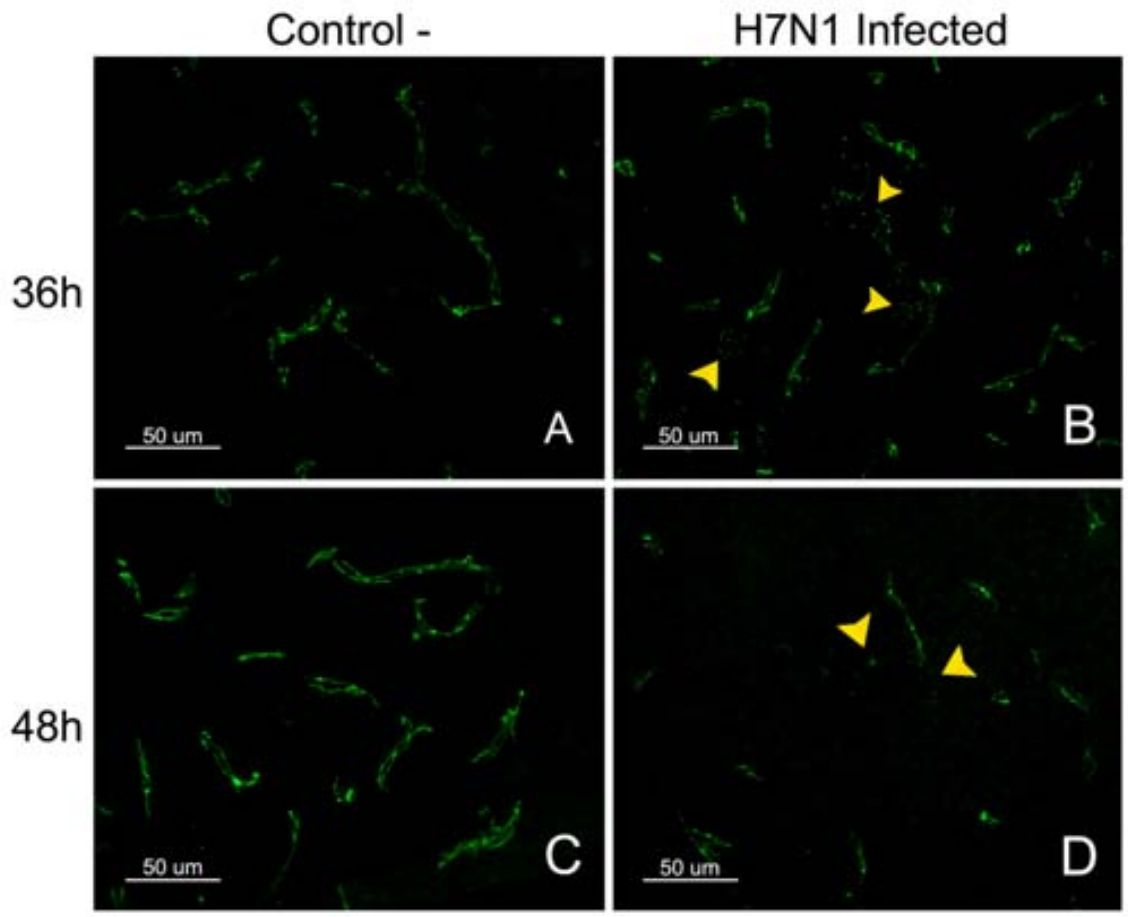

Figure 22. Representative images showing the pattern of staining for the TJs marker ZO-1, in the *telencephalic pallium* (Pall) of control and infected chickens sampled at 36 and 48 hpi. ZO-1 staining in control chickens was observed as a linear and continuous line in both sides of the vessels (A, B). In contrast, a granular and discontinuous appearance of the blood vessels was observed in the brain of infected chickens at 36 hpi (B). Loss of ZO-1 was multifocally observed in the brain of chickens after 48 hpi (D).

5.3.7. Double IF staining for the codetection of ZO-1 and influenza A virus antigen

To confirm that the abnormal pattern of ZO-1 staining or its absence could be the consequence of the direct replication of the H7N1 HPAI virus, a double IF was performed in brain samples of infected and control chickens at 18, 24, 36 and 48 hpi. This double staining made it possible to determine that the foci where there are loss of ZO-1 staining correspond to areas where viral antigen was present (Figure 23).

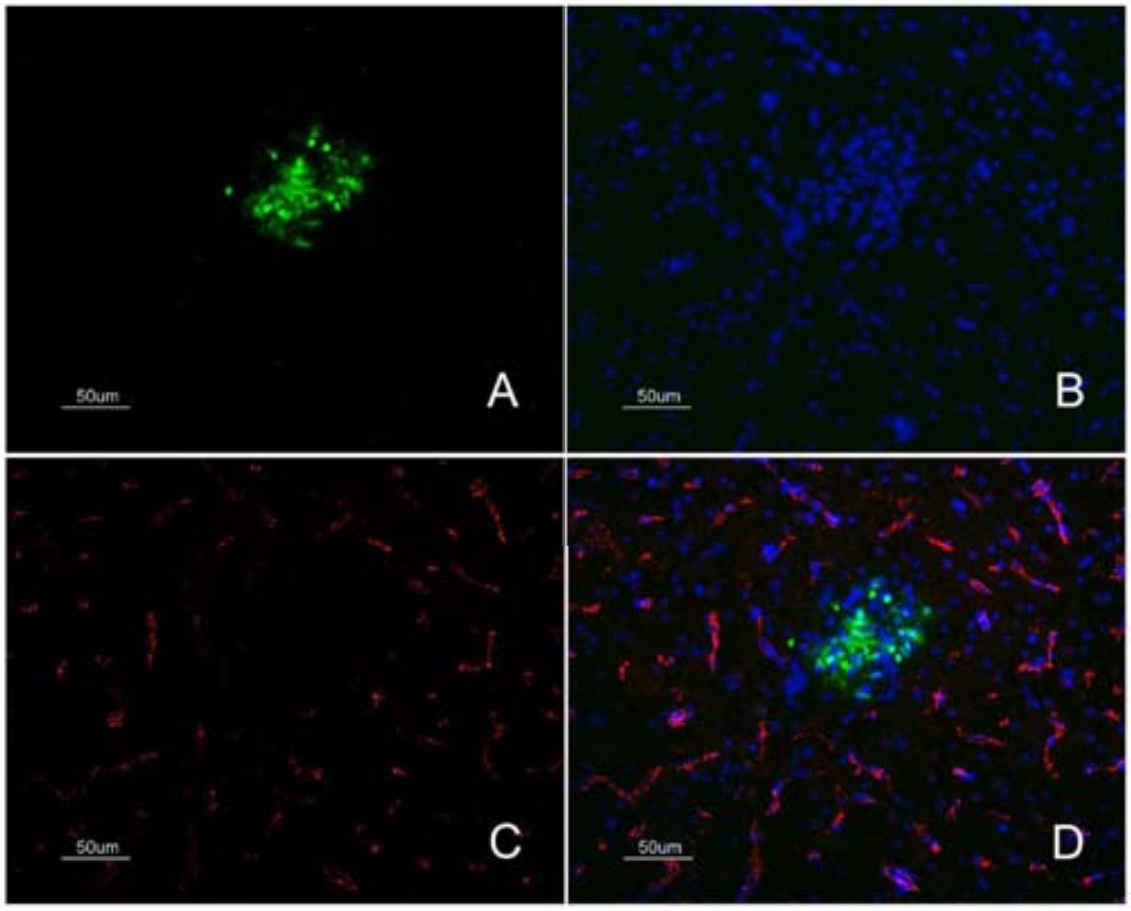

Figure 23. Codetection of influenza A viral antigen and ZO-1 in the brain of a chicken infected at 36 hpi (merge image D). Representative images showing the loss of ZO-1 marker (C) (labelled in red colour) in a focus of gliosis (B) positive for influenza viral antigen (A) (labelled in green colour) found in the *telencephalic pallium* (Pall).

5.3.8. Detection of viral antigen and pattern of distribution during the first hpi in formalin-fixed brain sections

Viral antigen was detected in formalin fixed tissues at 24, 36 and 48 hpi. At 24 hpi, the viral antigen detected was scarce and restricted to the nucleus of few individual endothelial cells in the *telencephalic pallium* (Lpall and Vpall), mesencephalon and *cerebellum* (Cb) of one chicken (Figure 24). At 36 and 48 hpi, multiple foci consisting of viral antigen positive endothelial cells, glial cells and neurons were found mainly in the *telencephalic pallium* (Dpall, Lpall, and Vpall) and the *cerebellum* (Cb). Viral antigen was also observed in the *subpallidum* (SPall), *prethalamus* (p3), *thalamus* (p2), mesencephalon, and the rhombomeres 3 and 4. These foci were composed of a variable number of positive cells (5-70 cells), in which the viral antigen staining was mainly found in

the nucleus of the cells and occasionally in the cytoplasm. At 48 hpi, there were also few foci where the neuropil showed positive granular staining. In general, the intensity of positive viral antigen was highest in the intermediate area of the telencephalon in comparison with the OB and most cranial areas of the brain. Viral antigen staining of ependymal cells was not detected until 48 hpi, and consisted of a line of positive cells (10-70) cells focally in the lateral, third and fourth ventricle. Similar to the other cells of the brain, the viral antigen staining was mainly nuclear. No viral antigen was observed in epithelial cell of the Chp. Evidence of bilateral staining was only observed in the *thalamus* (p2) at 36 and 48 hpi, and consisted of a scarce number of endothelial cells or neurons showing positivity. None of the CVOs evaluated (AP, ME) showed viral antigen staining at any time postinfection.

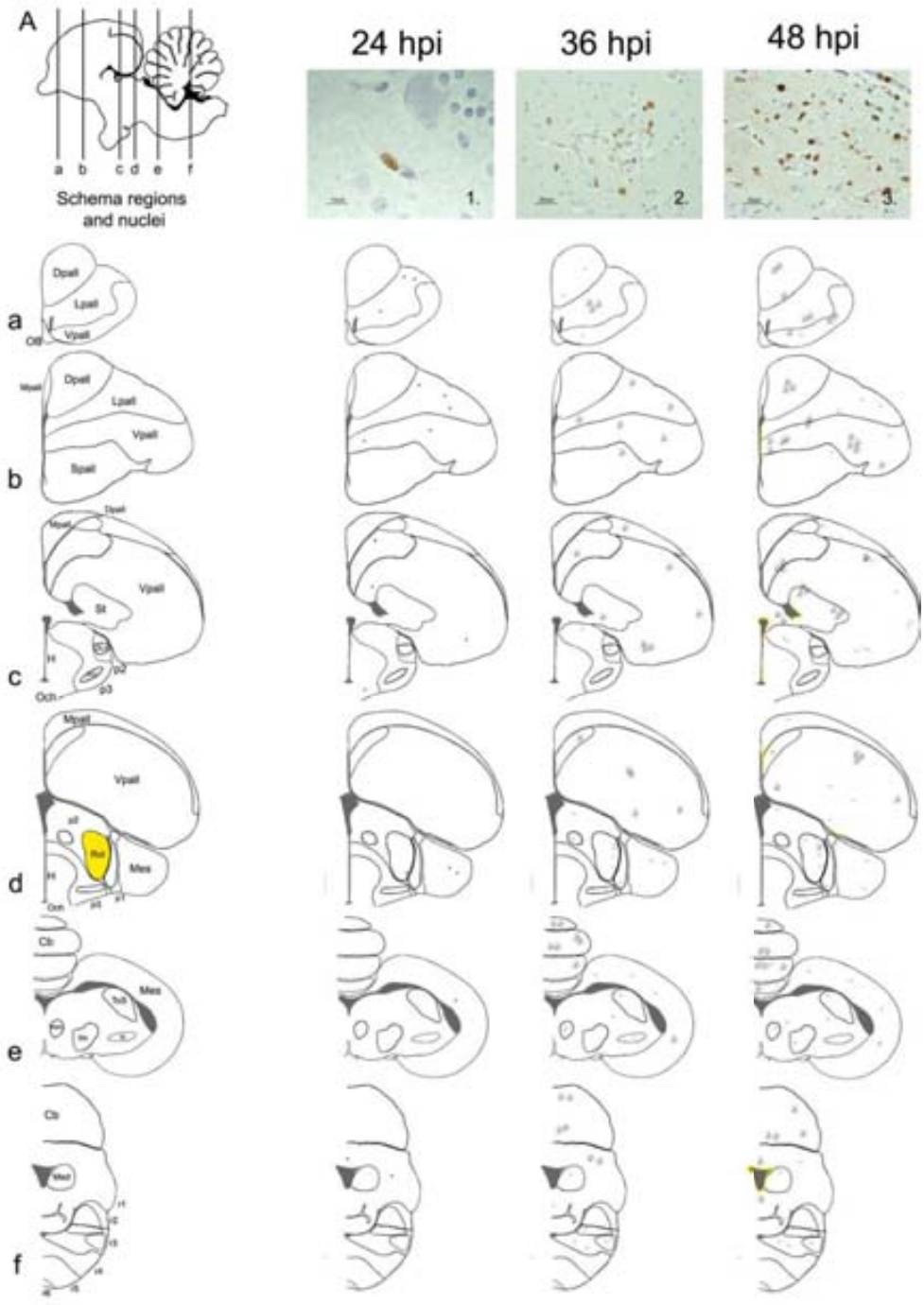

Figure 24. Shematic image showing the topographical distribution of the influenza A virus antigen detected at 24, 36 and 48 hpi, in chickens infected with a HPAI virus H7N1 detected by means of IHC. A. Schematic sagittal drawing of the chicken's brain showing the coronal levels represented in the diagrams below (a, b, c, d, e, f). In this study, the intensity of the staining was always scarce; consequently, in the diagram corresponding to 24 hpi, a dot was drawed in those regions where a positive cell was found. Microphotography 1. shows an endothelial cell with positive viral antigen staining in the nucleus. At 36 and 48 hpi, the intensity of influenza virus antigen staining was slight, varying the number of cell from 2 to 80 positive cells per foci. Bilateral staining was only found in the Rot (*thalamus*- p2) at these hours (labelled in yellow in the diagram of the left). Microphotography 2. shows several positive cells surrounding a disrupted capillary at 36 hpi, located in the Rot (p2). Positive viral antigen was detected in few ependymal cells until 48 hpi. Microphotography 3. shows the presence of viral antigen in endothelial cells, glial cells, neurons, and ependymal cells.

5.3.9. Quantification of viral RNA by RT-qPCR in the blood of chickens

Viral RNA copies in blood were firstly detected in 2 out of 8 chickens sampled at 18 hpi (4.52 Log_{10} viral RNA copies/mL). Similar viral load was detected in 3 out of 8 chickens at 24 hpi (4.72 Log_{10} viral RNA copies/mL). Viral RNA levels increased at 36 hpi (5.60 Log_{10} viral RNA copies/mL), and at this point were detected in 6 out of 8 chickens. This levels reached a peak at 48 hpi (6.24 Log_{10} viral RNA copies/mL), when all the sampled chickens showed high levels of viral genome in blood (Figure 25).

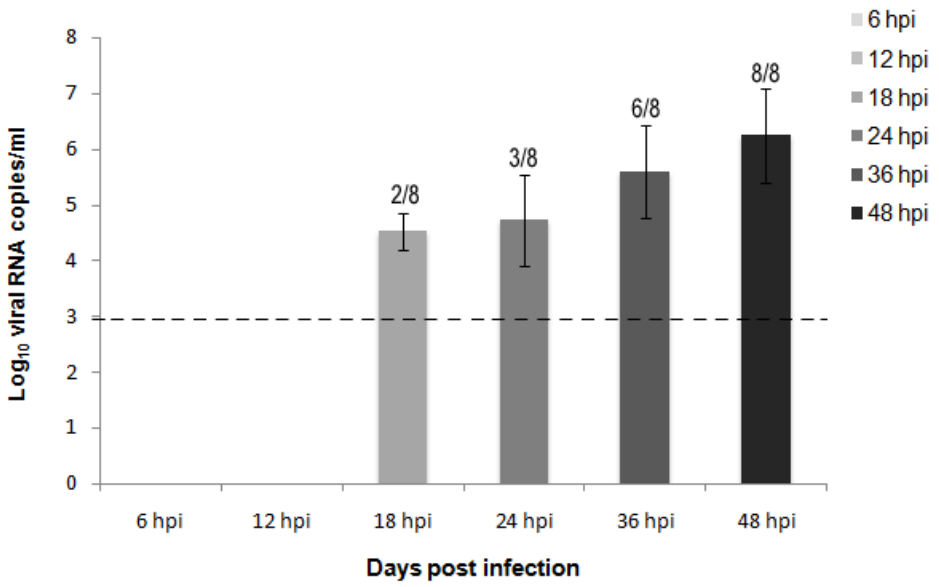

Figure 25. Influenza viral RNA detected by RT-qPCR in blood samples of chickens infected with a HPAI virus H7N1, collected at the indicated hpi. Viral RNA levels were expressed as log10 viral RNA copies/μl. Limit of detection is indicated with the dashed line. The number of positive samples from the total number of animals is indicated above each bar.

5.4. Discussion

HPAI viruses produce viraemia [106,223,224] and lesions in the CNS of chickens [119,138,144], which is hypothesized to occur by disruption of the BBB [144,204]. In general, the BBB can be disrupted by three mechanism that include: the paracellular and transcellular routes, the “Trojan horse” mechanism and the leakage of the infectious agent through the disrupted endothelial cells [305,315]. Then, in this study, SPF chickens infected with a HPAI virus H7N1 were examined during the first hpi, in order to evaluate the integrity of the BBB and determine the mechanism of the possible disruption. We proceeded to use three different methods to qualitatively evaluate the BBB permeability in chickens after inoculation with this HPAI virus.

The first method used to evaluate the integrity of the BBB consisted of the intracardial perfusion of the EB tracer at different hpi. This procedure has been frequently used on mice and rats to study different aspects of the pathogenesis of several infectious and non infectious diseases that affect the CNS, as well as to determine the efficacy of different therapies [316,317,318,319,320,321,322,323]. In contrast, this method has been scarcely used in chickens [324,325], and to our knowledge it has not been used to study the integrity of the BBB in chickens affected with infectious agents. In this study, chickens perfused with the fluorescence tracer EB every 6 hpi, demonstrated extravasation at 48 hpi. The most frequent zones where EB diffused from the circulating blood to the parenchyma were the *telencephalic pallium*, and the *cerebellum* followed by the *thalamus* (Rot), *subpallium* (Spall) and brain stem. EB leakage was observed as multiple foci, indicating that the loss of BBB function occurs simultaneously in multiple areas of the brain. Additionally, we were able to demonstrate the presence of viral antigen in some of these areas of extravasation, denoting that the EB leakage may be caused by the direct replication of the virus in brain cells. Evidence of the affinity of the virus for the *telencephalic pallium* (Pall) and the *cerebellum* (Cb) was also confirmed by conventional IHC, which shows that the viral antigen positive areas were mainly located in these same regions from 24 to 48 hpi. The distribution of the areas of EB extravasation and presence of viral antigen are in agreement with previous

studies in which three different HPAI viruses (A/chicken/Victoria/1/85 (H7N7), A/turkey/England/50-92/91 (H5N1), A/tern/South Africa/61 (H5N3), showed similar tropism in the brain [144]. Interestingly, we observed that the EB leakage occurs bilaterally in the *thalamus* (Rot), denoting that certain brain areas show different irrigation and could be more susceptible to the infection, as confirmed in the study of the topographical distribution of the virus. Similarly, in mice infected with influenza and humans affected with the influenza associated neurological disease (ANE) the lesions and viral antigen showed this distribution in the *thalamus* [270,272,326,327,328,329,330,331]. The affinity of the virus for these regions together with the increase extravasation of the EB marker in these areas could indicate that the BBB response may be different in each brain region, as is also suggested for other pathological insults [332,333,334].

With the second method, the integrity of the BBB was evaluated by means of the detection of increased vascular permeability of plasma proteins (IgY) at different hpi. In this study, extravascular distribution of the endogenous proteins IgY was demonstrated at 36 and 48 hpi. The deposition of IgY in the brain parenchyma increased with time, indicating a progressive increase in the severity of the BBB damage after infection. IgY extravasation areas coincided with EB leakage zones, however, the IgY staining was less intense and widespread than the EB staining. This discrepancy in the intensity of the staining and sensitivity in the detection of extravasion areas between both techniques may be related to differences in the sensitivity of both procedures and divergence in the molecular weight of both molecules which determine their penetration. That is, the IgY extravasated was detected using a less sensitive direct IF giving a slight staining [335], whereas, the EB perfusion technique made it possible to fix the sample at the same time that the animal is perfused given a bright colour in the zones of leakage [308]. Moreover, as the BBB did not allow the passage of soluble molecules greater than 400 Da [336,337], then the size of the molecules that are used as tracers may also determine the ability to detect minor changes in the permeability of the BBB. As a result, the IgY molecule (165000 Da) due to its large dimension [338] diffuses only when the damage to the BBB is severe and as also it spreads more slowly than small

molecules. Most of it remains trapped by the brain parenchyma close to the disrupted area [339]. For this reason, in this study the IgY molecule was found restricted to areas where viral antigen was present, indicating direct damage of the vessels and the nearest cells. In contrast, the EB molecule (960.81 Da) that binds to albumin (69000 Da) can spread easily from the point of disruption in the BBB to the parenchyma owing to its small size, which explained why it was found more widely distributed than the IgY protein and in areas where viral antigen was not detected. Both, the EB tracer and the IgY were found staining the cytoplasm and nucleus of the cells of the lesionated areas, which is in agreement with previous experiments were neuronal uptake of EB was related with presence of extravasation and injury to the CNS [308,316]. Similarly, the extravasation of plasma proteins (IgY) and the accumulation in neural cells, as observed in this study, has been related with permanent cell injury in the affected cells [339,340,341].

Finally, the third method consisted of the evaluation of the integrity of the BBB using the ZO-1 marker, which is a reliable indicator of the presence of undamaged TJs found between the endothelial cells of the BBB [342]. In this study, this marker helped to determine if the virus is able to enter into the brain by disrupting the TJs or by using transcellular or paracellular routes, as observed with other infectious agents, such as the West Nile virus that enter into the brain without impairing the integrity of the TJs [244,343]. On the contrary, in this study, we observed disorganization and loss of the continuous linear arrangement characteristic of ZO-1 in the brain of infected chickens sampled at 36 and 48 hpi. This pattern was mainly found as multiple foci in the telencephalon, diencephalon, mesencephalon and cerebellum. Besides this, there were focal areas where the ZO-1 marker was absent suggesting that the BBB was totally disrupted. The loss or dissociation of ZO-1 from the junctional complexes is associated with increased barrier permeability [344]. Similarly, decrease intensity of the staining with this marker has been observed in different pathological brain conditions reproduced in mice, and rat models such as those of ischemia [345], traumatic injury [346], stroke [347], as well as, human encephalitis caused by HIV [333], and in *in vitro* and *in vivo* models of HIV [348,349], SIV [350,351], and human T cell leukemia virus [352].

Codetection of ZO-1 and influenza A virus antigen made it possible to confirm that the core of the areas where there was lost of ZO-1 corresponded with viral antigen positive areas. This finding agrees with previous *in vivo* and *in vitro* studies which demonstrated loss of ZO-1 in the brain of mice (A/WSN/33) infected with influenza and *in vitro* in polarized epithelial cells infected with influenza [353].

Previous studies indicated that the TJs proteins, claudin-1, claudin-5, occludin and ZO-1 can be found in chicken endothelial cells [189]. However, in this study, claudin-1 was only found between the epithelial cells of the Chp and CVOs. This difference with respect to previous studies can be attributed to the use of antibodies that cross-react with claudin-3 in the old publications [189,303,354].

In a previous study from our group, influenza A antigen antigen was found in endothelial cells and the epithelium of the Chp, suggesting that these brain regions could be the initial sites of infection in the brain. Other viruses and other infectious agents use the Chp and CVOs, which form the BCSFB, to enter into the CNS, since these tissues have a fenestrated endothelium and a lower electrical resistance than the BBB. For example, the Chp is a portal of entry for canine distemper virus (CDV) [355], lymphocytic choriomeningitis virus (LCMV) [356], feline immunodeficiency virus (FIV) [357,358], and HIV [359]. Likewise, the CVOs may be a route of entry for *Trypanosoma brucei* parasites [268], Scrapie and BSE in sheep and goats [269,360,361]. In contrast, no alterations in the pattern and intensity of the staining with ZO-1 and claudin-1 were observed in the epithelial cells forming the Chp or in the tanycites (specialized ependymal cells of the CVOs) of infected chickens at any hpi. Therefore, evidence provided with this study indicates that the BCSFB did not contribute to the initial invasion of this HPAI virus H7N1 into the CNS.

Taken together our observations demonstrate that soon after inoculation, this HPAI virus H7N1 invades the bloodstream (18hpi), infecting first the

endothelial cells of the CNS where the virus replicates (24 hpi). Later, the virus surpasses the endothelial cells, causing alteration and disruption of the TJs (demonstrated by the loss of ZO-1) in the BBB (36-48 hpi). Soon after that or almost simultaneously, serum proteins leak from the bloodstream toward the tissue (IgY leakage) and the virus is found in the brain parenchymal cells (neurons and glial cells) (36-48 hpi).

6. General discussion

Several aspects of the HPAI virus infection in poultry have been repeatedly studied, especially the mechanisms of pathogenesis, immune response, transmission, and other features of the infection with H5 subtype HPAI viruses [81,104,108,112,126,135,143,149,152,230,362]. In contrast, investigations related to H7 subtype HPAI virus in poultry are designed to report the findings observed during natural outbreaks [111,212,220,222,233,363,364,365], which are informative, but do not provide deep knowledge about the pathogenesis of the disease. There are a few experimental studies using H7N7 [366,367], H7N3, and H7N6 HPAI viruses [117,367], in which similar lesions, plus replication of the virus in the endothelial and parenchymal cells of several organs have been observed. Some of these studies also demonstrated the high neurotropism of H7 HPAI viruses [366]. However, the early events leading to CNS lesions, during infections by HPAI viruses, have not yet been well characterized.

With the aim to understand the process of neural invasion by HPAI viruses, three studies were undertaken which have been presented in this thesis. In study I, the pathogenesis of the infection with a H7N1 HPAI virus was studied in SPF chickens and the effect of the dose in the clinical outcome and viral shedding was determined. In studies II and III, the neuropathogenesis induced by this H7N1 HPAI virus was studied with special emphasis upon elucidating the pathway of virus entry into the brain, and cell tropism. Additionally, in the third study, three different methods were applied to provide evidential support to the hypothesis of BBB disruption. The main findings obtained are critically reviewed in this general discussion, and the contributions and limitations of these findings to prove the hypothesis, are to be made clear. Other aspects which were central to each study were discussed at the end of each section and are not going to be repeated in this discussion.

In the first study, the model of H7N1 HPAI virus infection with chickens was set up, revealing that three different doses are able to infect the chickens with viral replication in different tissues and also that they are capable of induction of viral shedding. Additionally, it was determined that the highest dose enabled the study of the pathogenesis of the disease. This was due to the onset

of clinical signs and the type of gross and histopathological lesions being similar to those previously reported for other HPAI viruses [54,118,119]. One significant finding was that chickens receiving a very low dose of H7N1 HPAI virus ($10^{1.5}$ ELD_{50}) showed viral replication in different organs (brain and lung), and shed the virus in faeces and respiratory secretions. Similar findings have been reported in other studies of chickens infected with comparable doses of HPAI viruses ($10^{1.2}$ ELD_{50} to $10^{3.0}$) [368], indicating that chickens exposed to low doses can act as carriers, shedding viruses without showing any clinical signs. However, it has to be considered that in this study, the viral load was obtained using a RT-qPCR technique, which detects the vRNA, cRNA and mRNA [251]. This technique is unable to discriminate if the RNA is forming encapsidated and intact envelope viruses, or defective particles, which are not considered infectious [251,252]. Therefore, the use of other techniques such as VI in chicken eggs or titration in MDCK cells [217] would be helpful to confirm their infectiveness of these samples.

Within this study, the most important point of interest was the demonstration of the high neurotropism of this H7N1 HPAI virus. This was possible primarily because viral RNA was detected in the brain of chickens inoculated with the three doses of virus ($10^{5.5}$ ELD_{50}, $10^{3.5}$ ELD_{50} and $10^{1.5}$ ELD_{50}). Additionally, the presence of viral antigen in branches of the trigeminus nerves, in the nasal cavity, and the abundant replication of the virus in cells of the nasal cavity, suggests that the olfactory pathway possibly plays a role in the viral invasion of the CNS. According to this information, an initial hypothesis was established stating that the replicated virus in the nasal cavity could possibly enter into the brain using nervous and haematogenous routes. Other viruses, such as the Venezuelan equine encephalitis [369] and West Nile virus [370] are able to use both routes to arrive to the CNS, invading the OB after infection of the OSN, also causing BBB disruption and subsequently viral spreading into the brain. Similarly, in mice inoculated with H5N1 HPAI virus, it has been observed that the virus penetrates into the CNS using mainly cranial nerves, but also causes viraemia, indicating that the haematogenous route might also play a role in the invasion of the CNS [206]. Therefore, the indication that this H7N1 HPAI virus may use both pathways was not unexpected,

considering that in the first study, viral antigen was observed abundantly in the nasal cavity and the viral antigen was detected in branches of the trigeminus nerve innervating this cavity.

The nervous route may imply the infection of olfactory neurons, and/or direct axonal retrograde transport from the infected peripheral nerves. However, it has to be considered that the nerves in the peripheral nervous system are protected from infectious agents' attacks, by the perineurium and endoneural vessels. Moreover, there are also unprotected axonal endings which are responsible for the transport of macromolecules, which can serve as a route of entry for a series of pathogens [371]. The OSN of the olfactory epithelium appears within these unprotected areas where neurons are directly exposed to the environment. In fact, there are a number of infectious agents that use the olfactory pathway to reach the CNS, such as herpesvirus [372], bornavirus [373,374], Venezuelan equine encephalitis virus [256], and morbilivirus [375,376,377]. With mice, in which the neuropathogenicity of the influenza virus infection has been extensively studied, it has been proven that different influenza viruses (mouse-adapted viruses, recombinant, and nonadapted viruses) are able use the OB to enter the brain [206,378,379]. Then, in the second study, a double IHC technique was performed to determine if the OSN could be a virus target. Results demonstrated that in contrast to the viruses mentioned above, the H7N1 HPAI virus did not target the OSN of the nasal cavity. Besides, a topographical description of the distribution of the virus was performed in this study, with the aim to provide evidential support to discard or corroborate the hypothesis of the nervous route. From this topographical study, it was concluded that the olfactory pathway is not the main route used by this virus to enter into the brain of chickens, because the OB and the most cranial regions of the brain were scarcely stained in comparison with the intermediate area of the *telecephalic pallium* (Pall), the diencephalon and *cerebellum*. Similarly, in the first study no viral antigen was detected in samples of the *vagus* and Sciatic nerves at any dpi. Moreover, in the evaluation of the topographical distribution of the virus, there was no evidence of dissemination from the positive neural nucleus to the interconnected neural route, as observed in mice

where the virus disseminates following neural pathways [203,205,206,240,380,381].

The next step was to elucidate how the virus arrives to the brain from the bloodstream. From the first study, it was known that the viraemia could be detected early on during the infection (viral RNA was found in the blood and brain tissue at 1 dpi), indicating that the virus was able to penetrate through to the brain in the first 24 hpi. However, considering that the viral RNA detected in the CNS could belong to the viral RNA contained in the blood, further studies were necessary to confirm or discard this possibility. Thus, in the third study it was possible to determine that at 24 hpi the viral antigen was present in the brain, particularly within brain micro-vascular endothelial cells. It was also observed that the virus did not have to generate a high level of viraemia to invade the CNS, compared with other blood-borne neurotropic viruses, which are capable of inducing CNS lesions only when the host is at its peak of viraemia [382,383,384]. In contrast, this study detected viral antigen in the endothelium and brain cells (neurons and glial cells) at 36 hpi when the viral RNA load in the blood was low, showing that the virus arrived to the brain at the beginning of the infection process and not at the peak of viremia, which occurred at 3 dpi (as observed in the first study).

The ability of the virus to enter into the CNS early during the infection was further confirmed by the detection of viral RNA in the CSF at 1 dpi, indicating that the BCSFB was participating in the pathogenesis. The Chp is a permeable area of the brain [193,262] which is also a route of entry to the brain for viruses such as canine distemper virus [355], choriomeningitis virus [356], FIV [357,358] and HIV [359], which use circulating mononuclear cells to penetrate the BCSFB. Therefore, it was important to determine the contribution of this route to the initial penetration of this H7N1 HPAI virus into the CNS. In the second study, the presence of influenza receptors was investigated, observing that only the Siaα2-3Gal was present on the apical surface of the Chp epithelial cells, and viral antigen was found in epithelial cells of the Chp from 2 dpi onward, confirming that they are susceptible to the infection. However, in the third study it was evident that these cells were not the main or initial target

of the virus, since the viral antigen was first found in endothelial cells which form the BBB (24hours). Also the positivity observed in the Chp was mainly restricted to cells in the lumen of the vessel that belong to the bloodstream.

When studying the pattern of virus distribution and viral tropism, it is also important to consider the areas within the CNS, know as CVOs, where the vessels do not have a barrier function and where blood borne substances can have more direct access to the nervous parenchyma [262]. Some infectious agents take advantage of these more permeable zones to enter into the CNS, such as *trypanosome brucei* and prions causing BSE and Scrapie [268,269]. Therefore, these areas were evaluated to determine if they could be a portal of entry for the H7N1 HPAI virus to the CNS. In the second study, it was possible to observe the presence of viral antigen in the SPO, AP, VOLT and LSO from 2 dpi onward, indicating that they could be an entry route into the CNS for the virus. However, no evidence of viral dissemination from the CVOs to the nearest areas and to the rest of the brain parenchyma was detected. Furthermore, in the third study, the pattern of staining for the TJs markers ZO-1 and claudin-1 did not show loss or disorganization, proving that there was not endothelial and epithelial disruption of the CVOs. In addition, viral antigen was always observed, restricted to the lumen of the vessels of the CVOs, indicating that their role in the initial stages of virus entry is either minor or non-existent.

Another interesting finding from the second study was that the lesions and topographical distribution of the viral antigen tended to be allocated bilaterally and symmetrically. This pattern was observed in the diencephalon, mesencephalon, and rhombencephalon, especially in the Rot (*thalamus*) (p2), PG (p3), ToS (mesencephalon), and APT nuclei (p1). Moreover, what was especially remarkable from the third study was that the viral antigen began to show preference for the *thalamus* during the first hpi. This was significant considering that influenza A virus causes a series of CNS disorders in humans, and particularly for the ANE, bilateral and symmetrical lesions have also been described in the *thalamus*, *putamen*, cerebral and cerebellar white matter and brain stem *tegmentum* [272,292,293,385,386,387,388,389]. For this reason, and because as it is suggested that this disease is also caused by disruption of

the BBB, the chicken model has been proposed to understand its mechanism of pathogenesis [204]. However, this pattern where the *thalamus* is one of the main target regions in the brain, is also common to other infectious agents, such as rabies [390], herpes viruses [391], flaviviruses (Japanese Encephalitis, West Nile Encephalitis, and Murray Valley Encephalitis) [383,392,393,394], measles [395], and HIV [326]. Besides, in contrast to the chicken model, viral antigen and RNA is rarely detected in brain tissue and CSF of patients with ANE [270,272,289,396,397,398,399]. Hence, both diseases seem to be induced by different mechanisms; in chickens the lesions are caused by direct replication of the virus, while, in humans it is suggested that immune-mediated mechanisms are involved [288,400]. Regarding the viral distribution, it has been attributed to differences in the blood supply and the trans-synaptic transmission among thalamic neurons and other interconnected neural pathways [288].

Knowing that the BBB was the main route for virus entry, the third study aimed to evaluate the stability of the BBB, and to determine how and when the H7N1 HPAI virus disrupts the BBB. Three methods were used to evaluate the location and severity of the BBB disruption. Methods such as the intracardial perfusion of the EB tracer are frequently used in mice and rats to evaluate different CNS pathological condition [308,316,323,401] , but to the best of our knowledge, this is the first time that the intracardial perfusion with EB has been used to evaluate the stability of the BBB in chickens infected with an infectious agent. This method is based on the ability of the EB to emit a red bright fluoresce signal when it is bound to albumin. Consequently, when the EB is perfused in animals where the BBB is damaged, it stains the injured zone and the cells of the periphery that have taken the EB from the serum [308]. Therefore, a complementary method was used in this study to detect the presence of protein leakage and identify the presence of BBB disruption. This method consisted of the detection of IgY serum protein using a direct IF in brain tissue samples of animals perfused with EB and PBS. This method is usually used in mice and other mammalian models to detect the extravasation of IgG into the brain observed during different pathologies of the CNS [312,313,314,339]. Both techniques, the EB perfusion and the detection of IgY by IF, unequivocally indicated that serum proteins were leaking from the

bloodstream to the parenchyma [312,317]. In this study, both techniques indicated that the H7N1 HPAI virus was able to cause disruption of the BBB and leakage of serum proteins toward the brain tissue from 36 hpi onward.

There are several mechanisms that can be used by the infectious agents to gain entrance to the brain. Infectious agents can enter by passage of free virus using a paracellular route by disrupting the TJs between the endothelial cells or by using the transcellular route, which implies that the virus crosses through the endothelial cells of the BBB without disrupting the TJs. By the "Trojan horse" mechanism" that is observed when a infectious agent infects leukocytes or red blood cells, and penetrates into the CNS within these cells. And finally, by the direct infection of the microvascular endothelial cells of the BBB with cytotoxic effect and virus release into the brain parenchyma [305,315,402]. According to the results obtained in this research, the mechanism used by H7N1 HPAI virus to cross the BBB needs to be categorized with infectious agents that produce disruption of the TJs. In the third study, it was observed that the virus produces foci of disorganization or loss of the ZO-1 staining, which is indicative of the BBB's loss of stability [188]. Based on this data, it can be asserted that routes such as the transcellular mechanism can be totally discarded, because viruses using such routes do not disrupt the TJs of the BBB. On the other hand, the paracellular route could be a possibility during the initial stages of the disease. However, considering that the viral antigen was detected in the nucleus and cytoplasm of microvascular endothelial cells during this first hpi, its role is less probable. Similarly, the Trojan horse mechanism cannot be completely ruled out, since viral antigen positive cells were observed in the lumen of the vessels in the Chp cells and CVOs at 36 and 48 hpi. This indicates that the virus can be carried by these cells, to the brain. Consequently, this possibility has to be investigated further, for example using IF techniques to label the TJs components, viral antigens, and circulating infected leucocytes [403]. Finally, considering the results obtained from these studies, the most satisfactory mechanism to explain how the H7N1 HPAI virus enters into the brain is the fourth mechanism mentioned, where the virus directly infects the endothelial cells and the viral agent is released into the brain parenchyma. This mechanism is used by several viruses such as Rift valley fever virus [404],

Ebola virus [405,406], Marburg virus, Lassa virus, dengue virus [407] and Theiler's murine encephalomyelitis virus [261]. These viruses are also characterized by the induction of vascular leakage caused by alterations in the TJs proteins [193]. The mechanism of direct infection and damage to the endothelial cells is also supported because HPAI viruses are able to induce apoptosis of microvascular endothelial cells after infection in chickens [408]. This can also be observed in humans affected with acute encephalopathies and encephalitis associated to influenza [409]. More studies will be necessary to determine if the disruption of the TJs of the BBB occurs first, or if the damage to the microvascular endothelial cells of the BBB causes the disorganization of the TJs, and allows the entry of the virus. Furthermore, more research is required to fully understand the molecular mechanisms that lead to the severe and rapid damage of the endothelial cells, with the consequential leakage of serum protein and viral spreading toward the brain parenchyma.

In summary, the present work demonstrates that the H7N1 HPAI is strongly neurotropic; this is because even at very low doses the viral RNA can be detected in the brain of experimentally infected chickens. Also, after a detailed topographical study of H7N1 HPAI virus distribution in the chicken brain, it was concluded that the main route of entry and dissemination of this virus into the brain is haematogenous. Finally, by using three different methods to evaluate the stability of the BBB, it was determined that the H7N1 HPAI virus damages the endothelial cells directly, and disrupts the TJs, allowing the virus to enter the brain.

7. Conclusions

1. Experimental infection of SPF chickens with $10^{5.5}$ ELD_{50} of the H7N1 HPAI virus successfully reproduced the clinicopathological picture described in natural HPAI virus infection.

2. The H7N1 HPAI virus is highly neurotropic, inducing severe neurological signs and CNS lesions in experimentally infected chickens. The tropism by the CNS is also demonstrated by its capacity to replicate in the CNS in birds experimentally infected with a low dose of virus ($10^{1.5}$ ELD_{50}).

3. Chickens experimentally exposed to middle ($10^{3.5}$ ELD_{50}) or low doses ($10^{1.5}$ ELD_{50}) of H7N1 HPAI virus can shed viral RNA in their faeces and respiratory secretions, despite the absence of clinical signs, acting as viral carriers and contributing to viral spreading.

4. Viraemia occurs as early as 18 hpi in chickens experimentally infected with 10^{6} ELD_{50}H7N1 HPAI and is a key event for the viral dissemination to different organs and the CNS.

5. Expression of avian (Siaα2-3Gal) and human (Siaα2-6Gal) type receptors in chicken brain endothelial cells and infection of this cell type at 24 hpi demonstrates that chicken brain endothelial cells are the main target cell for the H7N1 HPAI virus at the early stages of infection.

6. Based in topographical studies and double staining techniques, it can be asserted that the H7N1 HPAI virus disseminates haematogenously to the CNS.

7. The Chp and CVOs are not main target sites for virus invasion into the CNS, as showed by the lack of dissemination of virus from these sites to the rest of the brain, the scarce to slight staining for the presence of viral antigen and because there was no alteration in the pattern of staining with both TJs markers (ZO-1 and claudin-1).

8. The H7N1 HPAI virus causes disruption of the BBB by means of the alteration of the TJs between the BBB endothelial cells, evidenced by disorganization and loss of ZO-1 staining in association with EB leakage and the extravasation of Ig Y protein.

8. References

1. Cox NJ, Subbarao K (2000) Global epidemiology of influenza: past and present. Annual Review of Medicine 51: 407-421.
2. Cunha BA (2004) Influenza: historical aspects of epidemics and pandemics. Infectious Disease Clinics of North America 18: 141-155.
3. Stubbs EL (1948) Fowl pest. In: Biester HE, Schwarte LH, editors. Diseases of poultry. 2nd ed. Iowa: Iowa State University Press, Ames. pp. 603-614.
4. Schäffr JR, Kawaoka Y, Bean WJ, Süss J, Senne D, et al. (1993) Origin of the pandemic 1957 H2 influenza A virus and the persistence of its possible progenitors in the avian reservoir. Virology 194: 781-788.
5. Shimizu K (1997) History of influenza epidemics and discovery of influenza virus. Nippon Rinsho 55: 2505-2511.
6. Smith W, Andrewes CH, Laidlaw PP (1933) A virus obtained from influenza patients. The Lancet i: 66-68.
7. Taubenberger JK, Reid AH, Fanning TG (2000) The 1918 influenza virus: a killer comes into view. Virology 274: 241-245.
8. Alexander DJ (2008) Orthomyxoviridae-avian influenza. In: Pattison M, McMullin PF, Bradbury JM, Alexander DJ, editors. Poultry Diseases. 6th ed. Philadelphia, PA: W.B. Saunders. pp. 317-332.
9. Glezen WP (1996) Emerging infections: pandemic influenza. Epidemiologic Reviews 18: 64-76.
10. Horimoto T, Kawaoka Y (2001) Pandemic threat posed by avian influenza A viruses. Clinical Microbiology Reviews 14: 129-149.
11. Easterday BC, Tumova B (1972) Avian influenza. In: Hofstad MS, Calnek BW, Helmbolt W, Reid M, Yoder HW, editors. Diseases of poultry. 6th ed. Iowa: Iowa State University Press, Ames. pp. 670-700.
12. Suarez DL (2008) Influenza A virus. In: Swayne DE, editor. Avian Influenza 1st ed. Iowa: Blackwell Publishing. pp. 3-22.
13. OIE (2011) Avian influenza. Manual of diagnostic test and vaccines for terrestrial animals 2011. 6th ed. Paris, France: World Organization for Animal Health.
14. Swayne DE, Halvorson DA (2008) Influenza In: Saif YM, editor. Diseases of poultry 12th ed. Ames, Iowa, USA: Blackwell Publishing Professional pp. 153-184.
15. Subbarao K, Klimov A, Katz J, Regnery H, Lim W, et al. (1998) Characterization of an avian influenza A (H5N1) virus isolated from a child with a fatal respiratory illness. Science 279: 393-396.
16. Tscherne DM, García-Sastre A (2011) Virulence determinants of pandemic influenza viruses. The Journal of Clinical Investigation 121: 6-13.
17. Jakeman KJ, Tisdale M, Russell S, Leone A, Sweet C (1994) Efficacy of 2'-deoxy-2'-fluororibosides against influenza A and B viruses in ferrets. Antimicrob Agents Chemother 38: 1864-1867.
18. Osterhaus ADME, Rimmelzwaan GF, Martina BEE, Bestebroer TM, Fouchier RAM (2000) Influenza B virus in seals. Science 288: 1051-1053.
19. Kimura H, Abiko C, Peng G, Muraki Y, Sugawara K, et al. (1997) Interspecies transmission of influenza C virus between humans and pigs. Virus Research 48: 71-79.
20. Yuanji G, Fengen J, Ping W, Min W, Jiming Z (1983) Isolation of influenza C virus from pigs and experimental infection of pigs with influenza C virus. Journal of General Virology 64: 177-182.
21. Yuanji G, Desselberger U (1984) Genome analysis of influenza C viruses isolated in 1981/82 from pigs in China. Journal of General Virology 65: 1857-1872.
22. Fujiyoshi Y, Kume NP, Sakata K, S.B. S (1994) Fine structure of influenza A virus observed by electron cryo-microscopy. EMBO J 13: 318-326. .
23. Clifford M, Twigg J, Upton C (2009) Evidence for a novel gene associated with human influenza A viruses. Virology Journal 6: 198.
24. Nayak DP, Hui EK-W, Barman S (2004) Assembly and budding of influenza virus. Virus Research 106: 147-165.

25. Karlsson Hedestam GB, Fouchier RAM, Phogat S, Burton DR, Sodroski J, et al. (2008) The challenges of eliciting neutralizing antibodies to HIV-1 and to influenza virus. Nature Reviews Microbiology 6: 143-155.
26. Rogers GN, Paulson JC (1983) Receptor determinants of human and animal influenza virus isolates: Differences in receptor specificity of the H3 hemagglutinin based on species of origin. Virology 127: 361-373.
27. Varki NM, Varki A (2007) Diversity in cell surface sialic acid presentations: implications for biology and disease. Lab Invest 87: 851-857.
28. Connor RJ, Kawaoka Y, Webster RG, Paulson JC (1994) Receptor specificity in human, avian, and equine H2 and H3 influenza virus isolates. Virology 205: 17-23.
29. Rogers GN, D'Souza BL (1989) Receptor binding properties of human and animal H1 influenza virus isolates. Virology 173: 317-322.
30. Matlin KS, Reggio H, Helenius A, Simons K (1981) Infectious entry pathway of influenza virus in a canine kidney cell line. The Journal of Cell Biology 91: 601-613.
31. Bouvier NM, Palese P (2008) The biology of influenza viruses. Vaccine 26: D49-D53.
32. Patterson S, Oxford JS, Dourmashkin RR (1979) Studies on the mechanism of influenza virus entry into cells. J Gen Virol 43: 223-229.
33. de Vries RP, de Vries E, Bosch BJ, de Groot RJ, Rottier PJM, et al. (2010) The influenza A virus hemagglutinin glycosylation state affects receptor-binding specificity. Virology 403: 17-25.
34. Steinhauer DA (1999) Role of hemagglutinin cleavage for the pathogenicity of influenza virus. Virology 258: 1-20.
35. Cross KJ, Langley WA, Russell RJ, Skehel JJ, Steinhauer DA (2009) Composition and functions of the influenza fusion peptide. Protein and Peptide Letters 16: 766-778.
36. Bullough PA, Hughson FM, Skehel JJ, Wiley DC (1994) Structure of influenza haemagglutinin at the pH of membrane fusion. Nature 371: 37-43.
37. Pinto LH, Lamb RA (2007) Controlling influenza virus replication by inhibiting its proton channel. Molecular BioSystems 3: 18-23.
38. O'Neill RE, Talon J, Palese P (1998) The influenza virus NEP (NS2 protein) mediates the nuclear export of viral ribonucleoproteins. EMBO J 17: 288-296.
39. Cros JF, Palese P (2003) Trafficking of viral genomic RNA into and out of the nucleus: influenza, Thogoto and Borna disease viruses. Virus Research 95: 3-12.
40. Dias A, Bouvier D, Crepin T, McCarthy AA, Hart DJ, et al. (2009) The cap-snatching endonuclease of influenza virus polymerase resides in the PA subunit. Nature 458: 914-918.
41. Perez JT (2010) Influenza A virus-generated small RNAs regulate the switch from transcription to replication. Proceedings of the National Academy of Sciences of the United States of America 107: 11525-11530.
42. Umbach JL, Yen HL, Poon LL, Cullen BR (2010) Influenza a virus expresses high levels of an unusual class of small viral leader RNAs in infected cells. mBio 1: e00204-e00210.
43. Barman S, Ali A, Hui EKW, Adhikary L, Nayak DP (2001) Transport of viral proteins to the apical membranes and interaction of matrix protein with glycoproteins in the assembly of influenza viruses. Virus Research 77: 61-69.
44. Enami M, Sharma G, Benham C, Palese P (1991) An influenza virus containing nine different RNA segments. Virology 185: 291-298.
45. Donald HB, Isaacs A (1954) Counts of influenza virus particles. Journal of General Microbiology 10: 457-464.
46. Seto JT, Chang FS (1969) Functional significance of sialidase during influenza virus multiplication: an electron microscope study. Journal of Virology 4: 58-66

47. Matrosovich MN, Matrosovich TY, Gray T, Roberts NA, Klenk H-D (2004) Neuraminidase is important for the initiation of influenza virus infection in human airway epithelium. The Journal of Virology 78: 12665-12667.
48. Flint JS, Enquist LW, Krug RM, Racaniello VR, Skalka AM (2000) Appendix, structure, genomic organization, and infectious cycles of selected animal viruses discussed in this book. Virology, molecular biology, pathogenesis and control. Washington, DC: American Society for Microbiology Press. pp. 759-761.
49. Wilson IA, Skehel JJ, Wiley DC (1981) Structure of the haemagglutinin membrane glycoprotein of influenza virus at 3 A resolution. Nature 29: 366-373.
50. Wiley DC, Skehel JJ (1987) The structure and function of the hemagglutinin membrane glycoprotein of influenza virus. Annual Review of Biochemistry 56: 365-394.
51. Wilson IA, Cox NJ (1990) Structural basis of immune recognition of influenza virus hemagglutinin. Annual Review of Immunology 8: 737-787.
52. Webster RG, Laver WG (1980) Determination of the number of nonoverlapping antigenic areas on Hong Kong (H3N2) influenza virus hemagglutinin with monoclonal antibodies and the selection of variants with potential epidemiological significance. Virology 104: 139-148.
53. Perdue ML (2008) Molecular determinants of pathogenicity for avian infuenza viruses. In: Swayne DE, editor. Avian Influenza. Ames, Iowa: Blackwell Piblishing pp. 23-41.
54. Swayne DE, Pantin-Jackwood M (2008) Pathobiology of avian influenza virus infections in birds and mammals In: Swayne DE, editor. Avian Influenza. 1st edition ed. Ames, Iowa, USA: Blackwell Publishing. pp. 87-122.
55. Klenk H-D, Garten W (1994) Host cell proteases controlling virus pathogenicity. Trends in Microbiology 2: 39-43.
56. Bosch FX, Orlich M, Klenk HD, Rott R (1979) The structure of the hemagglutinin, a determinant for the pathogenicity of influenza viruses. Virology 95: 197-207.
57. Gotoh B, Ogasawara T, Toyoda T, Inocencio NM, Hamaguchi M, et al. (1990) An endoprotease homologous to the blood clotting factor X as a determinant of viral tropism in chick embryo. The EMBO journal 9: 4189-4195.
58. Kido H, Niwa Y, Beppu Y, Towatari T (1996) Cellular proteases involved in the pathogenicity of enveloped animal viruses, human immunodeficiency virus, influenza virus A and Sendai virus. Advances in Enzyme Regulation 36: 325-347.
59. Kido H, Yokogoshi Y, Sakai K, Tashiro M, Kishino Y, et al. (1992) Isolation and characterization of a novel trypsin-like protease found in rat bronchiolar epithelial Clara cells. A possible activator of the viral fusion glycoprotein. Journal of Biological Chemistry 267: 13573-13579.
60. Klenk H-D, Rott R, Orlich M, Blödorn J (1975) Activation of influenza A viruses by trypsin treatment. Virology 68: 426-439.
61. Lazarowitz SG, Goldberg AR, Choppin PW (1973) Proteolytic cleavage by plasmin of the HA polypeptide of influenza virus: Host cell activation of serum plasminogen. Virology 56: 172-180.
62. Horimoto T, Nakayama K, Smeekens SP, Kawaoka Y (1994) Proprotein-processing endoproteases PC6 and furin both activate hemagglutinin of virulent avian influenza viruses. Journal of Virology 68: 6074-6078.
63. Horimoto T, Kawaoka Y (1997) Biologic effects of introducing additional basic amino acid residues into the hemagglutinin cleavage site of a virulent avian influenza virus. Virus Research 50: 35-40.
64. Jang H, Boltz D, Sturm-Ramirez K, Shepherd KR, Jiao Y, et al. (2009) Highly pathogenic H5N1 influenza virus can enter the central nervous system and induce neuroinflammation and neurodegeneration. Proceedings of the National Academy of Sciences 106: 14063-14068.

65. Fouchier RA (2004) Avian influenza A virus (H7N7) associated with human conjunctivitis and a fatal case of acute respiratory distress syndrome. Proc Natl Acad Sci USA 101: 1356-1361.
66. Webster RG, Bean WJ, Gorman OT, Chambers TM, Kawaoka Y (1992) Evolution and ecology of influenza A viruses. Microbiology and Molecular Biology Reviews 56: 152 - 179.
67. Gorman OT, Bean WJ, Kawaoka Y, Webster RG (1990) Evolution of the nucleoprotein gene of influenza A virus. The Journal of Virology 64: 1487-1497.
68. Stallknecht DE, Brown JD (2008) Ecology of avian influenza in wild birds. In: Swayne DE, editor. Avian Influenza. Blackwell Publishing ed. Ames, Iowa: Blackwell Publishing pp. 43-58.
69. Olsen B, Munster VJ, Wallensten A, Waldenström J, Osterhaus ADME, et al. (2006) Global patterns of influenza A virus in wild birds. Science 312: 384-388.
70. Hinshaw VS, Webster RG, Turner B (1980) The perpetuation of orthomyxoviruses and paramyxoviruses in Canadian waterfowl. Canadian Journal of Microbiology 26: 622-629.
71. Kaleta EF, Hergarten G, Yilmaz A (2005) Avian influenza A viruses in birds-an ecological, ornithological and virological view. Dtsch Tierarztl Wochenschr 112: 448-456.
72. Hinshaw VS, Bean WJ, Webster RG, Sriram G (1980) Genetic reassortment of influenza A viruses in the intestinal tract of ducks. Virology 102: 412-419.
73. Sharp GB, Kawaoka Y, Jones DJ, Bean WJ, Pryor SP, et al. (1997) Coinfection of wild ducks by influenza A viruses: distribution patterns and biological significance. The Journal of Virology 71: 6128-6135.
74. Markwell DD, Shortridge KF (1982) Possible waterborne transmission and maintenance of influenza viruses in domestic ducks. Applied and Environmental Microbiology 43: 110-115.
75. Swayne DE (2008) Epidemiology of avian influenza in agricultural and other man-made systems. In: Swayne DE, editor. Avian influenza. Ames, Iowa: Blackwell Publishing. pp. 59-85.
76. Peiris JSM, de Jong MD, Guan Y (2007) Avian influenza virus (H5N1): a threat to human health. Clinical Microbiology Reviews 20: 243-267.
77. Banks J, Speidel E, Alexander DJ (1998) Characterisation of an avian influenza A virus isolated from a human – is an intermediate host necessary for the emergence of pandemic influenza viruses? Archives of Virology 143: 781-787.
78. Koopmans M, Wilbrink B, Conyn M, Natrop G, van der Nat H, et al. (2004) Transmission of H7N7 avian influenza A virus to human beings during a large outbreak in commercial poultry farms in the Netherlands. The Lancet 363: 587-593.
79. Tweed SA, Skowronski DM, David ST, Larder A, Petric M, et al. (2004) Human illness from avian influenza H7N3, British Columbia. Emerging Infectious Diseases 10: 2196-2199.
80. Nguyen-Van-Tam JS, Nair P, Acheson P, Baker A, Barker M, et al. (2006) Outbreak of low pathogenicity H7N3 avian influenza in UK, including associated case of human conjunctivitis. Euro Surveillance 11: E060504.060502.
81. Shortridge KF, Zhou NN, Guan Y, Gao P, Ito T, et al. (1998) Characterization of avian H5N1 influenza viruses from poultry in Hong Kong. Virology 252: 331-342.
82. Guo Y, Wang M, Kawaoka Y, Gorman O, Ito T, et al. (1992) Characterization of a new avian-like influenza A virus from horses in China. Virology 188: 245-255.
83. Timoney PJ (1996) Equine influenza. Comparative Immunology, Microbiology and Infectious Diseases 19: 205-211.
84. Crawford PC, Dubovi EJ, Castleman WL, Stephenson I, Gibbs EPJ, et al. (2005) Transmission of equine influenza virus to dogs. Science 310: 482-485.

85. Song D, Kang B, Lee C, Jung K, Ha G, et al. (2008) Transmission of avian influenza virus (H3N2) to dogs. Emerging Infectious Diseases journal 14: 741–746.
86. Payungporn S, Crawford PC, Kouo TS, Chen LM, Pompey J, et al. (2008) Influenza A virus (H3N8) in dogs with respiratory disease, Florida. Emerging Infectious Diseases journal 14: 902-908.
87. Castleman WL, Powe JR, Crawford PC, Gibbs EPJ, Dubovi EJ, et al. (2010) Canine H3N8 influenza virus infection in dogs and mice. Veterinary Pathology Online 47: 507-517.
88. Kida H, Ito T, Yasuda J, Shimizu Y, Itakura C, et al. (1994) Potential for transmission of avian influenza viruses to pigs. Journal of General Virology 75: 2183-2188.
89. Ninomiya A, Takada A, Okazaki K, Shortridge KF, Kida H (2002) Seroepidemiological evidence of avian H4, H5, and H9 influenza A virus transmission to pigs in southeastern China. Veterinary Microbiology 88: 107-114.
90. Karasin AI, Brown IH, Carman S, Olsen CW (2000) Isolation and characterization of H4N6 avian influenza viruses from pigs with pneumonia in Canada. Journal of Virology 74: 9322-9327.
91. Van Reeth K (2007) Avian and swine influenza viruses: our current understanding of the zoonotic risk. Veterinary Research 38: 243-260.
92. Englund L (2000) Studies on influenza viruses H10N4 and H10N7 of avian origin in mink. Veterinary Microbiology 74: 101-107.
93. Klingeborn B, Englund L, Rott R, Juntti N, Rockborn G (1985) An avian influenza A virus killing a mammalian species - the mink. Archives of Virology 86: 347-351.
94. Callan RJ, Early G, Kida H, Hinshaw VS (1995) The appearance of H3 influenza viruses in seals. Journal of General Virology 76: 199-203.
95. Geraci, St Aubin DJ, Barker IK, Webster RG, Hinshaw VS, et al. (1982) Mass mortality of harbor seals: pneumonia associated with influenza A virus. Science 215: 1129-1131.
96. Hinshaw VS, Bean WJ, Webster RG, Rehg JE, Fiorelli P, et al. (1984) Are seals frequently infected with avian influenza viruses? J Virol 51: 863-865.
97. Webster RG, Hinshaw VS, Bean WJ, Van Wyke KL, Geraci JR, et al. (1981) Characterization of an influenza A virus from seals. Virology 113: 712-724.
98. Lvov DK, Zdanov VM, Sazonov AA, Braude NA, Vladimirtceva EA, et al. (1978) Comparison of influenza viruses isolated from man and from whales. Bull World Health Organ 56: 923-930.
99. Alexander DJ (2007) An overview of the epidemiology of avian influenza. Vaccine 25: 5637-5644.
100. Sinnecker R, Sinnecker H, Zilske E, Köhler D (1983) Surveillance of pelagic birds for influenza A viruses. Acta Virologica 27: 75-79.
101. Webster RG, Yakhno M, Hinshaw VS, Bean WJ, Murti KG (1978) Intestinal influenza: replication and characterization of influenza viruses in ducks. Virology 84: 268-278.
102. Stallknecht DE, Goekjian VH, Wilcox BR, Poulson RL, Brown JD (2010) Avian influenza virus in aquatic habitats: what do we need to learn? Avian Diseases 54: 461-465.
103. Kim JK, Negovetich NJ, Forrest HL, Webster RG (2009) Ducks: the "Trojan horses" of H5N1 influenza. Influenza and Other Respiratory Viruses 3: 121-128.
104. Spickler AR, Trampel DW, Roth JA (2008) The onset of virus shedding and clinical signs in chickens infected with high-pathogenicity and low-pathogenicity avian influenza viruses. Avian Pathology 37: 555 - 577.
105. Horimoto T, Rivera E, Pearson J, Senne D, Krauss S, et al. (1995) Origin and molecular changes associated with emergence of a highly pathogenic H5N2 influenza virus in Mexico. Virology 213: 223-230.

106. Swayne DE, Beck JR (2005) Experimental study to determine if low-pathogenicity and high-pathogenicity avian influenza viruses can be present in chicken breast and thigh meat following intranasal virus inoculation. Avian Diseases 49: 81-85.
107. Lu H, Castro AE, Pennick K, Liu J, Yang Q, et al. (2003) Survival of avian influenza virus H7N2 in SPF chickens and their environments. Avian Diseases 47: 1015-1021.
108. Swayne DE (1997) Pathobiology of H5N2 Mexican avian influenza virus infections of chickens. Veterinary pathology 34: 557-567.
109. Shalaby AA, Slemons RD, Swayne DE (1994) Pathological studies of A/chicken/Alabama/7395/75 (H4N8) influenza virus in specific-pathogen-free laying hens. Avian Diseases 38: 22-32.
110. van der Goot JA, de Jong MC, Koch G, Van Boven M (2003) Comparison of the transmission characteristics of low and high pathogenicity avian influenza A virus (H5N2). Epidemiology and Infection 131: 1003-1013.
111. Mutinelli F, Capua I, Terregino C, Cattoli G (2003) Clinical, gross, and microscopic findings in different avian species naturally infected during the H7N1 low- and high-pathogenicity avian influenza epidemics in Italy during 1999 and 2000. Avian Diseases 47: 844-848.
112. Swayne DE, Pantin-Jackwood M (2006) Pathogenicity of avian influenza viruses in poultry. Developmental Biology 124.
113. Ziegler AF, Davison S, Acland H, Eckroade RJ (1999) Characteristics of H7N2 (nonpathogenic) avian influenza virus infections in commercial layers, in Pennsylvania, 1997-98. Avian Diseases 43: 142-149.
114. Kinde H, Read DH, Daft BM, Hammarlund M, Moore J, et al. (2003) The occurrence of avian influenza A subtype H6N2 in commercial layer flocks in southern california (2000-02): clinicopathologic findings. Avian Diseases 47: 1214-1218.
115. van der Goot JA, Koch G, de Jong MCM, van Boven M (2005) Quantification of the effect of vaccination on transmission of avian influenza (H7N7) in chickens. Proceedings of the National Academy of Sciences of the United States of America 102: 18141-18146.
116. Kwon Y-K, Joh S-J, Kim M-C, Sung H-W, Lee Y-J, et al. (2005) Highly pathogenic avian influenza (H5N1) in the commercial domestic ducks of South Korea. Avian Pathology 34: 367-370.
117. Westbury HA, Turner AJ, Amon L (1981) Transmissibility of two avian influenza a viruses (H7 N6) between chickens. Avian Pathology 10: 481-487.
118. Jones YL, Swayne DE (2004) Comparative pathobiology of low and high pathogenicity H7N3 Chilean avian influenza viruses in Chickens. Avian Diseases 48: 119-128.
119. Perkins LEL, Swayne DE (2001) Pathobiology of A/Chicken/Hong Kong/220/97 (H5N1) avian influenza virus in seven gallinaceous species. Veterinary pathology 38: 149-164.
120. Lee MS, Deng MC, Lin YJ, Chang CY, Shieh HK, et al. (2007) Characterization of an H5N1 avian influenza virus from Taiwan. Veterinary Microbiology 124: 193-201.
121. Mase M, Eto M, Tanimura N, Imai K, Tsukamoto K, et al. (2005) Isolation of a genotypically unique H5N1 influenza virus from duck meat imported into Japan from China. Virology 339: 101-109.
122. Tumpey TM, Suarez DL, Perkins LEL, Senne DA, Lee J-g, et al. (2002) Characterization of a highly pathogenic H5N1 avian influenza A virus isolated from duck meat. The Journal of Virology 76: 6344-6355.
123. Bean WJ, Kawaoka Y, Wood JM, Pearson JE, Webster RG (1985) Characterization of virulent and avirulent A/chicken/Pennsylvania/83 influenza A viruses: potential role of defective interfering RNAs in nature. The Journal of Virology 54: 151-160.

124. Cappucci DT, Jr J, D.C., Brugh M, Smith TM, Jackson CF, et al. (1985) Isolation of avian influenza virus (subtype H5N2) from chicken eggs during a natural outbreak. Avian Diseases 29: 1195-1200.
125. Brown CC, Olander HJ, Senne DA (1992) A pathogenesis study of highly pathogenic avian influenza virus H5N2 in chickens, using immunohistochemistry. Journal of Comparative Pathology 107: 341-348.
126. Alexander DJ, Parsons G, Manvell RJ (1986) Experimental assessment of the pathogenicity of eight avian influenza a viruses of H5 subtype for chickens, turkeys, ducks and quail. Avian Pathology 15: 647-662.
127. Nakatani H, Nakamura K, Yamamoto Y, Yamada M, Yamamoto Y (2005) Epidemiology, pathology, and immunohistochemistry of layer hens naturally affected with H5N1 highly pathogenic avian influenza in Japan. Avian Diseases 49: 436-441.
128. Sims LD, Ellis TM, Liu KK, Dyrting K, Wong H, et al. (2003) Avian influenza in Hong Kong 1997-2002. Avian Diseases 47: 832-838.
129. Elbers AR, Holtslag JB, Bouma A, Koch G (2007) Within-flock mortality during the high-pathogenicity avian influenza (H7N7) epidemic in The Netherlands in 2003: implications for an early detection system. Avian Diseases 51: 304-308.
130. Savill NJ, St Rose SG, Keeling MJ, Woolhouse MEJ (2006) Silent spread of H5N1 in vaccinated poultry. Nature 442: 757-757.
131. Tiensin T, Nielen M, Vernooij H, Songserm T, Kalpravidh W, et al. (2007) Transmission of the highly pathogenic avian influenza virus H5N1 within flocks during the 2004 epidemic in Thailand. Journal of Infectious Diseases 196: 1679-1684.
132. Okamatsu M, Saito T, Yamamoto Y, Mase M, Tsuduku S, et al. (2007) Low pathogenicity H5N2 avian influenza outbreak in Japan during the 2005-2006. Veterinary Microbiology 124: 35-46.
133. Brown JD, Stallknecht DE, Beck JR, Suarez DL, Swayne DE (2006) Susceptibility of North American ducks and gulls to H5N1 highly pathogenic avian influenza viruses. Emerging Infectious Diseases journal 12: 1663-1670.
134. Sturm-Ramirez KM, Ellis T, Bousfield B, Bissett L, Dyrting K, et al. (2004) Reemerging H5N1 influenza viruses in Hong Kong in 2002 are highly pathogenic to ducks. The Journal of Virology 78: 4892-4901.
135. Perkins LE, Swayne DE (2003) Comparative susceptibility of selected avian and mammalian species to a Hong Kong-origin H5N1 high-pathogenicity avian influenza virus. Avian Diseases 47: 956-967.
136. Perkins LEL, Swayne DE (2002) Susceptibility of laughing gulls (Larus atricilla) to H5N1 and H5N3 highly pathogenic avian influenza viruses. Avian Diseases 46: 877-885.
137. Alexander DJ, Allan WH, Parsons DG, Parsons G (1978) The pathogenicity of four avian influenza viruses for fowls, turkeys and ducks. Research in Veterinary Science 24: 242-247.
138. Swayne DE (2007) Understanding the complex pathobiology of high pathogenicity avian influenza viruses in birds. Avian Diseases 51: 242-249.
139. Nguyen DC, Uyeki TM, Jadhao S, Maines T, Shaw M, et al. (2005) Isolation and characterization of avian influenza viruses, including highly pathogenic H5N1, from poultry in live bird markets in Hanoi, Vietnam, in 2001. Journal of Virology 79: 4201-4212.
140. Capua I, Marangon S, dalla Pozza M, Terregino C, Cattoli G (2003) Avian influenza in Italy 1997-2001. Avian Diseases 47: 839-843.
141. Capua I, Mutinelli F, Marangon S, Alexander DJ (2000) H7N1 avian influenza in Italy (1999-2000) in intensively reared chickens and turkeys. Avian Pathology 29: 537-543.

142. Spackman E, Gelb J, Preskenis L, Ladman B, Pope C, et al. (2010) The pathogenesis of low pathogenicity H7 avian influenza viruses in chickens, ducks and turkeys. Virology Journal 7: 331.
143. Suarez DL, Perdue ML, Cox N, Rowe T, Bender C, et al. (1998) Comparisons of highly virulent H5N1 influenza A viruses isolated from humans and chickens from Hong Kong. Journal of Virology 72: 6678-6688.
144. Kobayashi Y, Horimoto T, Kawaoka Y, Alexander DJ, Itakura C (1996) Neuropathological studies of chickens infected with highly pathogenic avian influenza viruses. Journal of Comparative Pathology 114: 131-147.
145. Ellis TM, Bousfield RB, Bissett LA, Dyrting KC, Luk GSM, et al. (2004) Investigation of outbreaks of highly pathogenic H5N1 avian influenza in waterfowl and wild birds in Hong Kong in late 2002. Avian Pathology 33: 492 - 505.
146. Klopfleisch R, Werner O, Mundt E, Harder T, Teifke JP (2006) Neurotropism of highly pathogenic avian influenza virus A/Chicken/Indonesia/2003 (H5N1) in experimentally infected pigeons (Columbia livia f. domestica). Veterinary Pathology Online 43: 463-470.
147. Teifke JP, Klopfleisch R, Globig A, Starick E, Hoffmann B, et al. (2007) Pathology of natural infections by H5N1 highly pathogenic avian influenza virus in mute (Cygnus olor) and whooper (Cygnus cygnus) swans. Veterinary Pathology 44: 137-143.
148. Pálmai N, Erdélyi K, Bálint Á, Márton L, Dán Á, et al. (2007) Pathobiology of highly pathogenic avian influenza virus (H5N1) infection in mute swans (Cygnus olor). Avian Pathology 36: 245 - 249.
149. Nakamura K, Imada T, Imai K, Yamamoto Y, Tanimura N, et al. (2008) Pathology of specific-pathogen-free chickens inoculated with H5N1 avian influenza viruses isolated in Japan in 2004. Avian Diseases Digest 3: e2-e2.
150. Yamamoto Y, Nakamura K, Kitagawa K, Ikenaga N, Yamada M, et al. (2007) Severe nonpurulent encephalitis with mortality and feather lesions in call ducks (Anas platyrhyncha var. domestica) inoculated intravenously with H5N1 highly pathogenic avian influenza virus. Avian Diseases 51: 52-57.
151. Pasick J, Weingartl H, Clavijo A, Riva J, Kehler H, et al. (2003) Characterization of avian influenza virus isolates submitted to the national centre for foreign animal disease between 1997 and 2001. Avian Diseases 47: 1208-1213.
152. Kwon YK, Swayne DE (2010) Different routes of inoculation impact infectivity and pathogenesis of H5N1 high pathogenicity avian influenza virus infection in chickens and domestic ducks. Avian Diseases 54: 1260-1269.
153. Brown JD, Stallknecht DE, Swayne DE (2008) Experimental infections of herring gulls (Larus argentatus) with H5N1 highly pathogenic avian influenza viruses by intranasal inoculation of virus and ingestion of virus-infected chicken meat. Avian Pathology 37: 393 - 397.
154. Breithaupt A, Kalthoff D, Dale J, Bairlein F, Beer M, et al. (2010) Neurotropism in blackcaps (Sylvia atricapilla) and red-billed queleas (Quelea quelea) after highly pathogenic avian influenza virus H5N1 infection. Veterinary Pathology Online.
155. Pantin-Jackwood MJ, Swayne DE (2007) Pathobiology of Asian highly pathogenic avian influenza H5N1 virus infections in ducks. Avian Diseases Digest 2: e15-e15.
156. Spackman E, Suarez DL, Senne DA (2008) Avian influenza diagnosis and survillance methods. In: Swayne DE, editor. Avian influenza. Ames, Iowa: Blackwell Publishing.
157. Woolcock PR (2008) Avian influenza virus isolation and propagation in chicken eggs. In: Spackman E, editor. Avian influenza virus. Totowa, NJ.: Humana Press. pp. 35-46.
158. Killian ML (2008) Hemagglutination assay for the avian influenza virus. In: E. S, editor. Avian influenza virus. Totowa, NJ.: Humana Press. pp. 47-52.

159. Swayne DE, Senne D, Beard CW (1998) Avian Influenza. A laboratory manual for the isolation and identification of avian pathogens. Kennett Square, PA.: American Association of Avian Pathologist.
160. Pendersen JC (2008) Neuraminidase-inhibition assay for the identification of influenza A virus neuraminidase subtype or neuraminidase antibody specificity. In: Spackman E, editor. Avian influenza virus. Totowa, NJ.: Humana Press. pp. 67-75.
161. Van Deusen RA, Hinshaw VS, Senne DA, Pellacani D (1983) Micro neuraminidase-inhibition assay for classification of influenza A virus neuraminidases. Avian Dis 27: 745-750.
162. Pendersen JC (2008) Hemagglutination-inhibition test for avian influenza virus subtype identification and the detection and quatification of serum antibodies to the avian influenza virus. In: Spackman E, editor. Avian influenza virus. Totowa, NJ.: Humana Press. pp. 53-66.
163. Pantin-Jackwood MJ (2008) Immunohistochemical staining for the detection of the avian influenza virus in tissues. In: Spackman E, editor. Avian influenza virus. NJ, USA: Humana Press. pp. 77-83.
164. Satterly N, Tsai P-L, van Deursen J, Nussenzveig DR, Wang Y, et al. (2007) Influenza virus targets the mRNA export machinery and the nuclear pore complex. Proceedings of the National Academy of Sciences 104: 1853-1858.
165. Guarner J, Shieh W-J, Dawson J, Subbarao K, Shaw M, et al. (2000) Immunohistochemical and in situ hybridization studies of influenza A virus infection in human lungs. American Journal of Clinical Pathology 114: 227-233.
166. Watters AD (2005) In situ hibridization. In: Walker JM, Rapley R, editors. Medical Biomethods handbook. Totowa, NJ.: Humana Press. Inc. . pp. 409-428.
167. Ellis JS, Zambon MC (2002) Molecular diagnosis of influenza. Reviews in Medical Virology 12: 375-389.
168. Wang R, Taubenberger JK (2010) Methods for molecular surveillance of influenza. Expert Review of Anti-infective Therapy 8: 517-527.
169. Vascellari M, Granato A, Trevisan L, Basilicata L, Toffan A, et al. (2007) Pathologic findings of highly pathogenic avian influenza virus A/Duck/Vietnam/12/05 (H5N1) in experimentally infected pekin ducks, based on immunohistochemistry and in situ hybridization. Veterinary Pathology 44: 635-642.
170. Spackman E, Suarez DL (2008) Type A influenza virus detection and quatification by real-time RT-PCR. . In: Spackman E, editor. Avian influenza virus. Totowa, NJ.: Humana Press. Inc. pp. 19-33.
171. OIE (2011) Terrestrial Animal Health Code. 2011 ed: OIE Terrestrial Animal Health Code. pp. Section 10. Chapter 10.14.
172. Swayne DE (2008) Avian influenza control strategies. In: Swayne DE, editor. Avian influenza. Ames, Iowa: Backwell publishing. pp. 287-296.
173. FAO (2011) Approaches to controlling, preventing and eliminating H5N1 Highly Pathogenic Avian Influenza in endemic countries. Animal Production and Health Paper. Rome. pp. 13-24.
174. Swayne DE, Kapczynski DR (2008) Vaccines, vaccination and immunology for avian influenza viruses in poultry. In: Swayne DE, editor. Avian influenza. Ames, Iowa: Blackwell Publising. pp. 407-424.
175. van den Berg T, Lambrecht B, Marché S, Steensels M, Van Borm S, et al. (2008) Influenza vaccines and vaccination strategies in birds. Comparative Immunology, Microbiology and Infectious Diseases 31: 121-165.
176. Wareing MD, Tannock GA (2001) Live attenuated vaccines against influenza; an historical review. Vaccine 19: 3320-3330.
177. Ellebedy AH, Webby RJ (2009) Influenza vaccines. Vaccine 27, Supplement 4: D65-D68.

178. Pertmer TM, Oran AE, Moser JM, Madorin CA, Robinson HL (2000) DNA vaccines for influenza virus: differential effects of maternal antibody on immune responses to hemagglutinin and nucleoprotein. The Journal of Virology 74: 7787-7793.
179. Onur G (2005) Avian and mammalian prefrontal cortices: Limited degrees of freedom in the evolution of the neural mechanisms of goal-state maintenance. Brain Research Bulletin 66: 311-316.
180. Onur G (2005) The avian prefrontal cortex and cognition. Current Opinion in Neurobiology 15: 686-693.
181. Reiner A, Yamamoto K, Karten HJ (2005) Organization and evolution of the avian forebrain. The Anatomical Record Part A: Discoveries in Molecular, Cellular, and Evolutionary Biology 287A: 1080-1102.
182. Kirsch JA, Güntürkün O, Rose J (2008) Insight without cortex: Lessons from the avian brain. Consciousness and Cognition 17: 475-483.
183. Durstewitz D, Kröner S, Güntürkün O (1999) The dopaminergic innervation of the avian telencephalon. Progress in Neurobiology 59: 161-195.
184. Leutgeb S, Husband S, Riters LV, Shimizu T, Bingman VP (1996) Telencephalic afferents to the caudolateral neostriatum of the pigeon. Brain Research 730: 173-181.
185. Puelles L, Martinez-de-la-Torre M, Paxinos G, Watson C, Martinez S (2007) The chick brain in stereotaxic coordinates: an atlas featuring neuromeric subdivisions and mammalian homologies. New York: Elseiver Inc
186. Jarvis ED, Gunturkun O, Bruce L, Csillag A, Karten H, et al. (2005) Avian brains and a new understanding of vertebrate brain evolution. Nature Reviews Neuroscience 6: 151-159.
187. Stewart PA, Wiley MJ (1981) Structural and histochemical features of the avian blood-brain barrier. The Journal of comparative neurology 202: 157-167.
188. Wolburg H, Lippoldt A (2002) Tight junctions of the blood-brain barrier: development, composition and regulation. Vascular Pharmacology 38: 323-337.
189. Liebner S, Kniesel U, Kalbacher H, Wolburg H (2000) Correlation of tight junction morphology with the expression of tight junction proteins in blood-brain barrier endothelial cells. European Journal of Cell Biology 79: 707-717.
190. Hawkins BT, Davis TP (2005) The blood-brain barrier/neurovascular unit in health and disease. Pharmacological Reviews 57: 173-185.
191. Nitta T, Hata M, Gotoh S, Seo Y, Sasaki H, et al. (2003) Size-selective loosening of the blood-brain barrier in claudin-5 deficient mice. The Journal of Cell Biology 161: 653-660.
192. Abbott NJ, Patabendige AAK, Dolman DEM, Yusof SR, Begley DJ (2010) Structure and function of the blood-brain barrier. Neurobiology of Disease 37: 13-25.
193. Wolburg H, Paulus W (2010) Choroid plexus: biology and pathology. Acta Neuropathologica 119: 75-88.
194. Wolburg H, Wolburg-Buchholz K, Liebner S, Engelhardt B (2001) Claudin-1, claudin-2 and claudin-11 are present in tight junctions of choroid plexus epithelium of the mouse. Neuroscience Letters 307: 77-80.
195. Duvernoy HM, Risold P-Y (2007) The circumventricular organs: An atlas of comparative anatomy and vascularization. Brain Research Reviews 56: 119-147.
196. Sisó S, Jeffrey M, González L (2010) Sensory circumventricular organs in health and disease. Acta Neuropathologica 120: 689-705.
197. Joly J-S, Osório J, Alunni A, Auger H, Kano S, et al. (2007) Windows of the brain: Towards a developmental biology of circumventricular and other neurohemal organs. Seminars in Cell & Developmental Biology 18: 512-524.
198. Bardet SM, Cobos I, Puelles E, Martínez-De-La-Torre M, Puelles L (2006) Chicken lateral septal organ and other circumventricular organs form in a

striatal subdomain abutting the molecular striatopallidal border. The Journal of Comparative Neurology 499: 745-767.
199. Goren O, Adorján I, Kálmán M (2006) Heterogeneous occurrence of aquaporin-4 in the ependyma and in the circumventricular organs in rat and chicken. Anatomy and Embryology 211: 155-172.
200. Rodríguez EM, Rodríguez S, Hein S (1998) The subcommissural organ. Microscopy Research and Technique 41: 98-123.
201. Ziegels J (1979) Effects of light and of testosterone derivatives or antiandrogens on the secretory content of the subcommissural organ of the quail, Coturnix coturnix japonica. Journal of Neural Transmission 44: 317-326.
202. Ziegels J (1977) Histochemical study of the subcommissural organ in chickens during development. CR Seances Soc Biol Fi 171: 1306-1308.
203. Tanaka H, Park C-H, Ninomiya A, Ozaki H, Takada A, et al. (2003) Neurotropism of the 1997 Hong Kong H5N1 influenza virus in mice. Veterinary Microbiology 95: 1-13.
204. Park CH, Ishinaka M, Takada A, Kida H, Kimura T, et al. (2002) The invasion routes of neurovirulent A/Hong Kong/483/97 (H5N1) influenza virus into the central nervous system after respiratory infection in mice. Archives of Virology 147: 1425-1436.
205. Shinya K, Shimada A, Ito T, Otsuki K, Morita T, et al. (2000) Avian influenza virus intranasally inoculated infects the central nervous system of mice through the general visceral afferent nerve. Archives of Virology 145: 187-195.
206. Iwasaki T, Itamura S, Nishimura H, Sato Y, Tashiro M, et al. (2004) Productive infection in the murine central nervous system with avian influenza virus A (H5N1) after intranasal inoculation. Acta Neuropathologica 108: 485-492.
207. Lu X, Tumpey TM, Morken T, Zaki SR, Cox NJ, et al. (1999) A mouse model for the evaluation of pathogenesis and immunity to influenza A (H5N1) viruses isolated from humans. The Journal of Virology 73: 5903-5911.
208. Gao P, Watanabe S, Ito T, Goto H, Wells K, et al. (1999) Biological heterogeneity, including systemic replication in mice, of H5N1 influenza A virus isolates from humans in Hong Kong. Journal of Virology 73: 3184-3189.
209. de Jong MD, Hien TT (2006) Avian influenza A (H5N1). Journal of Clinical Virology 35: 2-13.
210. Nishimura H, Itamura S, Iwasaki T, Kurata T, Tashiro M (2000) Characterization of human influenza A (H5N1) virus infection in mice: neuro-, pneumo- and adipotropic infection. Journal of General Virology 81: 2503-2510.
211. Feldmann A, Looser N, Wagner R, Klenk H-D (2001) Targeted influenza virus infection of endothelial cells and leucocytes. International Congress Series 1219: 557-571.
212. Capua I, Mutinelli F, Marangon S, Alexander DJ (2000) H7N1 avian influenza in Italy (1999-2000) in intensively reared chickens and turkeys. Avian Pathol 29: 537-543.
213. Reed LJ, Muench H (1938) A simple method of estimating fifty percent endpoints. The American Journal of Hygiene 27: 493–497.
214. Campitelli L, Di Martino A, Spagnolo D, Smith GJD, Di Trani L, et al. (2008) Molecular analysis of avian H7 influenza viruses circulating in Eurasia in 1999-2005: detection of multiple reassortant virus genotypes. Journal of General Virology 89: 48-59.
215. Kreijtz JHCM, Bodewes R, van Amerongen G, Kuiken T, Fouchier RAM, et al. (2007) Primary influenza A virus infection induces cross-protective immunity against a lethal infection with a heterosubtypic virus strain in mice. Vaccine 25: 612-620.
216. Rimmelzwaan GF, Kuiken T, van Amerongen G, Bestebroer TM, Fouchier RAM, et al. (2001) Pathogenesis of influenza A (H5N1) virus infection in a primate model. The Journal of Virology 75: 6687-6691.

217. Spackman E, Senne DA, Myers TJ, Bulaga LL, Garber LP, et al. (2002) Development of a real-time reverse transcriptase PCR assay for type A influenza virus and the avian H5 and H7 hemagglutinin subtypes. Journal of clinical microbiology 40: 3256-3260.
218. Busquets N, Alba A, Napp S, Sánchez A, Serrano E, et al. (2010) Influenza A virus subtypes in wild birds in North-Eastern Spain (Catalonia). Virus Research 149: 10-18.
219. Fronhoffs S, Totzke G, Stier S, Wernert N, Rothe M, et al. (2002) A method for the rapid construction of cRNA standard curves in quantitative real-time reverse transcription polymerase chain reaction. Molecular and Cellular Probes 16: 99-110.
220. Zanella A (2003) Avian influenza attributable to serovar H7N1 in light layers in Italy. Avian Diseases 47: 1177-1180.
221. Perkins LEL, Swayne DE (2002) Pathogenicity of a Hong Kong-origin H5N1 highly pathogenic avian influenza virus for emus, geese, ducks, and pigeons. Avian Diseases 46, 1: 53-63.
222. van Riel D, van den Brand J, Munster VJ, Besteboer TM, Fouchier RA, et al. (2009) Pathology and virus distribution in chickens naturally infected with highly pathogenic avian influenza A virus (H7N7) during the 2003 outbreak in the Netherlands. Veterinary Pathology.
223. Kishida N, Sakoda Y, Eto M, Sunaga Y, Kida H (2004) Co-infection of Staphylococcus aureus or Haemophilus paragallinarum exacerbates H9N2 influenza A virus infection in chickens. Archives of Virology 149: 2095-2104.
224. Beato MS, Toffan A, De Nardi R, Cristalli A, Terregino C, et al. (2007) A conventional, inactivated oil emulsion vaccine suppresses shedding and prevents viral meat colonisation in commercial (Pekin) ducks challenged with HPAI H5N1. Vaccine 25: 4064-4072.
225. Toffan A, Serena Beato M, De Nardi R, Bertoli E, Salviato A, et al. (2008) Conventional inactivated bivalent H5/H7 vaccine prevents viral localization in muscles of turkeys infected experimentally with low pathogenic avian influenza and highly pathogenic avian influenza H7N1 isolates. Avian Pathology 37: 407 - 412.
226. Feldmann A, Schafer MKH, Garten W, Klenk H-D (2000) Targeted infection of endothelial cells by avian influenza virus A/FPV/Rostock/34 (H7N1) in chicken embryos. The Journal of Virology 74: 8018-8027.
227. Capua I, Mutinelli F, Hablovarid MH (2002) Avian embryo susceptibility to Italian H7N1 avian influenza viruses belonging to different genetic lineages: Brief Report. Archives of Virology 147: 1611-1621.
228. Kobayashi Y, Horimoto T, Kawaoka Y, Alexander DJ, Itakura C (1996) Pathological studies of chickens experimentally infected with two highly pathogenic avian influenza viruses. Avian Pathology 25: 285-304.
229. Mo IP, Brugh M, Fletcher OJ (1997) Comparative pathology of chickens experimentally inoculated with avian influenza viruses of low and high pathogenicity. Avian Diseases 41: 125.
230. Muramoto Y, Ozaki H, Takada A, Park CH, Yuji S, et al. (2006) Highly pathogenic H5N1 influenza virus causes coagulopathy in chickens. Microbiology Immunology 50 (1): 73-81.
231. Chutinimitkul S, van Riel D, Munster VJ, van den Brand JM, Rimmelzwaan GF, et al. (2010) In vitro assessment of attachment pattern and replication efficiency of H5N1 influenza A viruses with altered receptor specificity. Journal of Virology 84: 6825-6833.
232. Pasick J, Berhane Y, Hisanaga T, Kehler H, Hooper-McGrevy K, et al. (2010) Diagnostic test results and pathology associated with the 2007 Canadian H7N3 highly pathogenic avian influenza outbreak. Avian Diseases 54: 213-219.

233. Capua I, Marangon S, Selli L, Alexander DJ, Swayne DE, et al. (1999) Outbreaks of highly pathogenic avian influenza (H5N2) in Italy during October 1997 to January 1998. Avian Pathology 28: 455-460.
234. Bingham J, Green DJ, Lowther S, Klippel J, Burggraaf S, et al. (2009) Infection studies with two highly pathogenic avian influenza strains (Vietnamese and Indonesian) in Pekin ducks (Anas platyrhynchos), with particular reference to clinical disease, tissue tropism and viral shedding. Avian Pathology 38: 267 - 278.
235. Rigoni M, Shinya K, Toffan A, Milani A, Bettini F, et al. (2007) Pneumo- and neurotropism of avian origin Italian highly pathogenic avian influenza H7N1 isolates in experimentally infected mice. Virology 364: 28-35.
236. Goletić T, Gagić A, Rećidbegović E, Kustura A, Kavazović A, et al. (2010) Highly pathogenic avian influenza virus subtype H5N1 in mute swans (Cygnus olor) in central Bosnia. Avian Diseases 54: 496-501.
237. Lipatov AS, Krauss S, Guan Y, Peiris M, Rehg JE, et al. (2003) Neurovirulence in mice of H5N1 influenza virus genotypes isolated from Hong Kong poultry in 2001. The Journal of Virology 77: 3816-3823.
238. Löndt BZ, Nunez A, Banks J, Nili H, Johnson LK, et al. (2008) Pathogenesis of highly pathogenic avian influenza A/turkey/Turkey/1/2005 H5N1 in Pekin ducks (Anas platyrhynchos) infected experimentally. Avian Pathology 37: 619 - 627.
239. Majde JA, Bohnet SG, Ellis GA, Churchill L, Leyva-Grado V, et al. (2007) Detection of mouse-adapted human influenza virus in the olfactory bulbs of mice within hours after intranasal infection. Journal of Neurovirology 13: 399-409.
240. Matsuda K, Park CH, Sunden Y, Kimura T, Ochiai K, et al. (2004) The vagus nerve is one route of transneural invasion for intranasally inoculated influenza A virus in mice. Veterinary Pathology 41: 101-107.
241. Mori I, Komatsu T, Takeuchi K, Nakakuki K, Sudo M, et al. (1995) Viremia induced by influenza virus. Microbial Pathogenesis 19: 237-244.
242. Lossinsky AS, Shivers RR (2004) Structural pathways for macromolecular and cellular transport across the blood-brain barrier during inflammatory conditions. Review. Histology and Histopathology 19: 535-564.
243. Liu NQ, Lossinsky AS, Popik W, Li X, Gujuluva C, et al. (2002) Human immunodeficiency virus type 1 enters brain microvascular endothelia by macropinocytosis dependent on lipid rafts and the mitogen-activated protein kinase signaling pathway. The Journal of Virology 76: 6689-6700.
244. Verma S, Lo Y, Chapagain M, Lum S, Kumar M, et al. (2009) West Nile virus infection modulates human brain microvascular endothelial cells tight junction proteins and cell adhesion molecules: Transmigration across the in vitro blood-brain barrier. Virology 385: 425-433.
245. Matsuda K, Shibata T, Sakoda Y, Kida H, Kimura T, et al. (2005) In vitro demonstration of neural transmission of avian influenza A virus. Journal of General Virology 86: 1131-1139.
246. Mori I, Kimura Y (2001) Neuropathogenesis of influenza virus infection in mice. Microbes and Infection 3: 475-479.
247. Silvano FD, Kanata Y, Takeuchi M, Shimada A, Otsuki K, et al. (1997) Avian influenza A virus induced stunting syndrome-like disease in chicks. The Journal of Veterinary Medical Science 59: 205-207.
248. Suzuki K, Okada H, Itoh T, Tada T, Mase M, et al. (2009) Association of increased pathogenicity of asian H5N1 highly pathogenic avian influenza viruses in chickens with highly efficient viral replication accompanied by early destruction of innate immune responses. The Journal of Virology 83: 7475-7486.
249. Yao L, Korteweg C, Hsueh W, Gu J (2008) Avian influenza receptor expression in H5N1-infected and noninfected human tissues. The FASEB Journal 22: 733-740.

250. Shibuya N, Tazaki K, Song Z, Tarr GE, Goldstein IJ, et al. (1989) A comparative study of bark lectins from three elderberry (Sambucus) species. Journal of Biochemistry 106: 1098-1103.
251. Busquets N, Abad FX, Alba A, Dolz R, Allepuz A, et al. (2010) Persistence of highly pathogenic avian influenza virus (H7N1) in infected chickens: feather as a suitable sample for diagnosis. Journal of General Virology 91: 2307-2313.
252. Spackman E, Senne DA, Bulaga LL, Myers TJ, Perdue ML, et al. (2003) Development of real-time RT-PCR for the detection of avian influenza virus. Avian Diseases 47: 1079-1082.
253. Yamada T (1996) Viral etiology of Parkinson's disease: Focus on influenza A virus. Parkinsonism & Related Disorders 2: 113-121.
254. Mori I, Nishiyama Y, Yokochi T, Kimura Y (2005) Olfactory transmission of neurotropic viruses. Journal of Neurovirology 11: 129-137.
255. Chaves AJ, Busquets N, Campos N, Ramis A, Dolz R, et al. (2011) Pathogenesis of highly pathogenic avian influenza A virus (H7N1) infection in chickens inoculated with three different doses. Avian Pathology 40: 163-172.
256. Charles PC, Walters E, Margolis F, Johnston RE (1995) Mechanism of neuroinvasion of Venezuelan equine encephalitis virus in the mouse. Virology 208: 662-671.
257. Sun N, Perlman S (1995) Spread of a neurotropic coronavirus to spinal cord white matter via neurons and astrocytes. The Journal of Virology 69: 633-641.
258. Barnett EM, Cassell MD, Perlman S (1993) Two neurotropic viruses, herpes simplex virus type 1 and mouse hepatitis virus, spread along different neural pathways from the main olfactory bulb. Neuroscience 57: 1007.
259. Brown JD, Stallknecht DE, Berghaus RD, Swayne DE (2009) Infectious and lethal doses of H5N1 highly pathogenic avian influenza virus for house sparrows (Passer domesticus) and rock pigeons (Columbia livia). Journal of Veterinary Diagnostic Investigation 21: 437-445.
260. Beineke A, Puff C, Seehusen F, Baumgärtner W (2009) Pathogenesis and immunopathology of systemic and nervous canine distemper. Veterinary Immunology and Immunopathology 127: 1-18.
261. Ha-Lee YM, Dillon K, Kosaras B, Sidman R, Revell P, et al. (1995) Mode of spread to and within the central nervous system after oral infection of neonatal mice with the DA strain of Theiler's murine encephalomyelitis virus. Journal of Virology 69: 7354-7361.
262. Engelhardt B, Sorokin L (2009) The blood–brain and the blood–cerebrospinal fluid barriers: function and dysfunction. Seminars in Immunopathology 31: 497-511.
263. Flint SJ, Enquist LW, Racaniello VR, Skalka AM (2004) Dissemination, virulence and epidemiology In: Flint JS, Enquist LW, Racaniello VR, Skalka AM, editors. Principles of virology: molecular biology, pathogenesis, and control of animal viruses. 2 ed. Washington, D.C: Asm Press.
264. Liu P, Hudson L, Tompkins M, Vahlenkamp T, Colby B, et al. (2006) Cerebrospinal fluid is an efficient route for establishing brain infection with feline immunodeficiency virus and transfering infectious virus to the periphery. Journal of Neurovirology 12: 294-306.
265. Hurtrel M, Ganière J, Guelfi J, Chakrabarti L, Maire M, et al. (1992) Comparison of early and late feline immunodeficiency virus encephalopathies. AIDS 6: 399-406.
266. Hurtrel B, Chakrabarti L, Hurtrel MM, MA. Dormont D, Montagnier L (1991) Early SIV encephalopathy. Journal of Medical Primatology 20: 159-166.
267. Budka H (1991) Neuropathology of human immunodeficiency virus infection. Brain Pathology 1: 163-175.
268. Schultzberg M, Ambatsis M, Samuelsson EB, Kristensson K, van Meirvenne N (1988) Spread of Trypanosoma brucei to the nervous system: Early attack on

circumventricular organs and sensory ganglia. Journal of Neuroscience Research 21: 56-61.
269. Sisó S, Jeffrey M, González L (2009) Neuroinvasion in sheep transmissible spongiform encephalopathies: the role of the haematogenous route. Neuropathology and Applied Neurobiology 35: 232-246.
270. Fujimoto Y, Shibata M, Tsuyuki M, Okada M, Tsuzuki K (2000) Influenza A virus encephalopathy with symmetrical thalamic lesions. European Journal of Pediatrics 159: 319-321.
271. Nagai T, Yagishita A, Tsuchiya Y, Asamura S, Kurokawa H, et al. (1993) Symmetrical thalamic lesions on CT in influenza A virus infection presenting with or without Reye syndrome. Brain & Development 15: 67-73.
272. Mizuguchi M, Abe J, Mikkaichi K, Noma S, Yoshida K, et al. (1995) Acute necrotising encephalopathy of childhood: a new syndrome presenting with multifocal, symmetric brain lesions. Journal of Neurology, Neurosurgery & Psychiatry 58: 555-561.
273. Nelli R, Kuchipudi S, White G, Perez B, Dunham S, et al. (2010) Comparative distribution of human and avian type sialic acid influenza receptors in the pig. BMC Veterinary Research 6: 4.
274. Lawrenson JG, Cassella JP, Hayes AJ, Firth JA, Allt G (2000) Endothelial glycoconjugates: a comparative lectin study of the brain, retina and myocardium. Journal of Anatomy 196: 55-60.
275. Pillai S, Lee C (2010) Species and age related differences in the type and distribution of influenza virus receptors in different tissues of chickens, ducks and turkeys. Virology Journal 7: 5.
276. Kirkeby S, Jensen N-E, Mandel U, Poulsen S (2008) Asthma induction in mice leads to appearance of α2–3- and α2–6-linked sialic acid residues in respiratory goblet-like cells. Virchows Archiv 453: 283-290.
277. Kirkeby S, Martel CJM, Aasted B (2009) Infection with human H1N1 influenza virus affects the expression of sialic acids of metaplastic mucous cells in the ferret airways. Virus Research 144: 225-232.
278. Yasukawa Z, Sato C, Kitajima K (2005) Inflammation-dependent changes in α2,3-, α2,6-, and α2,8-sialic acid glycotopes on serum glycoproteins in mice. Glycobiology 15: 827-837.
279. Kaplan HA, Woloski BM, Hellman M, Jamieson JC (1983) Studies on the effect of inflammation on rat liver and serum sialyltransferase. Evidence that inflammation causes release of Gal beta 1 leads to 4GlcNAc alpha 2 leads to 6 sialyltransferase from liver. Journal of Biological Chemistry 258: 11505-11509.
280. Delmotte P, Degroote S, Merten MD, Van Seuningen I, Bernigaud A, et al. (2001) Influence of TNFα on the sialylation of mucins produced by a transformed cell line MM-39 derived from human tracheal gland cells. Glycoconjugate Journal 18: 487-497.
281. Süer Gökmen S, Kazezoğlu C, Sunar B, Özçelik F, Güngör Ö, et al. (2006) Relationship between serum sialic acids, sialic acid-rich inflammation-sensitive proteins and cell damage in patients with acute myocardial infarction. Clinical Chemistry and Laboratory Medicine 44: 199-206.
282. Crook M, Haq M, Haq S, Tutt P (1994) Plasma sialic acid and acute-phase proteins in patients with myocardial infarction. Angiology 45: 709-715.
283. Daly JM, Whitwell KE, Miller J, Dowd G, Cardwell JM, et al. (2010) Investigation of equine influenza cases exhibiting neurological disease: coincidence or association? Journal of Comparative Pathology 134: 231-235.
284. Songserm T, Amonsin A, Jam-on R, Sae-Heng N, Meemak N, et al. (2006) Avian influenza H5N1 in naturally infected domestic cat. Emerging Infectious Diseases journal 12.
285. Shinya K, Suto A, Kawakami M, Sakamoto H, Umemura T, et al. (2005) Neurovirulence of H7N7 influenza A virus: Brain stem encephalitis

accompanied with aspiration pneumonia in mice. Archives of Virology 150: 1653-1660.
286. Rowe T, Cho DS, Bright RA, Zitzow LA, Katz JM (2003) Neurological manifestations of avian influenza viruses in mammals. Avian Diseases 47: 1122-1126.
287. Chen H (2005) Avian flu: H5N1 virus outbreak in migratory waterfowl. Nature 436: 191-192.
288. Toovey S (2008) Influenza-associated central nervous system dysfunction: A literature review. Travel Medicine and Infectious Disease 6: 114-124.
289. Togashi T, Matsuzono Y, Narita M, Morishima T (2004) Influenza-associated acute encephalopathy in Japanese children in 1994-2002. Virus Research 103: 75-78.
290. Maricich SM, Neul JL, Lotze TE, Cazacu AC, Uyeki TM, et al. (2004) Neurologic complications associated with influenza A in children during the 2003-2004 influenza season in Houston, Texas. Pediatrics 114: e626-e633.
291. Long SS (2005) Emerging infections in children: influenza and acute necrotizing encephalopathy. Advances in Experimental Medicine and Biology 568: 1-9.
292. Martin A, Reade EP (2010) Acute necrotizing encephalopathy progressing to brain death in a pediatric patient with novel influenza A (H1N1) infection. Clinical Infectious Diseases 50: e50-e52.
293. Yoshikawa H, Yamazaki S, Watanabe T, Abe T (2001) Study of influenza-associated encephalitis/encephalopathy in children during the 1997 to 2001 influenza seasons. Journal of Child Neurology 16: 885-890.
294. Shinya K, Silvano FD, Morita T, Shimada A, Nakajima M, et al. (1998) Encephalitis in mice inoculated intranasally with an influenza virus strain originated from a water bird. The Journal of Veterinary Medical Science 60: 627-629.
295. Dybing JK, Schultz-Cherry S, Swayne DE, Suarez DL, Perdue ML (2000) Distinct pathogenesis of Hong Kong-origin H5N1 viruses in mice compared to that of other highly pathogenic H5 avian influenza viruses. The Journal of Virology 74: 1443-1450.
296. Ravenholdt RT, Foege WH (1982) 1918 Influenza, encephalitis lethargica, Parkinsonism. Lancet 2: 860-863.
297. Togashi T, Matsuzono Y, Morishima T, Narita M (2001) Acute encephalitis-encephalopathy during influenza epidemics in Japanese children. International Congress Series 1219: 609-613.
298. Levin M, Kay JDS, Gould JD, Hjelm M, Pincott JR, et al. (1983) Haemorrhagic shock and encephalopathy: a new syndrome with a high mortality in young children. The Lancet 322: 64-67.
299. Davis LE, Blisard KS, Kornfeld M (1990) The influenza B virus mouse model of Reye's syndrome: clinical, virologic and morphologic studies of the encephalopathy. J Neurol Sci 97: 221-231.
300. Salinas S, Schiavo G, Kremer EJ (2010) A hitchhiker's guide to the nervous system: the complex journey of viruses and toxins. Nature Reviews Microbiology 8: 645-655.
301. Weiss N, Miller F, Cazaubon S, Couraud P-O (2009) The blood-brain barrier in brain homeostasis and neurological diseases. Biochimica et Biophysica Acta (BBA) - Biomembranes 1788: 842-857.
302. Furuse M, Hirase T, Itoh M, Nagafuchi A, Yonemura S, et al. (1993) Occludin: a novel integral membrane protein localizing at tight junctions. The Journal of Cell Biology 123: 1777-1788.
303. Redzic Z (2011) Molecular biology of the blood-brain and the blood-cerebrospinal fluid barriers: similarities and differences. Fluids and Barriers of the CNS 8: 3.

304. Grant Maxie M, Youssef S, Maxie MG (2007) Inflammation in the central nervous system. Jubb, Kennedy & Palmer's Pathology of Domestic Animals (Fifth Edition). Edinburgh: Elsevier. pp. 393-446.
305. Fletcher NF, Meeker RB, Hudson LC, Callanan JJ (2011) The neuropathogenesis of feline immunodeficiency virus infection: Barriers to overcome. The Veterinary Journal 188: 260-269.
306. Kramer-Hämmerle S, Rothenaigner I, Wolff H, Bell JE, Brack-Werner R (2005) Cells of the central nervous system as targets and reservoirs of the human immunodeficiency virus. Virus Research 111: 194-213.
307. Albright A, Soldan S, González-Scarano F (2003) Pathogenesis of human immunodeficiency virus-induced neurological disease. Journal of Neurovirology 9: 222-227.
308. del Valle J, Camins A, Pallàs M, Vilaplana J, Pelegrí C (2008) A new method for determining blood-brain barrier integrity based on intracardiac perfusion of an Evans Blue-Hoechst cocktail. Journal of Neuroscience Methods 174: 42-49.
309. Davison F, Magor KE, Kaspers B, Fred D, Bernd K, et al. (2008) Structure and evolution of avian immunoglobulins. Avian Immunology. London: Academic Press. pp. 107-127.
310. Hädge D, Fiebig H, Ambrosius H (1980) Evolution of low molecular weight immunoglobulins I. Relationship of 7S immunoglobulins of various vertebrates to chicken IgY. Developmental and Comparative Immunology 4: 501-513.
311. Hädge D, Fiebig H, Puskas E, Ambrosius H (1980) Evolution of low molecular weight immunoglobulins II. No antigenic cross-reactivity of human IgD, human IgG and IgG3 to chicken IgY. Developmental and Comparative Immunology 4: 725-736.
312. Pelegrí C, Canudas AM, del Valle J, Casadesus G, Smith MA, et al. (2007) Increased permeability of blood-brain barrier on the hippocampus of a murine model of senescence. Mechanisms of Ageing and Development 128: 522-528.
313. Jullien-Vitoux D, Voisin GA (1973) Studies in vascular permeability. ii. comparative extravasation of different immunoglobulin classes in normal guinea pig skin. European Journal of Immunology 3: 663-667.
314. Kuang F, Wang B-R, Zhang P, Fei L-L, Jia YI, et al. (2004) Extravasation of blood-borne immunoglobulin G through blood brain barrier during adrenaline induce trasient hypertension in the rat. International Journal of Neuroscience 114: 575-591.
315. Mims CA, Dimmock NJ, Nash A, Stephen J (1995) Mims' pathogenesis of infectious disease. London: Academic Press.
316. Kaptanoglu E, Okutan O, Akbiyik F, Solaroglu I, Kilinc A, et al. (2004) Correlation of injury severity and tissue Evans blue content, lipid peroxidation and clinical evaluation in acute spinal cord injury in rats. Journal of Clinical Neuroscience 11: 879-885.
317. del Valle J, Duran-Vilaregut J, Manich G, Camins A, Pallàs M, et al. (2009) Time-course of blood-brain barrier disruption in senescence-accelerated mouse prone 8 (SAMP8) mice. International Journal of Developmental Neuroscience 27: 47-52.
318. Tanno H, Nockels RP, Pitts LH, Noble LJ (1992) Breakdown of the blood-brain barrier after fluid percussion brain injury in the rat: Part 2: Effect of hypoxia on permeability to plasma proteins. Journal of Neurotrauma 9: 335-347.
319. Morrey JD, Olsen AL, Siddharthan V, Motter NE, Wang H, et al. (2008) Increased blood-brain barrier permeability is not a primary determinant for lethality of West Nile virus infection in rodents. Journal of General Virology 89: 467-473.
320. Liu T-H, Liang L-C, Wang C-C, Liu H-C, Chen W-J (2008) The blood-brain barrier in the cerebrum is the initial site for the Japanese encephalitis virus entering the central nervous system. Journal of Neurovirology 14: 514-521.

321. Oshima S, Nemoto E, Kuramochi M, Saitoh Y, Kobayashi D (2009) Penetration of oseltamivir and its active metabolite into the brain after lipopolysaccharide-induced inflammation in mice. Journal of Pharmacy and Pharmacology 61: 1397-1400.
322. Chaturvedi UC, Dhawan R, Khanna M, Mathur A (1991) Breakdown of the blood-brain barrier during dengue virus infection of mice. Journal of General Virology 72: 859-866.
323. Hawkins BT, Egleton RD (2006) Fluorescence imaging of blood-brain barrier disruption. Journal of Neuroscience Methods 151: 262-267.
324. Delorme P, Gayet J, Grignon G (1975) Diffusion of horseradish peroxidase perfused through the lateral ventricle of the chick telencephalon. Cell and Tissue Research 157: 535-540.
325. Anderson DK, Heisey SR (1975) Creatinine, potassium, and calcium flux from chicken cerebrospinal fluid. American Journal of Physiology -- Legacy Content 228: 415-419.
326. Hegde AN, Mohan S, Lath N, Lim CCT (2011) Differential diagnosis for bilateral abnormalities of the basal ganglia and thalamus. Radiographics 31: 5-30.
327. Bentivoglio M, Kristensson K (2004) Thalamus in flame: targeting of infectious agents to thalamic nuclei. Thalamus & Related Systems 2: 297-314.
328. Yagishita A, Nakano I, Ushioda T, Otsuki N, Hasegawa A (1995) Acute encephalopathy with bilateral thalamotegmental involvement in infants and children: imaging and pathology findings. American Journal of Neuroradiology 16: 439-447.
329. Shinjoh M, Bamba M, Jozaki K, Takahashi E, Koinuma G, et al. (2000) Influenza A-associated encephalopathy with bilateral thalamic necrosis in Japan. Clinical Infectious Diseases 31: 611-613.
330. Mori I, Diehl AD, Chauhan A (1999) Selective targeting of habenular, thalamic midline and monoaminergic brainstem neurons by neurotropic influenza A virus in mice. Journal of Neurovirology 5: 355.
331. Sugaya N (2002) Influenza-associated encephalopathy in Japan. Seminars in Pediatric Infectious Diseases 13: 79-84.
332. Nitsch C, Klatzo I (1983) Regional patterns of blood-brain barrier breakdown during epileptiform seizures induced by various convulsive agents. Journal of the Neurological Sciences 59: 305-322.
333. Dallasta LM, Pisarov LA, Esplen JE, Werley JV, Moses AV, et al. (1999) Blood-brain barrier tight junction disruption in human immunodeficiency virus-1 encephalitis. American Journal of Pathology 155: 1915-1927.
334. Ge S, Song L, Pachter JS (2005) Where is the blood–brain barrier … really? Journal of Neuroscience Research 79: 421-427.
335. Swayne DE, Fletcher OJ, Schierman LW (1989) Marek's disease virus induced transient paralysis in chickens. 1. Time course association between clinical signs and histological brain lesions. Avian Pathology 18: 385-396.
336. Pardridge WM (2007) Blood-brain barrier delivery. Drug Discovery Today 12: 54-61.
337. Ohtsuki S, Terasaki T (2007) Contribution of carrier-mediated transport systems to the blood-brain barrier as a supporting and protecting interface for the brain; importance for CNS drug discovery and development. Pharmaceutical Research 24: 1745-1758.
338. Davidson F, Magor KE, Kaspers B (2008) Structure and evolution of avian immunoglobulins. In: Davidson F, Kaspers B, Schat KA, editors. Avian Immunology. 1rst ed. London, UK: Academic Press, Elseiver Ltd.
339. Tanno H, Nockels RP, Pitts LH, Noble LJ (1992) Breakdown of the blood-brain barrier after fluid percussive brain injury in the rat. Part 1: Distribution and time course of protein extravasation. Journal of Neurotrauma 9: 21-32.

340. Sokrab TEO, Johansson BB, Kalimo H, Olsson Y (1988) A transient hypertensive opening of the blood-brain barrier can lead to brain damage. Acta Neuropathologica 75: 557-565.
341. Levin EC, Acharya NK, Han M, Zavareh SB, Sedeyn JC, et al. (2010) Brain-reactive autoantibodies are nearly ubiquitous in human sera and may be linked to pathology in the context of blood-brain barrier breakdown. Brain Research 1345: 221-232.
342. Tsukita S, Furuse M, Itoh M (1999) Structural and signalling molecules come together at tight junctions. Current Opinion in Cell Biology 11: 628-633.
343. Hasebe R, Suzuki T, Makino Y, Igarashi M, Yamanouchi S, et al. (2010) Transcellular transport of West Nile virus-like particles across human endothelial cells depends on residues 156 and 159 of envelope protein. BMC Microbiology 10: 165.
344. Mark KS, Davis TP (2002) Cerebral microvascular changes in permeability and tight junctions induced by hypoxia-reoxygenation. American Journal of Physiology - Heart and Circulatory Physiology 282: H1485-H1494.
345. Lin B, Ginsberg MD (2000) Quantitative assessment of the normal cerebral microvasculature by endothelial barrier antigen (EBA) immunohistochemistry: application to focal cerebral ischemia. Brain research 865: 237-244.
346. Lin B, Ginsberg MD, Zhao W, Alonso OF, Belayev L, et al. (2001) Quantitative Analysis of Microvascular Alterations in Traumatic Brain Injury by Endothelial Barrier Antigen Immunohistochemistry. Journal of Neurotrauma 18: 389-397.
347. Gursoy-Ozdemir Y, Qiu J, Matsuoka N, Bolay H, Bermpohl D, et al. (2004) Cortical spreading depression activates and upregulates MMP-9. The Journal of Clinical Investigation 113: 1447-1455.
348. Gandhi N, Saiyed Z, Napuri J, Samikkannu T, Reddy P, et al. (2010) Interactive role of human immunodeficiency virus type 1 (HIV-1) clade-specific Tat protein and cocaine in blood-brain barrier dysfunction: Implications for HIV-1-associated neurocognitive disorder. Journal of Neurovirology 16: 294-305.
349. Nakamuta S, Endo H, Higashi Y, Kousaka A, Yamada H, et al. (2008) Human immunodeficiency virus type 1 gp120 mediated disruption of tight junction proteins by induction of proteasome-mediated degradation of zonula occludens-1 and -2 in human brain microvascular endothelial cells. Journal of Neurovirology 14: 186-195.
350. MacLean AG, Belenchia GE, Bieniemy DN, Moroney-Rasmussen TA, Lackner AA (2005) Simian immunodeficiency virus disrupts extended lengths of the blood–brain barrier. Journal of Medical Primatology 34: 237-242.
351. Luabeya MK, Dallasta LM, Achim CL, Pauza CD, Hamilton RL (2000) Blood–brain barrier disruption in simian immunodeficiency virus encephalitis. Neuropathology and Applied Neurobiology 26: 454-462.
352. Afonso PV, Ozden S, Prevost M-C, Schmitt C, Seilhean D, et al. (2007) Human blood-brain barrier disruption by retroviral-infected lymphocytes: role of myosin light chain kinase in endothelial tight-junction disorganization. The Journal of Immunology 179: 2576-2583.
353. Wang S, Le TQ, Kurihara N, Chida J, Cisse Y, et al. (2010) Influenza virus cytokine-protease cycle in the pathogenesis of vascular hyperpermeability in severe influenza. Journal of Infectious Diseases 202: 991-1001.
354. Wolburg H, Noell S, Wolburg-Buchholz K, Mack A, Fallier-Becker P (2009) Agrin, aquaporin-4, and astrocyte polarity as an important feature of the blood-brain barrier. The Neuroscientist 15: 180-193.
355. Rudd PA, Cattaneo R, von Messling V (2006) Canine distemper virus uses both the anterograde and the hematogenous heathway for neuroinvasion. The Journal of Virology 80: 9361-9370.
356. Christensen JE, de Lemos C, Moos T, Christensen JP, Thomsen AR (2006) CXCL10 is the key ligand for CXCR3 on CD8+ effector T cells involved in

immune surveillance of the lymphocytic choriomeningitis virus-infected central nervous system. The Journal of Immunology 176: 4235-4243.
357. Ryan G, Klein D, Knapp E, Hosie MJ, Grimes T, et al. (2003) Dynamics of viral and proviral loads of feline immunodeficiency virus within the feline central nervous system during the acute phase following intravenous infection. The Journal of Virology 77: 7477-7485.
358. Ryan G, Grimes T, Brankin B, Mabruk MJ, Hosie MJ, et al. (2005) Neuropathology associated with feline immunodeficiency virus infection highlights prominent lymphocyte trafficking through both the blood-brain and blood-choroid plexus barriers. Journal of Neurovirology 11: 337-345.
359. Falangola MF, Hanly A, Galvao-Castro B, Petito CK (1995) HIV infection of human choroid plexus: A possible mechanism of viral entry into the CNS. Journal of Neuropathology & Experimental Neurology 54: 497-503.
360. González L, Martin S, Hawkins SAC, Goldmann W, Jeffrey M, et al. (2010) Pathogenesis of natural goat scrapie: modulation by host PRNP genotype and effect of co-existent conditions. Vet Res 41: 48.
361. Siso S, Gonzalez L, Jeffrey M (2010) Neuroinvasion in prion diseases: the roles of ascending neural infection and blood dissemination. Interdisciplinary perspectives on infectious diseases 2010: 747892.
362. Suzuki K, Okada H, Itoh T, Tada T, Mase M, et al. (2009) Association of increased pathogenicity of Asian H5N1 highly pathogenic avian influenza viruses in chickens with highly efficient viral replication accompanied by early destruction of innate immune responses. Journal of Virology 83: 7475-7486.
363. Capua I, Marangon S (2000) The avian influenza epidemic in Italy, 1999-2000: A review. Avian Pathology 29: 289 - 294.
364. Capua I, Mutinelli F, Pozza MD, Donatelli I, Puzelli S, et al. (2002) The 1999-2000 avian influenza (H7N1) epidemic in Italy: veterinary and human health implications. Acta Tropica 83: 7-11.
365. Elbers ARW, Fabri THF, de Vries TS, de Wit JJ, Pijpers A, et al. (2004) The highly pathogenic avian influenza A (H7N7) virus epidemic in the Netherlands in 2003-Lessons learned from the first five outbreaks. Avian Diseases 48: 691-705.
366. Wood GW, Parsons G, Alexander DJ (1995) Replication of influenza A viruses of high and low pathogenicity for chickens at different sites in chickens and ducks following intranasal inoculation. Avian Pathology 24: 545 - 551.
367. Hooper PT, Russell GW, Selleck PW, Stanislawek WL (1995) Observations on the relationship in chickens between the virulence of some avian influenza viruses and their pathogenicity for various organs. Avian Diseases 39: 458-464.
368. Swayne DE, Slemons RD (2008) Using mean infectious dose of high- or low-pathogenicity avian influenza viruses originating from wild duck and poultry as one measure of infectivity and adaptation to poultry. Avian Diseases Digest 3: e15-e15.
369. Schafer A, Brooke CB, Whitmore AC, Johnston RE (2011) The role of the blood brain barrier during Venezuelan equine encephalitis virus infection. The Journal of Virology: JVI.05032-05011.
370. Samuel MA, Diamond MS (2006) Pathogenesis of West Nile virus infection: a balance between virulence, innate and adaptative immunity, and viral evasion. The Journal of Virology 80: 9349-9360.
371. Kristensson K, Olsson Y (1973) Diffusion pathways and retrograde axonal transport of protein tracers in peripheral nerves. Progress in Neurobiology 1: 87-109.
372. Harberts E, Yao K, Wohler JE, Maric D, Ohayon J, et al. (2011) Human herpesvirus-6 entry into the central nervous system through the olfactory pathway. Proceedings of the National Academy of Sciences.

373. Morales JA, Herzog S, Kompter C, Frese K, Rott R (1988) Axonal transport of Borna disease virus along olfactory pathways in spontaneously and experimentally infected rats. Medical Microbiology and Immunology 177: 51-68.
374. Gonzalez-Dunia D, Sauder C, de la Torre JC (1997) Borna disease virus and the brain. Brain Research Bulletin 44: 647-664.
375. Urbanska EM, Chambers BJ, Ljunggren H-G, Norrby E, Kristensson K (1997) Spread of measles virus through axonal pathways into limbic structures in the brain of TAP1 -/- mice. Journal of Medical Virology 52: 362-369.
376. Cosby SL, Duprex WP, Hamill LA, Ludlow M, McQuaid S (2002) Approaches in the understanding of morbillivirus neurovirulence. Journal of Neurovirology 8: 85-90.
377. Techangamsuwan S, Haas L, Rohn K, Baumgärtner W, Wewetzer K (2009) Distinct cell tropism of canine distemper virus strains to adult olfactory ensheathing cells and Schwann cells in vitro. Virus Research 144: 195-201.
378. Aronsson F, Robertso B, Ljunggren H-G, Kristensson K (2003) Invasion and persistence of the neuroadapted influenza virus A/WSN/33 in the mouse olfactory system. Viral Immunology 16: 415-423.
379. Reinacher M, Bonin J, Narayan O, Scholtissek C (1983) Pathogenesis of neurovirulent influenza A virus infection in mice. Laboratory Investigation 49: 686.
380. Silvano DF, Yoshikawa M, Shimada A, Otsuki K, Umemura T (1997) Enhanced neuropathogenicity of avian influenza A virus by passages through air sac and brain of chicks. The Journal of Veterinary Medical Science 59: 143-148.
381. Ito T, Goto H, Yamamoto E, Tanaka H, Takeuchi M, et al. (2001) Generation of a highly pathogenic avian influenza A virus from an avirulent field isolate by passaging in chickens. The Journal of Virology 75: 4439-4443.
382. Chambers TJ, Diamond MS (2003) Pathogenesis of flavivirus encephalitis. Advances in Virus Research 60: 273-342.
383. Hollidge B, González-Scarano F, Soldan S (2010) Arboviral encephalitis: Transmission, emergence, and pathogenesis. Journal of NeuroImmune Pharmacology 5: 428-422.
384. Wang P, Dai J, Bai F, Kong K-F, Wong SJ, et al. (2008) Matrix metalloproteinase 9 facilitates West Nile virus entry into the brain. The Journal of Virology 82: 8978-8985.
385. Mizuguchi M, Tomonaga M, Fukusato T, Asano M (1989) Acute necrotizing encephalopathy with widespread edematous lesions of symmetrical distribution. Acta Neuropathologica 78: 108-111.
386. Mizuguchi M (1997) Acute necrotizing encephalopathy of childhood: a novel form of acute encephalopathy prevalent in Japan and Taiwan. Brain and Development 19: 81-92.
387. Yoshikawa H, Watanabe T, Abe T, Oda Y (1999) Clinical diversity in acute necrotizing encephalopathy. Journal of Child Neurology 14: 249-255.
388. Weitkamp J-H, Spring MD, Brogan T, Moses H, Bloch KC, et al. (2004) Influenza A virus-associated acute necrotizing encephalopathy in the United States. The Pediatric Infectious Disease Journal 23: 259-263.
389. Protheroe SM, Mellor DH (1991) Imaging in influenza A encephalitis. Archives of Disease in Childhood 66: 702-705.
390. Suja MS, Mahadevan A, Madhusudhana SN, Vijayasarathi SK, Shankar SK (2009) Neuroanatomical mapping of rabies nucleocapsid viral antigen distribution and apoptosis in pathogenesis in street dog rabies-an immunohistochemical study. Clinical Neuropathology 28: 113-124.
391. Anderson JR, Field HJ (1983) The distribution of herpes simplex type 1 antigen in mouse central nervous system after different routes of inoculation. Journal of the Neurological Sciences 60: 181-195.

392. Solomon T (2004) Flavivirus encephalitis. New England Journal of Medicine 351: 370-378.
393. Kimura T, Sasaki M, Okumura M, Kim E, Sawa H (2010) Flavivirus encephalitis. Veterinary Pathology Online 47: 806-818.
394. Schweitzer BK, Chapman NM, Iwen PC (2009) Overview of the Flaviviridae with an emphasis on the Japanese Encephalitis group viruses. Lab Medicine 40: 493-499.
395. Ruggieri M, Polizzi A, Pavone L, Musumeci S (1998) Thalamic syndrome in children with measles infection and selective, reversible thalamic involvement. pediatrics 101: 112-119.
396. Steininger C, Popow-Kraupp T, Laferl H, Seiser A, Gōdl I, et al. (2003) Acute encephalopathy associated with influenza A virus infection. Clinical Infectious Diseases 36: 567-574.
397. Fujimoto S, Kobayashi M, Uemura O (1998) PCR on cerebrospinal fluid to show influenza-associated acute encephalopathy or encephalitis. The Lancet 352: 873.
398. Fujimoto S, Kobayashi M, Uemura O (1998) PCR on cerebrospinal fluid to show influenza-associated acute encephalopathy or encephalitis. Lancet 352: 873.
399. Mukherjee A, Peterson J, Sandberg G, Takei H, Adesina A, et al. (2011) Central nervous system pathology in fatal swine-origin influenza A H1N1 virus infection in patients with and without neurological symptoms: an autopsy study of 15 cases. Acta Neuropathologica 122: 371-373.
400. Yokota S (2003) Influenza-associated encephalopathy-pathophysiology and disease mechanims. Nihon Rinsho 61: 1953-1958.
401. Duran-Vilaregut J, del Valle J, Camins A, Pallàs M, Pelegrí C, et al. (2009) Blood-brain barrier disruption in the striatum of rats treated with 3-nitropropionic acid. NeuroToxicology 30: 136-143.
402. Kim KS (2008) Mechanisms of microbial traversal of the blood-brain barrier. Nature Reviews Microbiology 6: 625-634.
403. Huang S-H, Jong AY (2001) Cellular mechanisms of microbial proteins contributing to invasion of the blood–brain barrier. Cellular Microbiology 3: 277-287.
404. Rippy MK, Topper MJ, Mebus CA, Morrill JC (1992) Rift valley fever virus-induced encephalomyelitis and hepatitis in calves. Veterinary Pathology Online 29: 495-502.
405. Geisbert TW, Young HA, Jahrling PB, Davis KJ, Larsen T, et al. (2003) Pathogenesis of ebola hemorrhagic fever in primate models: evidence that hemorrhage is not a direct effect of virus-induced cytolysis of endothelial cells. The American Journal of Pathology 163: 2371-2382.
406. Hensley LE, Geisbert TW (2005) The contribution of the endothelium to the development of coagulation disorders that characterize Ebola hemorrhagic fever in primates. Thromb Haemost 94: 254-261.
407. Chen JP, Cosgriff TM (2000) Hemorrhagic fever virus-induced changes in hemostasis and vascular biology. Blood Coagulation & Fibrinolysis 11: 461-483.
408. Ito T, Kobayashi Y, Morita T, Horimoto T, Kawaoka Y (2002) Virulent influenza A viruses induce apoptosis in chickens. Virus Research 84: 27-35.
409. Nakai Y, Itoh M, Mizuguchi M, Ozawa H, Okazaki E, et al. (2003) Apoptosis and microglial activation in influenza encephalopathy. Acta Neuropathologica 105: 233-239.
410. Tumpey TM, Suarez DL, Perkins LEL, Senne DA, Lee J, et al. (2003) Evaluation of a high-pathogenicity H5N1 avian influenza A virus isolated from duck meat. Avian Diseases 47: 951-955.
411. Keawcharoen J, van Riel D, van Amerongen G, Bestebroer T, Beyer WE, et al. (2008) Wild ducks as long-distance vectors of highly pathogenic avian influenza virus (H5N1). Emerging Infectious Diseases journal 14.

412. Bröjer C, Ågren EO, Uhlhorn H, Bernodt K, Mörner T, et al. (2009) Pathology of natural highly pathogenic avian influenza H5N1 infection in wild tufted ducks (Aythya fuligula). Journal of Veterinary Diagnostic Investigation 21: 579-587.
413. Costa TP, Brown JD, Howerth EW, Stallknecht DE, Swayne DE (2011) Homo- and heterosubtypic low pathogenic avian influenza exposure on H5N1 highly pathogenic avian influenza virus infection in wood ducks (Aix sponsa). PLoS ONE 6: e15987.
414. Kwon YK, Thomas C, Swayne DE (2010) Variability in pathobiology of South Korean H5N1 high-pathogenicity avian influenza virus infection for 5 species of migratory waterfowl. Veterinary Pathology Online 47: 495-506.
415. Zhou J-Y, Shen H-G, Chen H-X, Tong G-Z, Liao M, et al. (2006) Characterization of a highly pathogenic H5N1 influenza virus derived from bar-headed geese in China. Journal of General Virology 87: 1823-1833.
416. Brown JD, Stallknecht DE, Swayne DE (2008) Experimental infection of swans and geese with highly pathogenic avian influenza virus (H5N1) of Asian lineage. Emerging Infectious Diseases 14: 136-142.
417. Kalthoff D, Breithaupt A, Teifke JP, Globig A, Harder T, et al. (2008) Pathogenicity of highly pathogenic avian influenza virus (H5N1) in adult mute swans. Emerging Infectious Diseases 14.
418. Jia B, Shi J, Li Y, Shinya K, Muramoto Y, et al. (2008) Pathogenicity of Chinese H5N1 highly pathogenic avian influenza viruses in pigeons. Archives of Virology 153: 1821-1826.
419. Tanimura N, Tsukamoto K, Okamatsu M, Mase M, Imada T, et al. (2006) Pathology of fatal highly pathogenic H5N1 avian influenza virus infection in large-billed crows (*Corvus macrorhynchos*) during the 2004 outbreak in Japan. Veterinary Pathology Online 43: 500-509.
420. Kwon YK, Joh SJ, Kim MC, Lee YJ, Choi JG, et al. (2005) Highly pathogenic avian influenza in magpies (*Pica pica serice*a) in South Korea. Journal of Wildlife Diseases 41: 618-623.
421. Kwon KY, Joh SJ, Kim MC, Kang MS, Lee YJ, et al. (2010) The susceptibility of magpies to a highly pathogenic avian influenza virus subtype H5N1. Poultry Science 89: 1156-1161.
422. Perkins LEL, Swayne DE (2003) Varied pathogenicity of a Hong Kong-origin H5N1 avian influenza virus in four passerine species and budgerigars. Veterinary Pathology 40: 14-24.
423. Müller T, Hlinak A, Freuling C, Mühle RU, Engelhardt A, et al. (2009) Virological monitoring of white storks (*Ciconia ciconia*) for avian influenza. Avian Diseases 53: 578-584.

Annex 1

Summary of the literature of free living bird species showing CNS lesions after infection with a HPAI virus.

Bird species	Virus strain	Histopathological findings	Influenza viral antigen positive cells and regions	Ref.
Domestic geese (*Anser anser domesticus*)	A/Hong Kong/156/1997 (H5N1)	Cerebral malacia and meningo-encephalitis	nr	[221]
Domestic ducks (*Anas platyrhynchos*)	A/Gs/Hong Kong/139.2/02 (H5N1)	Neuronal degeneration and necrosis. Heterophilic infiltrates in the neuropil and perivascular mononuclear infiltrates, oedema	nr	[221]
Call ducks (*Anas platyrhynchos var domestica*): 1 d, 2 and 4 wks old.	A/chicken/Yamaguchi/7/04 (H5N1) Experimental	Multifocal neuronal necrosis, lymphoplasmacytic perivascular cuffing, gliosis in OB, *cerebelum*, brain stem. Myelitis in the gray matter and necrosis of ependymal cell in the cervical and lumbar spinal cord.	nr	[150]
***Pekin white ducks (A. platyrhynchos domestica*) (2 wks- 5 wks)**	A/Vietnam/1203/2004- A/Crow/ Thailand/04, and A/Egret/HK/757.2/02	Malacia with gliosis, mild lymphoplasmacytic perivascular cuffs, and mild perivascular oedema. Neuronal degeneration and necrosis and vacuolation of the neuropil in birds found death.	Neurons, glial Vascular endothelium negative	[155]
Pekin white ducks (*A. platyrhynchos domestica*) (2 wks)	A/Duck/Anyang/AVL-1/01 (H5N1)	Mild perivascular lymphoplasmacytic cuffs around a few localized cerebral vessels and associated small foci of gliosis.	Ependymal cells	[410]
Pekin white ducks (*A. platyrhynchos domestica*) (2 wks)	A/Duck/Vietnam/12/05 (H5N1) Experimental	Necrosis of neurons and glial cells, occasional neuronophagia in the gray matter of the cerebrum. Rarely multifocal lymphohistiocytic perivascular cuffing. No lesions in *cerebellum* and brain stem	Neurons, glial cells (*cerebrum* - brain stem) Viral RNA in nervous cells of the submucosal plexus of the duodenum	[169]
Pekin white ducks (*A. platyrhynchos domestica*) (5 wks)	A/Muscovy duck/Vietnam/453/04 (H5N1) A/Duck/Indramayu/BBVW/109/06 (H5N1) Experimental	Mononuclear cell cuffs, gliosis, oedema of the neuropil, neural degeneration.	Neurons and neuropil Ependymal cells (Indonesian strain)	[234]
Tufted ducks (*Aythya fuligula*) (8-11 ms)	A/turkey/Turkey/1/05 (H5N1) Experimental	Severe multifocal encephalitis, ganglioneuritis	Neurons, glial cells (brain), Neurons and satellite cells (submucosal and myenteric plexuses, mesenteric ganglia of the small intestine)	[411]
Tufted ducks (*A. fuligula*)	HPAI virus H5N1 Natural cases	Non-supurative encephalitis or meningoencephalitis	Neurons, macrophages, glial cells. Ganglion cell of peripheral nerves. Submucosal Meissner and myenteric plexuses	[412]
Wood ducks (*Aix sponsa*)	A/whooper swan/Mongolia/244/05 (H5N1)	Non-suppurative encephalitis and neuronal necrosis. Choroiditis, meningitis, gliosis, vacuolar degeneration (associated or not with lymphoplasmacytic infiltrate). Neuritis and necrosis of myenteric plexus of small intestine	Neurons, glial cells (*cerebrum, cerebellum*, brain stem). Neurons of submucosal and myenteric plexuses. Sporadic in the meninges and epithelial cells of choroid plexus	[413]
Wood ducks (*Aix sponsa*) (10-16 wks)	A/ws/Mongolia/244/05 and A/Duck Meat/Anyang/01 (H5N1)	Severe multifocal to diffuse neuronal necrosis in the *cerebrum* and less commonly, in the *cerebellum*. Survival birds: Lymphoplasmacytic perivascular encephalitis	Neurons, glial cells, ependymal cells, endothelial cells, gitter cells and parasympathetic ganglia in the submucosal and muscular plexuses of the small intestine	[133]
White-faced Whistling duck (*Dendrocygna viduata*)	H5N1 HPAI virus Natural infection	Non-supurative meningo-encephalitis	Brain tissue positive	[145]
Ruddy shelduck (*Tadorna ferruginea*) (7-12 wks)	A/chicken/South Korea/IS/06 (H5N1) Experimental	Non-supurative meningo-encephalitis and neuronal degeneration and necrosis. Lymphocytic meningitis. Lymphocytic perivascular cuffs, gliosis, oedema.	Neurons, glial cells, neuropil, ependymal cells, cerebellar Purkinje cells and granular layer. Infrequent in ganglion cells in the myeteric plexus	[414]
Mandarin ducks (*Aix galericulata*) (7-12 wks)	A/chicken/South Korea/IS/06 (H5N1) Experimental	Non-suppurative encephalitis and neuronal degeneration and necrosis. Lymphocytic meningitis. Lymphocytic perivascular cuffs, gliosis, oedema.	Neurons, glial cells, neuropil, ependymal cells, epithelium of the choroid plexus.	[414]
Duck	A/Bar headed goose/Qinghai /05 Experimental	Hemorrhagic meningitis and perivascular cuffing with infiltration of lymphocytes and foci of gliosis	Neurons	[415]

Mute swan (*Cygnus color*) (5–6 wks)	A/ whooper swan /Mongolia/244/05 (H5N1)	Multifocal to coalescing necrosis with mild to moderate heterophilic inflammation.	Neurons, astrocytes, and other parenchymal cells of the brain	[416]
Mute swan (*Cygnus color*) (1-4 yrs)	A/Cygnus cygnus /Germany/R65/06 (H5N1) Experimental	-	Neurons, glial cells, ependymal cells in brain, spinal cord, and peripheral nerves innervating the adrenal glands, the ovary, or area located adjacent to the cecal tonsil.	[417]
Mute swan (*Cygnus color*)		Lymphocytic meningoencephalitis or meningo-encephalomyelitis: focal gliosis, neuronal necrosi, neuronophagia.		[148]
Mute swan (*Cygnus color*) (7–12 wks)	A/chicken/South Korea/IS/06 (H5N1). Experimental	Non-supurative encephalitis and neuronal degeneration and necrosis. Lymphocytic perivascular cuffs, gliosis, edema	Neurons, glial cells, neuropil, Endothelium, epithelium of the choroid plexus, cerebellar Purkinje cells and granular layer. Infrequent in neurons of submucosal and myenteric plexuses.	[414]
Mute swans (*Cygnus cygnus*) (Adult)	HPAI virus H5N1 Natural cases	Lymphoplasmacytic encephalitis in the *cerebrum* and severe necrosis and loss of Purkinje cells in the *cerebellum*. Oedema, lymphoplasmacytic cuffs. Neuronal necrosis, neuronophagia, gliosis	Neurons, glial cells (brain), Purkinje cells and cells of the granular layer (*cerebellum*). Ependymal cells lining the central canal of the spinal cord.	[147]
Black swan (*C.atratus*) (5–6 wks)	A/ws/Mongolia/244 /05 (H5N1) Experimental	Necrosis and inflammation.	Endothelial cell predominantly	[416]
Trumpeter swan (*C.buccinator*) (5–6 wks)	A/ws/Mongolia/244 /05 (H5N1) Experimental	Multifocal to coalescing necrosis with mild to moderate heterophilic inflammation.	Neurons, astrocytes, and other parenchymal cells of the brain	[416]
Whooper swans (*Cygnus olor*) (Adult)	HPAI virus H5N1 Natural cases	Lymphoplasmacytic encephalitis (*cerebrum*). Multiple foci of neuronal necrosis, neuronophagia, gliosisl. Necrosis and loss of Purkinje cells in the *cerebellum*. Rarely, spinal cord ependymal cells were hypeeosinophilic and necrotic.	Neurons and glial cells (brain and brain stem). Purkinje cells and cells of the granular layer (*cerebellum*). Ependymal cells lining the central canal of the spinal cord.	[147]
Bar-headed goose (*Anser indicus*) (12 wks)	A/whopper swan/Mongolia/24 4/05 (H5N1) Experimental	Moderate perivascular encephalitis and neuronal necrosis and mild perivascular encephalitis.	Widespread in the brain	[416]
Cackling goose (*B.hutchinsii*) (12 wks)	A/ws/Mongolia/244 /05 (H5N1) Experimental	Multiple foci of necrosis with moderate heterophilic to lymphoplasmocytic encephalitis	Neurons	[416]
Bar-headed geese (*Anser indicus*)	A/Bar-headed goose/Qinghai/051 0/05 (H5N1). Experimental		Brain +	[415]
Hawaiian Goose, (*Branta sandvicensis*)	H5N1 HPAI virus Natural infection	Non-supurative encephalitis with foci of necrosis	Brain +	[145]
Greylag geese (*Anser anser*) (7-12 wks)	A/chicken/South Korea/IS/06 (H5N1) Experimental	Malacia, neuronal loss, dystrophic calcification of necrotic neurons, gitter cell, and lymphocytic perivascular cuffs, focal hemorrhage, spongiform degeneration. Lymphocytic meningitis.	Neurons, neuropil, glial cells, gitter cells (cerebrum and midbrain)	[414]
Canada goose (*Branta canadensis*)	A/chicken/Vietnam/ 14/05 (H5N1) A/mallard/British Columbia/373/05 (H5N2)	Congestion and hemorrhages in the surface of the brain, spinal cord and parasympathetic ganglia	Neurons, glial cells, ependymal cells (brain, brain stem, spinal cord). Purkinje cell and neurons of granular layer, parasympathic ganglia of the submucosal and myenteric plexuses.	[221]
Canada goose (*Branta canadensis*)	A/chicken/Hong Kong/220/97 (H5N1)	Multifocal non-suppurative meningo-encephalitis, multiple small foci of necrosis with some gliosis in brain	-	[221]
Herring gulls (*Larus argentatus*) (12 wks)	A/ws/Mongolia/244 /05 (H5N1) Experimental	Severe and diffuse neuronal necrosis	Neurons, glial cells (*cerebrum* and *cerebellum*).	[153]
Black-headed Gull, (*Larus ridibundus*)	H5N1 HPAI virus Natural infection	Marked brain congestion, multiple small foci of necrosis and gliosis, few perivascular lymphoid cuffs	Brain +	[221]
Laughing gulls (*Larus atricilla*) (10-16 wks)	A/ws/Mongolia/244 /05 and A/Duck Meat/Anyang/01 (H5N1) Experimental	Lymphoplasmacytic perivascular encephalitis	Neurons, glial cells, endothelial cells, ependymal cells	[133]
Laughing gulls (*Passer domesticus*) wild capture	A/ws/Mongolia/244 /05 (H5N1)	Neuronal degeneration and necrosis (*cerebrum* and *cerebellum*), lymphoplasmacytic perivascular encephalitis, lymphocytic ganglioneuritisin peripheral nerves innervating heart and adrenal gland.	Neurons of CNS and peripheral nervous system	[259]
Rock pigeons (*Columbia livia*) Wild capture	A/ws/Mongolia/244 /05 (H5N1)	Lymphoplasmacytic encephalitis or meningoencephalitis and marked neuronal necrosis	Neurons	[259]

Pigeons		Necrosis of neurons and neuropil in the brain, and neurons of the autonomous nervous system, ganglioneuritis. Malacia, perivascular cuffing of mononuclear cells.	Neurons, glial cell (brain), autonomic nervous system, and ependymal cells.	[146, 418]
American crows (*Corvus brachyrhychos*)	A/crow/Thailand/1 C/2005 (H5N1)	Nonsuppurative encephalitis with neuron necrosis		[419]
Magpies (*Pica pica sericea*)	HPAI virus H5N1 Natural cases	Lymphocytic meningoencephalitis, malacia, gliosis, momonuclear perivascular cuffs.	Neurons, Purkinje cells, ependymal cells of the telencephalon, medulla oblongata and pons)	[420]
Korean wild magpies *(Pica pica sericea*) Wild capture	A/chicken/ Korea/ES/03 (H5N1) Experimenal	Neuronal degeneration, necrosis and vacuolation of the neuropil *(cerebrum, cerebellum* and medulla), lymphoplasmacytic perivascular cuffs, oedema, gliosis (*cerebrum* and *cerebellum*)	Neurons, glial cell (brain), ependymal cells, epithelium of the choroid plexus, cerebellar Purkinje cells neurons molecular layer, Infrequently in parasympathetic ganglia within the submucosal and myenteric plexus (small and large intestine).	[421]
Budgerigars (*Melopsittacus undulatus*).	A/Hong Kong/156/1997 (H5N1)	Perivascular edema and necrosis of cells containing viral antigen, minimal heterophilic inflammation was observed in the stroma of the choroid plexus	Neurons, glial cells, ependymal cells, epithelium of the choroid plexus	[135]
Zebra finches (*Taeniopygia guttata*) (young adult)	A/chicken/Hong Kong/220/97 (H5N1)	Minimal to mild perivascular edema and infrequent foci of a few necrotic cells	Neurons, ependymal cells, epithelial cells of the choroid plexus, glia, and endothelial cells. Neurons of peripheral ganglia	[422]
House finches (*Carpodacus mexicanus*) (wild-captured)	A/chicken/Hong Kong/220/97 (H5N1)	Foci of necrosis	Neurons, glial cells, and ependymal cells, peripheral ganglia	[422]
House finches (*Carpodacus mexicanu*s) (Wild-captured adult)	A/Hong Kong/156/1997 (H5N1)	Severe neurological disease being the result of viral neurotropism	nr	[135]
Emus (*Dramaius novaehollandia*) (2-week-old)	A/chicken/Hong Kong/220/97 (H5N1)	Meningo-encephalitis	nr	[221] [135]
Gadwall (*A. strepera*) (8-11 ms)	A/turkey/Turkey /1/05 (H5N1) Experimental	Mild encephalitis	Rarely in neurons	[411]
Little Egret (F), (*Egretta garzetta*)	H5N1 HPAI virus Natural infection	Severe brain congestion		[145]
Rosybill Pochard, (*Netta peposaca*)	H5N1 HPAI virus Natural infection	Congestion and multifocal non-suppurative meningo-encephalitis	Brain +	[145]
Eurasian pochard (*Aythya ferina*) (8-11 ms)	A/turkey/Turkey /1/05 (H5N1) Experimental	Multifocal encephalitis	Neurons, glial cells	[411]
Coscoroba Swan, (*Coscoroba coscoroba*)	H5N1 HPAI virus Natural infection	Congestion and multifocal non-suppurative encephalitis	Brain +	[221]
Chestnut-breasted Teal *(Anas castanea*)	H5N1 HPAI virus Natural infection	Congested brain with multiple small foci of necrosis	Brain +	[221]
Greater Flamingo (*Phoenicopterus ruber*)	H5N1 HPAI virus Natural infection	Non-suppurative meningo-encephalitis;	Brain +	[221]
Large-billed crows (*Corvus macrorhynchos*)	A/crow/Kyoto/53/ 04 (H5N1) A/crow/Osaka/53/ 04 (H5N1) Natural infection	Neuronal degeneration, necrosis of neurons and glial cells (*cerebrum, cerebellum*, brain stem, and spinal cord). Fibrin deposition in blood vessels, mild macrophages infiltration in meninges.	Neurons, glial cells (*cerebrum, cerebellum*, brain stem, spinal cord), ependymal cells. Neurons in interlobular connective tissue of pancreas, ganglion cells of the pericardium, lung adrenal gland. peripheral ganglia.	[419]
White storks (*Ciconia ciconia*)	H5N1 HPAI virus Natural infection	Neuronal degeneration and necrosis, spongiosis (brain stem), mild inflammatory reaction.	Neurons (*cerebrum*), glial cells of granular (*cerebellum*), brain stem, spinal cord), ependymal cells. Nuclei and cytoplasm of degenerate ganglion cells of the submucous and myenteric plexuses.	[423]
Blackcaps *(Sylvia atricapilla*) (wild-captured)	A/Cygnus cygnus/Germany/R 65/06 (H5N1)	Neuronal necrosis, neuronophagia, neuropil vaculozation.	Neurons, glial cells, ependymal cells, endothelial cells, neurons of peripheral nervous system (intestinal tract, adrenal gland, nervus *trigeminus*).	[154]
Red-billed queleas (*Quelea queleas*) (wild-captured)	A/Cygnus cygnus/Germany/R 65/06 (H5N1)	Neuronal necrosis, neuronophagia, neuropil vaculozation	Neurons, glial cells, ependymal cells, endothelial cells	[154]